

The oxidative ammonolysis of ethylene to acetonitrile over supported molybdenum catalysts

Citation for published version (APA):

Peeters, I. (1996). *The oxidative ammonolysis of ethylene to acetonitrile over supported molybdenum catalysts*. [Phd Thesis 1 (Research TU/e / Graduation TU/e), Chemical Engineering and Chemistry]. Technische Universiteit Eindhoven. <https://doi.org/10.6100/IR469707>

DOI:

[10.6100/IR469707](https://doi.org/10.6100/IR469707)

Document status and date:

Published: 01/01/1996

Document Version:

Publisher's PDF, also known as Version of Record (includes final page, issue and volume numbers)

Please check the document version of this publication:

- A submitted manuscript is the version of the article upon submission and before peer-review. There can be important differences between the submitted version and the official published version of record. People interested in the research are advised to contact the author for the final version of the publication, or visit the DOI to the publisher's website.
- The final author version and the galley proof are versions of the publication after peer review.
- The final published version features the final layout of the paper including the volume, issue and page numbers.

[Link to publication](#)

General rights

Copyright and moral rights for the publications made accessible in the public portal are retained by the authors and/or other copyright owners and it is a condition of accessing publications that users recognise and abide by the legal requirements associated with these rights.

- Users may download and print one copy of any publication from the public portal for the purpose of private study or research.
- You may not further distribute the material or use it for any profit-making activity or commercial gain
- You may freely distribute the URL identifying the publication in the public portal.

If the publication is distributed under the terms of Article 25fa of the Dutch Copyright Act, indicated by the "Taverne" license above, please follow below link for the End User Agreement:

www.tue.nl/taverne

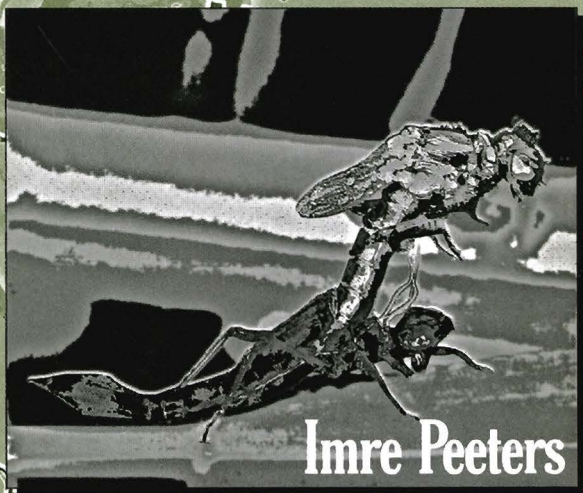
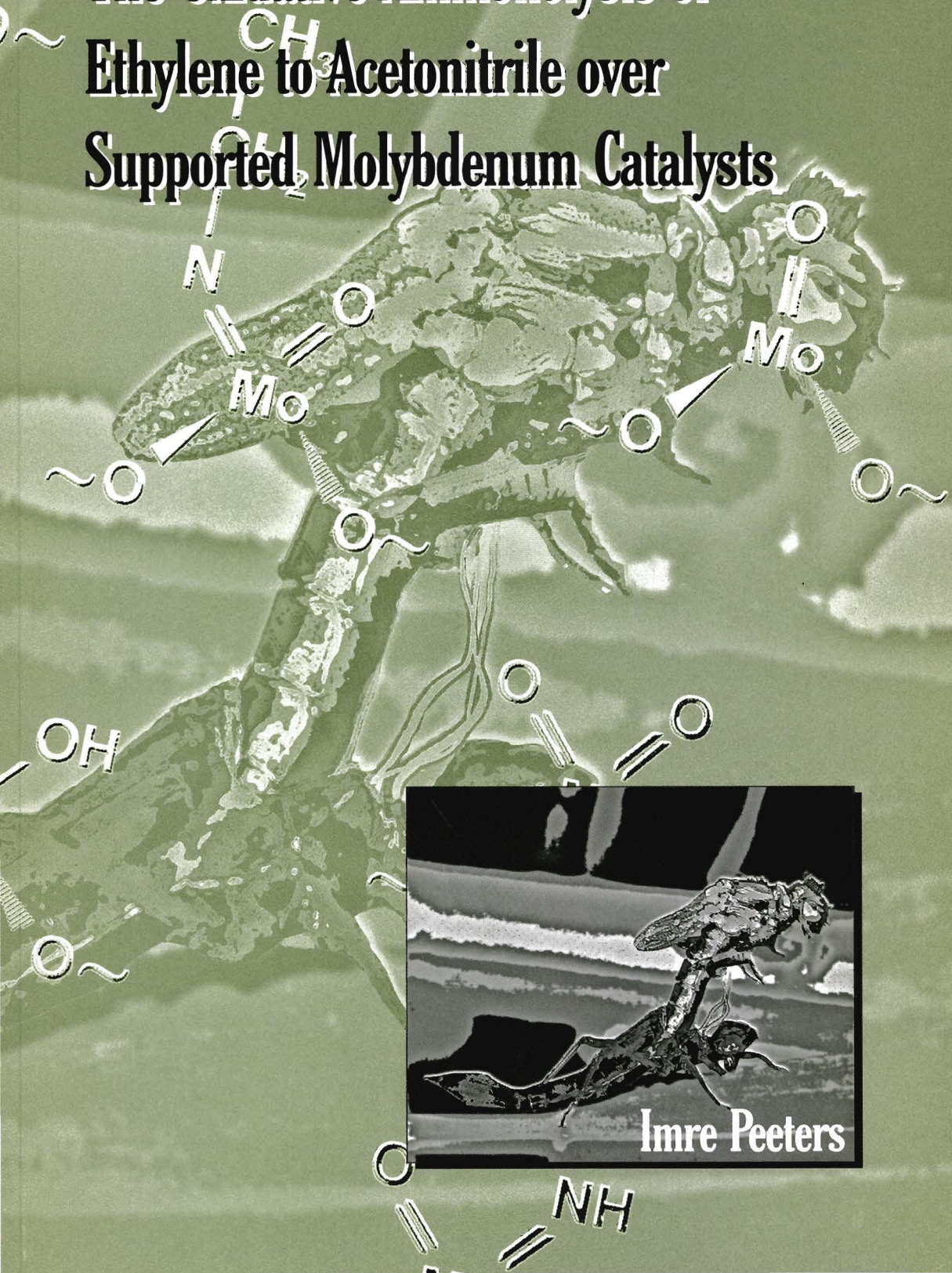
Take down policy

If you believe that this document breaches copyright please contact us at:

openaccess@tue.nl

providing details and we will investigate your claim.

The Oxidative Ammonolysis of Ethylene to Acetonitrile over Supported Molybdenum Catalysts



Imre Peeters

**The Oxidative Ammonolysis
of
Ethylene to Acetonitrile
over
Supported Molybdenum Catalysts**

PROEFSCHRIFT

ter verkrijging van de graad doctor aan de Technische
Universiteit Eindhoven, op gezag van de Rector
Magnificus, prof.dr. M. Rem, voor een commissie
aangewezen door het College van Dekanen in het openbaar
te verdedigen op maandag 18 november 1996 om 16.00 uur

door

IMRE PEETERS

Geboren te Den Haag

Dit proefschrift is goedgekeurd door de promotoren:

prof.dr. R.A. van Santen

en

prof.dr. J.A.R. van Veen

druk: Universiteitsdrukkerij,
Technische Universiteit Eindhoven.

Peeters, Imre

The oxidative ammonolysis of ethylene to acetonitrile over
supported molybdenum catalysts / Imre Peeters. - Eindhoven :
Technische Universiteit Eindhoven
Proefschrift Technische Universiteit Eindhoven. - Met lit. opg.
- Met samenvatting in het Nederlands.
ISBN 90-386-0079-8

The work described in this thesis was carried out at the Schuit Institute of Catalysis,
Laboratory of Inorganic Chemistry and Catalysis, Eindhoven University of Technology (P.O.
Box 513, 5600 MB Eindhoven) with financial support of the Dutch Organization for
Scientific Research (NWO).

*If anything can go wrong,
fix it !!!!!
Then shoot Murphy*

A.I.O.'s Law.

Contents

1 Introduction	1
1 In general	1
2 Nitrogen coupling to ethylene	2
3 The ammoxidation of propylene over molybdenum catalysts	3
4 Preparation γ -Al ₂ O ₃ supported molybdenum catalysts	6
5 Catalyst pretreatment	9
6 Characterisation of active sites of MoO ₃ / γ -Al ₂ O ₃ catalysts	13
7 Scope of this thesis	14
2 Catalyst preparation and characterisation	17
1 Introduction	17
2 Preparation of various catalysts	18
2.1 Alumina supported molybdenum oxide catalysts	18
2.2 Silica supported molybdenum oxide catalysts	18
2.3 Alumina supported mixed oxide catalysts containing molybdenum	18
3 Catalyst characterisation	20
3.1 Atomic Absorption Spectroscopy	20
3.2 BET surface area and pore volume by N ₂ -adsorption	20
3.3 Temperature Programmed Reduction/Oxidation	21
3.4 Fourier-Transform Infrared Spectroscopy	22
3.5 X-ray Photoelectron Spectroscopy	23
3.6 Low Energy Ion Scattering	24
3.7 X-ray Diffraction	26
3.8 High Resolution Transmission Electron Microscopy	26
4 Outline of the TPD and TPRE apparatus	26
3 Supported molybdenum oxide catalysts; temperature programmed techniques	29
Abstract	29
1 Introduction	30
2 Temperature programmed desorption of ammonia	31
2.1 Introduction	31
2.2 Experimental procedure	32
2.3 Results and discussion	32
3 Temperature programmed reaction of ethylene and ammonia; the method of sequentially introducing of the reactants	38
3.1 Experimental procedure	38
3.2 Results and discussion	39
3.2-1 The influence of the sequence of introducing reactants	39
3.2-2 Silica versus alumina support	41
3.2-3 Formation of organic products during a pulse of ethylene	42
3.2-4 γ -Al ₂ O ₃ supported molybdenum catalysts with various loading ...	44
4 Proposed N-containing (reactive) surface species	46
5 Conclusions.....	48

4	γ-Al₂O₃ supported MoO_x catalysts; structure-activity relationships	51
	Abstract	51
1	Introduction	52
2	Experimental procedure	53
3	Results and discussion	53
3.1	Characteristic regions of the activity profile	53
3.1-1	The semi-steady-state period	54
3.1-2	Transition period	59
3.1-3	Steady-state period	61
3.2	Characterisation of Mo/ γ -Al ₂ O ₃ catalysts	64
3.2-1	X-ray Diffraction	64
3.2-2	High Resolution Transmission Electron Microscopy	67
3.2-3	X-ray Photoelectron Spectroscopy	70
3.2-4	Low Energy Ion Scattering	74
3.2-5	Fourier-Transform Infrared Spectroscopy	81
3.3	Proposed reaction mechanisms	85
4	Conclusions	90
5	Molybdenum mixed oxides on γ-Al₂O₃	93
	Abstract	93
1	Introduction	94
2	Catalytic tests by sequentially introducing the reactants	96
2.1	Experimental procedure	96
2.2	Results and discussion	98
2.3	In summary	100
3	Catalytic tests under semi-flow conditions	101
3.1	Experimental procedure	101
3.2	Results and discussion	101
3.2-1	Catalytic tests	101
3.2-2	Catalyst characterisation	103
	High Resolution Electron Microscopy	103
	X-ray Diffraction	104
	X-ray Photoelectron Spectroscopy	104
4	Conclusions	107
6	Concluding remarks and summary	111
6	Conclusie en samenvatting	115
	Appendix I.....	119
	Dankwoord	122
	Curriculum Vitae	123

1

INTRODUCTION

1 In general.

Over eighty-five percent of industrial organic chemicals are currently produced by catalytic processes from petroleum and natural gas sources. About one quarter is produced by heterogeneous oxidation catalysis and can be classified by mechanistically related reactions, namely allylic oxidation and ammoxidation, epoxidation, aromatic and paraffinic oxidation (see Table 1.1) [1].

Almost all of the catalysts used in these processes are based on transition metal mixed oxides or oxysalts, which have the characteristic that a combination of surface properties, such as acid-base and redox, determines the route for the selective transformation [2,3]. The formation of carbon dioxide and water, which are the thermodynamically favoured products, always competes with the desired reaction. So, all products of partial oxidation are obtained by kinetic control of the reaction, which is a difficult task if one takes into account that usually the C-H bonds in the reactants are stronger than in the products of selective oxidation. Therefore, it is necessary to understand the relationship between catalyst surface reactivity and the formation of the desired product, and to control this reaction in order to prevent overoxidation to other products or carbon oxides.

★ Table 1.1 Some heterogeneous catalytic oxidation processes [1].

Oxidation class	Starting material	Product	End use
allylic	propylene	acrylonitrile	acrylic fibre resins, rubbers,
	C_3H_6	C_3H_3N	adiponitrile
epoxidation	ethylene	ethylene oxide	ethylene glycol, antifreeze,
	C_2H_4	C_2H_4O	polyesters, surfactants
aromatic	<i>o</i> -xylene	phthalic anhydride	polyesters, plasticisers, fine
	$C_6H_6(CH_3)_2$	$C_6H_4(C_2O_3)$	chemicals
paraffinic	n-butane	maleic anhydride	unsaturated polyester resins, fumaric
	C_4H_{10}	$C_4H_2O_3$	acid, insecticides, fungicides

Selective oxidation usually consists of complex multi-electron, multi-step and polyfunctional reactions [3]. The relative rates of these different routes depend not only on the presence or absence of specific sites, but can also depend on the surface transformation dynamics, *e.g.* the lifetime and mobility of adsorbed species, the redox dynamics, the evolution of the surface characteristics during the reaction, the presence of competitive adsorption phenomena, the population and surface distribution of adsorbed species, and the geometry of the active surface.

Supported and unsupported molybdenum oxide catalysts have been the subject of extensive research because of their wide applications in the petroleum, chemical and environmental control industries [4] and are known, amongst others, for their performance in selective oxidation. These catalysts are usually prepared by depositing the catalytically active molybdenum oxide component on the surface of an oxidic support, such as Al_2O_3 , TiO_2 , ZrO_2 , SiO_2 and MgO .

2 Nitrogen coupling to ethylene.

Allylic (amm)oxidation, that is, the selective (amm)oxidation of olefins at the allylic position, represents a substantial contribution to the production of important organic chemicals by heterogeneous oxidation. In addition, the development and study of selective catalysts for allylic oxidation has led to more understanding concerning selective oxidation and the phenomena of catalysis in general.

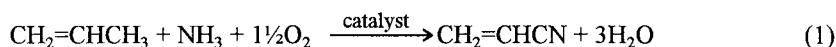
The (ep)oxidation of ethylene has been the subject of extensive research. Much of the reaction mechanism of the epoxidation of ethylene is now understood [5]. A well-known

homogeneous catalytic reaction for the selective oxidation of ethylene is the Wacker reaction, catalysed by palladium to form vinylacetate [6,7]. However, little is known about vinylic ammoxidation of olefins in a heterogeneous catalytic reaction. The formation of acetonitrile from ethylene and ammonia has only been mentioned in patents and literature of several decades ago [8,9]. To study the probable pathways of the ammoxidation of ethane over Sc-Mo catalysts, the rate and selectivity was compared with those of ethylene and acetaldehyde [10]. Only recently, the formation of acetonitrile with ethylene and ammonia over Zn^{2+} and Cd^{2+} exchanged Y-zeolites was reported by Takahashi *et al.* [11]. More understanding in the reaction mechanism of vinylic ammoxidation could be of great interest when extrapolated to more complicated olefins. This can lead to the reduction of synthesis steps in some industrial processes required in the near future for environmental considerations. Ethylene, due to its simplicity, is a good reactant for studying the vinylic ammoxidation, and is for this reason applied in the study reported here. The ammoxidation of ethylene seems to be analogous to the ammoxidation of propylene. But if one considers that the abstraction of an allylic hydrogen is much easier than the abstraction of a vinylic hydrogen (85 vs. 105 kcal/mole), and a hydrogen shift has to occur, forming a methyl group, some differences in reaction mechanism are to be expected. To illustrate this, the ammoxidation of propylene will be discussed in more detail in the next section.

Acetonitrile is conventionally produced by catalytic dehydration of acetamide or catalytic dehydrogenation of ethylamine. Also reactions of ammonia with acetic acid, acetic anhydride or ethanol, thermal decomposition of several nitrogen containing compounds, and reactions of cyanogen, hydrocyanic acid or ammonia with hydrocarbons lead to the formation of acetonitrile [9,12]. Also much research has been done on the formation of acetonitrile with carbon monoxide, hydrogen and ammonia as starting materials [9,13]. Acetonitrile and hydrocyanic acid are important side products from the ammoxidation of propylene (*vide infra*), and in some plants acetonitrile is recovered from the reaction stream and purified [14].

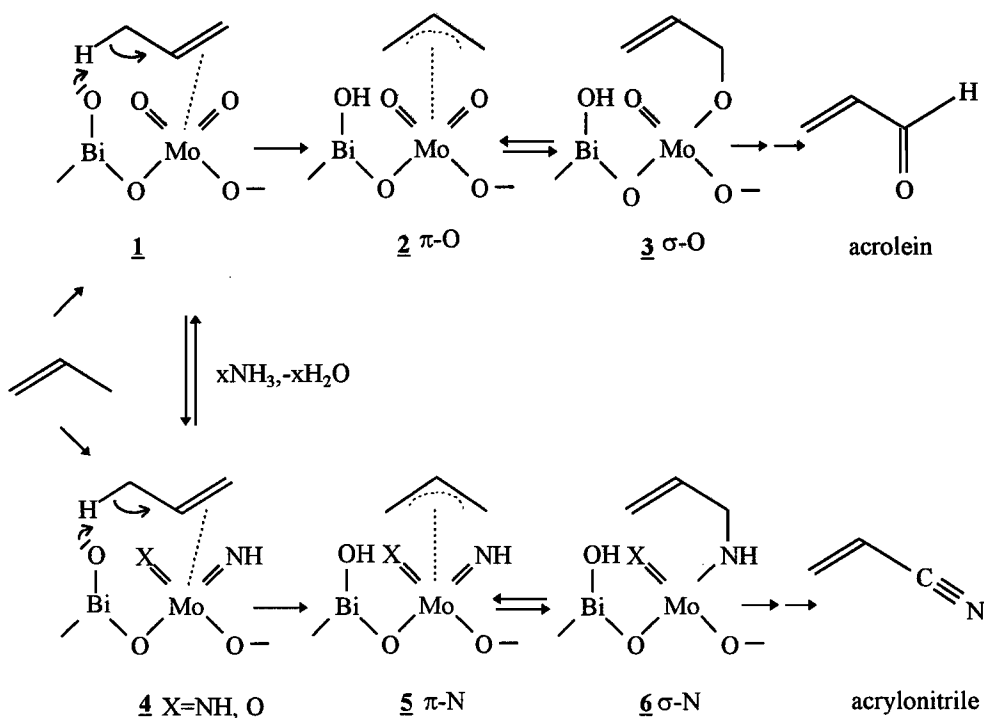
3 The ammoxidation of propylene over molybdenum catalysts.

Commercially, the most important member of allylic oxidation is the ammoxidation of propylene with ammonia and air to acrylonitrile,



This Sohio-discovered process [15] accounts for the majority of the acrylonitrile currently produced world-wide. It displaced the more expensive acetylene-HCN-based route in the early 1960's as well as other obsolete processes which also used expensive reagents (*e.g.* ethylene oxide and acetaldehyde) and oxidants (*e.g.* NO). The oxidation reaction, producing acrolein, which is also an important chemical intermediate, shows mechanistic analogies. Both reactions proceed via similar catalysts and in the temperature region of 300 to 460 °C. The most active and selective catalyst systems are based on oxides of either molybdenum (*e.g.* Bi₂Mo₃O₁₂) or antimony (Fe-Sb-O_x). The selective oxidation and ammoxidation of olefins is an example where 30 years of research has elucidated most of the reaction mechanism [15,16].

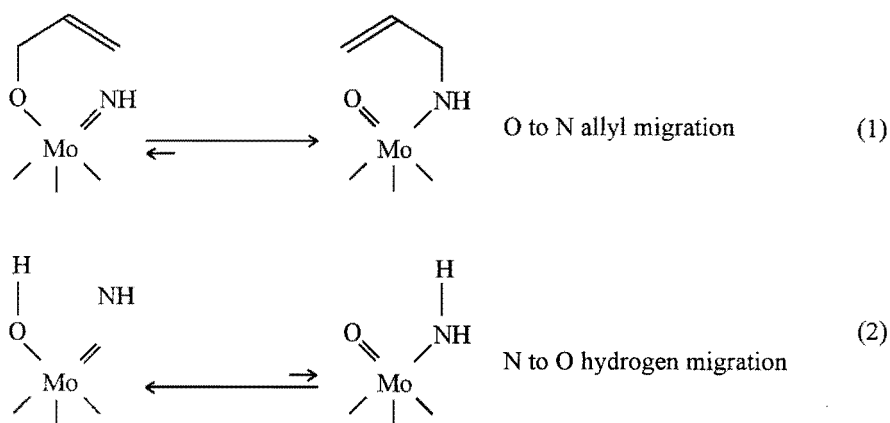
Mechanistic work on bismuth/molybdate catalysts reveals that the active sites for selective oxidation contain Mo-dioxo groups, which are responsible for the propylene chemisorption and O-insertion. Bridged Bi-O groups are the sites for the abstraction of an α -H (Scheme 1.1; **1**), which is the rate determining step. The α -H abstraction results in the formation of a π -allylic molybdate intermediate (**2**), which is in a rapid equilibrium with the σ -O form (**3**), the acrolein precursor [15,16]. In the ammoxidation reaction, ammonia is



★ **Scheme 1.1** Reaction mechanism of the selective oxidation and ammoxidation of propylene over bismuth/molybdate catalysts [16].

activated via a condensation reaction, forming an imido (Mo=NH) group (4), while water is released. The formation of acrylonitrile proceeds via the analogous π -N (5) and σ -N allyl (6) species. This reaction mechanism is supported by experiments with probe molecules [17].

Experiments by Burrington *et al.* [16] revealed that the activation of ammonia can take place in pairs. Also, two N-inserting species existed. The first pair is activated 2.5 times faster than the second pair of ammonia molecules. This pairwise activation of ammonia results in the successive formation of Mo-diimido groups. The activity of the two different Mo sites varies under different turnover conditions. At low turnover conditions both sites participate, one as inserting and the other as redox species. At higher turnover conditions only one Mo site reacts and the surface reoxidation proceeds via bulk lattice. Also, experiments with *d*-containing probe molecules proved the occurrence of allyl and H migration. The allyl migration from O to N appears to be favoured (see Scheme 1.2; reaction (1)), whereas the H migration preferably occurs from N to O (reaction (2)). The correct position of these two equilibria is the secret of a successful selective ammoxidation catalyst.



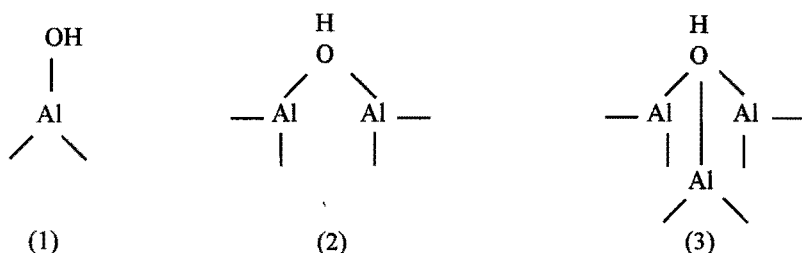
★ Scheme 1.2 Migration equilibria of allyl (1.) and hydrogen (2.) on the mixed oxo-imido molybdate surface.

Not only the performance of supported molybdenum catalysts has been extensively studied, but also the preparation of these catalysts, which appeared to be a complex process dependent on the deposition method of the active material as well as on the pretreatment. A number of characterisation techniques have been optimised and applied, which has resulted in almost full understanding of the processes occurring during catalyst preparation. As an example of this, the preparation, pretreatment and characterisation of γ -Al₂O₃ supported

molybdenum catalysts will be discussed in the following sections, because this type of catalyst has been applied in this study of the reaction of ethylene with ammonia.

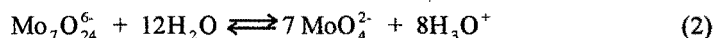
4 Preparation of $\gamma\text{-Al}_2\text{O}_3$ supported molybdenum catalysts.

The supported molybdenum oxide catalyst has been the subject of a large number of studies. Most common supports used for transition metal oxide catalysts are active C, SiO_2 and $\gamma\text{-Al}_2\text{O}_3$. The major difference in characteristics between the three supports is that active C and SiO_2 are relatively inert, whereas $\gamma\text{-Al}_2\text{O}_3$, due to its surface chemistry, can influence more strongly the nature of the supported species. The surface of $\gamma\text{-Al}_2\text{O}_3$ contains three different OH configurations, which can be distinguished by infrared spectroscopy (IR). The high frequency band is due to structures of the basic type (1), while the middle and low frequency bands are due to neutral and acidic structures of types (2) and (3), respectively (see Figure 1.1) [18].



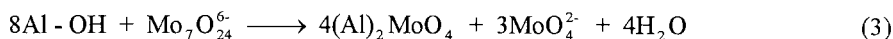
★ Figure 1.1 Three specific surface hydroxyl configurations of $\gamma\text{-Al}_2\text{O}_3$.

$\text{Mo}/\gamma\text{-Al}_2\text{O}_3$ catalysts are often prepared by aqueous impregnation with ammonium hepta molybdate (AHM) solutions. In the solution an equilibrium exists between hepta molybdate (HM) and molybdate ions (equation (2)):



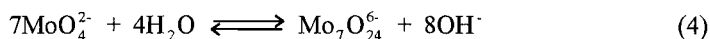
Clearly, changing the pH of the solution influences this equilibrium, resulting in a shift of the concentration of either molybdate species.

The interaction between AHM and the $\gamma\text{-Al}_2\text{O}_3$ surface has been the subject of many studies. According to van Veen *et al.* [19,20] two reactions are involved, when AHM solutions are used that are not acidified or alkalised. First, HM reacts irreversibly with the basic hydroxyl groups (equation(3)):



The fact that only the basic hydroxyl groups react is confirmed by IR. Only the high-frequency band, which is ascribed to the basic hydroxyl groups [21], disappears in the IR spectrum of the $\gamma\text{-Al}_2\text{O}_3$ support. Raman and EXAFS measurements proved the tetrahedral coordination of the adsorbed molybdenum species whereas molybdenum is octahedral coordinated in AHM [22]. The second reaction consists of a reversible physisorption of AHM on the coordinatively unsaturated sites (c.u.s.) Al^{3+} present on the alumina surface [23].

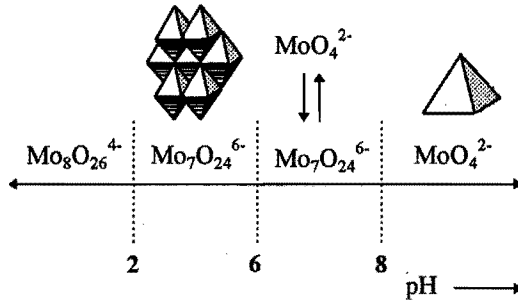
At a pH of 9-10, the AHM solution contains only MoO_4^{2-} ions (see Figure 1.2; (A)). Since the pH is substantially higher than the point of zero charge (pzc) of $\gamma\text{-Al}_2\text{O}_3$ (pH=8), initially no interaction occurs between the solute and the negatively charged alumina surface (see Figure 1.2; (B)). While drying the catalyst, ammonia desorbs at a lower temperature than water, which leads to a drop of the pH, shifting the equilibrium (equation (4)) to the right, forming HM ions. This shift starts at a pH of approximately 7.



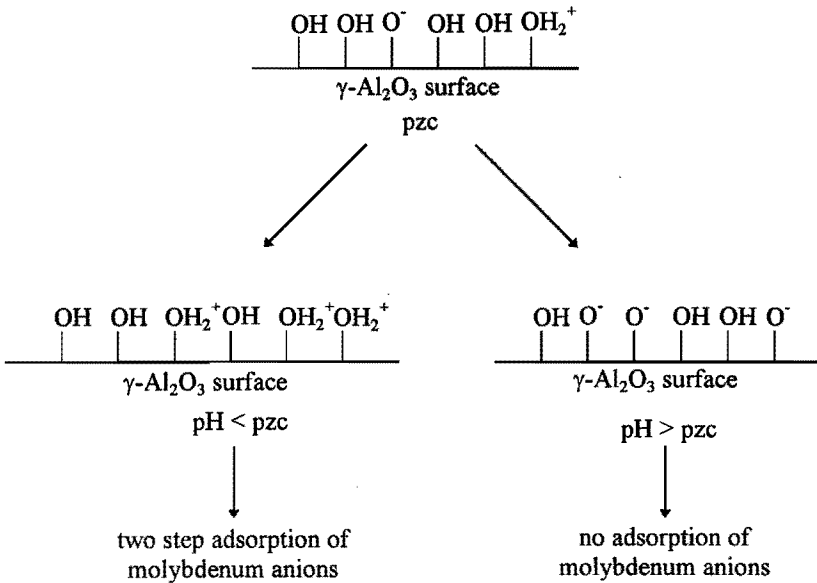
The HM formed can then participate in the process discussed above, except that the physisorption of AHM precedes the reaction of HM with the basic hydroxyl groups of alumina (equation (3)). This is confirmed by Raman spectroscopy. When the spectra of dried and wet samples were compared with one of an AHM solution, similarities were found [24], implying that the same oxo-molybdenum species are present on the surface as observed in solution. When the AHM impregnation solution is acidified to pH=2, the maximum adsorption level is higher than when near neutral solutions are used [23-25]. The dominating molybdenum species exist now in the form of $\text{Mo}_8\text{O}_{26}^{4-}$ ions (see Figure 1.2; (A)), while the surface charge of the alumina has increased (see Figure 1.2; (B)). On the basis of charge compensation one might expect an increase in the adsorption amount of at least a factor 2. However, only an increase of 30% is observed. Considering that there are other anions present in the solution (NO_3^-), (co)adsorption could oppose this effect. Since IR spectra did not show significant nitrate adsorption at high molybdenum loading, it is concluded that the adsorption of molybdate anions on alumina is not controlled by surface charge compensation [23]. Spanos *et al.* [26] concluded that not only neutral hydroxyls participate in the adsorption process, but also protonated surface hydroxyls are involved and furthermore, that adsorption of monomolybdate takes place through reaction with two neutral hydroxyl groups,

forming a surface complex (see Figure 1.3). It was also noted that raising the impregnation temperature, at pH=5, leads to a considerable increase of adsorption of $\text{Mo}_7\text{O}_{24}^{6-}$ ions. In contrast, the further deposition of monomolybdate ions through surface reaction is suppressed, while the adsorption of monomolybdate is not influenced substantially.

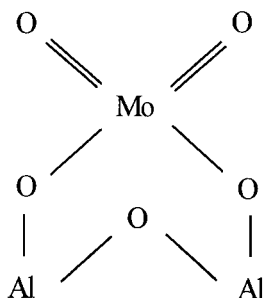
A.



B.



★ Figure 1.2 (A) The dominant molybdenum oxyanions present at various pH regions [27, 28]. (B) The adsorption scheme of molybdenum anions on the $\gamma\text{-Al}_2\text{O}_3$ surface.



★ **Figure 1.3** The surface complex of the reaction of MoO_4^{2-} ions with neutral surface hydroxyl groups of $\gamma\text{-Al}_2\text{O}_3$ [26].

A good technique to study the character of the adsorbed species is temperature programmed reduction (TPR). The temperature at which the rate of reduction is maximal (T_{max}) and the amount of hydrogen consumed per mole Mo, representing the extent of reduction, gives information about the reducibility of the adsorbed species. It appears that at low molybdenum content (< 4 wt% Mo) the species present on the alumina surface are hard to reduce, because T_{max} is high and the amount of hydrogen consumption is low [23]. This is characteristic for adsorbed MoO_4^{2-} . At mediate molybdenum content (~ 7 wt% Mo) a second species can be detected at a lower T_{max} with a high hydrogen consumption. This is due to the presence of $\text{Mo}_7\text{O}_{24}^{6-}$. When a catalyst, impregnated with an acidified AHM solution, is submitted to TPR, a third species is observed at high molybdenum content. The T_{max} lies in between the other two, while the hydrogen consumption is the highest. Since at pH=2 octamolybdate anions (OM; $\text{Mo}_8\text{O}_{26}^{4-}$; see Figure 1.2; (A)) are present, they can probably be identified with the third species[23]. The fact that OM is not observed at low and intermediate molybdenum content, leads to the conclusion that it can also react in acidic environment with the basic OH groups on the alumina surface, followed by decomposition to HM and monomolybdate.

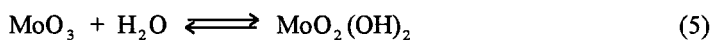
5 Catalyst pretreatment.

Having discussed the process of impregnation, it is also of great importance to understand the processes that can occur when the catalyst is submitted to thermal treatment. The conditions used in this heat treatment (oxygen, hydrogen or inert gas treatments) can influence the final

state of the catalyst. In the process of subsequent drying and calcining the adsorbed species become chemically bonded to the support surface replacing the OH groups. At higher molybdenum concentrations also precipitation of non-adsorbed ions occurs, which could be responsible for the formation of polymolybdate species, during removal of the solvent. The difference between the surface and the bulk oxide has been reported for the first time for molybdenum catalysts by Hall and Massoth [29,30] and Schuit and Gates [31]. Disagreement existed on the coordination of molybdenum. Hall and Massoth, along with other investigators [32,33], assumed one-dimensional chains of MoO_2 -species with a third O located in the underlying oxide layer, implying an octahedral coordination. Others have described the surface phase as a layer of highly dispersed aluminium molybdate, which has a tetrahedral coordination of molybdenum [34]. It appears that both coordinations can be present, and that the octahedral/tetrahedral molybdate ratio strongly depends on preparation method and molybdenum content.

Because NH_3 is easier expelled than water, the pH also changes during heat treatment, shifting the equilibrium of the molybdate anions (*vide supra*). This leads to ambiguities, which could be avoided by using very dilute impregnating solutions, controlling the loading [35] by varying pH and determining final pH values [36]. Raman spectra were compared of wet, dried and calcined catalysts with those from solutions with the same final pH. At low pH the signals, clearly indicating the existence of polymolybdate species, did not change upon drying and calcining. It was also concluded that all samples contained tetrahedral monomeric species, regardless of pH, and that the ratio of tetrahedral monomeric to octahedrally coordinated polymolybdate species decreased with increasing molybdenum content.

Upon calcining, also spreading of the molybdenum oxide on the alumina surface can occur. Raman microscopy on an alumina wafer in close contact with a molybdenum oxide wafer indicated transport of molybdenum for several hundred micrometers after thermal treatment, at 800 K, in a stream of dry oxygen or saturated with water vapour [37]. When the atmosphere contained dry oxygen, only X-ray amorphous MoO_3 could be detected, whereas with moistened O_2 a surface polymolybdate was formed after spreading. Transport through the gas phase was excluded at the applied temperature region. This indicates that in the presence of water vapour, besides spreading, also a chemical transformation occurs. The intermediate in the surface polymolybdate formation is supposed to be $\text{MoO}_2(\text{OH})_2$ [38,39] according to equation (5):



This oxyhydroxide is then assumed to react with surface hydroxyl groups $[\text{OH}]_s$ to form a surface monomolybdate $[\text{MoO}_4^{2-}]_s$ according to equation (6):



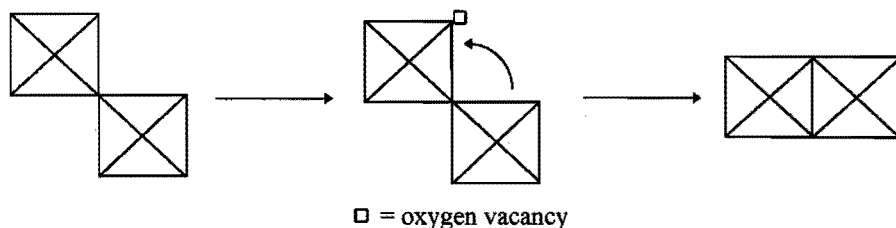
The surface molybdate species are detected as intermediates [39]. When the concentration becomes too high, they undergo condensation, forming the surface polymolybdate. Since this spreading phenomenon does not occur on SiO_2 surfaces, sublimation of a molybdenum phase could be excluded. According to Leyrer *et al.* [37], the spreading can best be described as a solid-solid wetting process, in which the decrease in surface free energy is to be considered as the dominant driving force. The different behaviour of Al_2O_3 and SiO_2 is explained by assuming "chemical" interactions between MoO_3 and Al_2O_3 , leading to a favourable interface energy, which is not possible for MoO_3 and SiO_2 . This is supported by experiments with various physical mixtures of powders of the oxides concerned [38]. It is suggested that, particularly for supported oxides, wetting processes of this kind may play an important role in catalyst preparation and regeneration.

Although the spreading of molybdenum on silica is controversial, some examples are known that it can occur under certain conditions. Stencel *et al.* [40] used LEIS to demonstrate that molybdenum spreads upon calcination, whereas exposure to water results in agglomeration, and this is a reversible process. More recently, LEIS experiments also clearly established the spreading of molybdenum [41]. However, this spreading is not expected on the basis of solid-solid wetting, as was suggested by Leyrer *et al.* [37]. In the highly dispersed silica supported molybdenum catalyst studied by Stencel *et al.* [40] and Brongersma *et al.* [41], the spreading can be assigned to the destruction of so-called Keggin units (silicomolybdic acid, $\text{H}_2\text{SiMo}_{12}\text{O}_{40} \cdot \text{H}_2\text{O}$), which can be restored upon water treatment.

The reactions (5) and (6) were also reported by Liu *et al.* [42] in an investigation on physical and chemical loss of MoO_3 on alumina and silica. On alumina, significant loss of molybdenum in an inert atmosphere, defined as physical loss, occurred at temperatures exceeding 800 °C. In a water vapour atmosphere, significant loss, defined as chemical loss, occurred already at temperatures exceeding 600 °C. The chemical loss was ascribed to the reactions (5) and (6), where the $\text{MoO}_2(\text{OH})_2$ formed by the chemical reaction with the water vapour, is more volatile than MoO_3 . This loss mechanism can not only occur during catalyst preparation, but is one of the main reasons of deactivation during heterogeneous catalytic oxidation reactions.

When a $\gamma\text{-Al}_2\text{O}_3$ supported molybdenum catalyst is heated in a hydrogen flow, the reduction is presumed to go through formation of Mo-OH groups which can recombine,

forming water and an oxygen vacancy. These vacancies are known to form ordered arrays, followed by facile rearrangement of the layers of initially cornered-linked into edge-linked metal-oxygen octahedra, resulting in the formation of a shear plane (see Figure 1.4) [43].



★ Figure 1.4 The formation of a shear plane upon reduction of MoO_3 .

The reduction process starts at relatively low temperatures, forming a variety of reduced Mo states. It was reported by Segawa and Hall [44] that all Brønsted acidity disappeared from these catalysts upon reduction, while the Lewis acid sites of the molybdenum and the γ - Al_2O_3 could not be distinguished. Chemisorption experiments, using IR spectroscopy, revealed that NO is selective for the coordinatively unsaturated sites (c.u.s.) of reduced molybdena surfaces, and NO chemisorbs in pairs [45]. Also the strong irreversible chemisorption of H_2 has been studied on these catalysts [46], which showed similarities with NO chemisorption. By applying NMR it was suggested that dissociative adsorption occurred on the same sites as those involved in NO chemisorption [47]. The selective chemisorption of CO_2 on alumina is well-known. These selective chemisorptions can be used as a powerful tool to characterise directly adsorption on sites where undetectable catalytic intermediates are presumed to form, especially when the chemisorption takes place on different sites independently, which is the case for NO and CO_2 [48]. Using this technique, some interesting features have been revealed concerning phenomena that occur during the reduction of supported molybdena catalysts. It was confirmed that the surface OH groups of the alumina are replaced by molybdate species, but a fraction is regenerated upon reduction with H_2 . A maximum of 50% recovery was found, which was in agreement with CO_2 chemisorption. This suggests that some of the surface bonds of molybdena to alumina, formed upon calcining, are broken and a part of the alumina surface remained bonded to the reduced molybdenum. During the reduction reconstruction takes place into MoO_2 -like

structures, which is reversible, so redox cycles can be carried out without significant modification of the catalyst surface.

XPS measurements by Grünert *et al.* [49] showed that at thermal treatment in an inert atmosphere a part of the Mo(VI) present on the surface is reduced to Mo(V). These authors also claimed the formation of Mo(IV) and Mo(0) states upon reductive treatment at 700 °C.

6 Characterisation of active sites of MoO₃/γ-Al₂O₃ catalysts.

Catalysts based upon Mo/Al₂O₃ are remarkable for the multiplicity of the reactions they promote. This has resulted in a large number of investigations, attempting to clear up the relationship between catalytic activity and catalyst composition. The combination of spectroscopic techniques, such as IR, UV, Raman, EXAFS and NMR, have provided information on the molecular nature of supported molybdena on alumina catalysts and the mechanism for the formation of such structures during the impregnation, drying and calcination stages. The reason this has been emphasised is that the molecular nature of molybdenum in the Mo/γ-Al₂O₃ catalyst is strongly dependent on the method of preparation, as described in the preceding paragraphs. Obviously, this has important effects on the activity of these catalysts. So, even more important is characterisation of the catalyst surface under reaction conditions. A large number of spectroscopic measurements has been applied to elucidate the surface structures of the molybdenum oxide species, however, not all have been successful in yielding independently a definitive structural determination. Transmission FTIR can in principle provide this information, but due to strong absorption of the IR signal by the oxide support below 1000 cm⁻¹ it is not possible to collect spectra in this important region. Due to its broad UV features, UV-vis does not provide sufficiently detailed structural information on the surface molybdenum oxide species. EXAFS can discriminate between different metal oxide structures, but averages the signal from all sites, so different structures present in the catalyst cannot be separately identified with EXAFS. The coordination number of molybdenum oxide species (octahedral or tetrahedral) can be obtained by XANES, but it has, also due to averaging the signal of all sites, difficulty in discriminating between structures possessing the same coordination number. Solid-state ⁹⁵Mo NMR can provide detailed structural information of the supported molybdenum oxide species, but the low sensitivity of the ⁹⁵Mo NMR signal generally makes it difficult to obtain useful spectra. Most promising seems to be Raman spectroscopy. It can provide the desired information concerning the surface structures of molybdenum oxide species on oxide supports, but it has also the advantage that it can discriminate between the different molecular states of the supported metal oxide. Each state possesses a unique vibrational spectrum directly related to

its structure. However, the occurrence of fluorescence and the correct assignment can cause difficulties in applying this technique.

7 Scope of this thesis.

As illustrated in the previous sections, extensive research on heterogeneous oxidation catalysts, in particular those containing molybdenum, has elucidated both mechanistic aspects and structure-reactivity phenomena to some extent. The ammoxidation of propylene is an example where the knowledge obtained has led to a world-wide industrial application and extrapolation to the allylic ammoxidation of more complex compounds (*e.g.* toluene). However, little is known about the vinylic ammoxidation of olefins.

The objective of the research described in this thesis was to investigate the possibility of N-addition to olefins over supported molybdenum catalysts. Industrial interest is focused on nitrile formation with more complicated compounds, such as styrene and dienes. The formation of acetonitrile from ethylene and ammonia over supported molybdenum catalysts was studied as test reaction. No molecular oxygen was added to the reaction stream, thus the focus was on the reactivity of the lattice oxygen, excluding surface reoxidation effects. An attempt was made to elucidate some aspects of the reaction mechanism and to find a correlation of reactivity with the surface structure of the catalyst, which are well-known to exist in (amm)oxidation reactions, by using various physical characterisation techniques. Also, an attempt was made to improve catalytic performance by the addition secondary compounds.

Chapter 2 describes in detail the preparation and pretreatment of various catalysts and the experimental set-up with corresponding methods of sample preparation. In Chapter 3 and 4 the catalytic activity of various supported molybdenum catalysts is described. Chapter 3 focuses on temperature programmed desorption and reaction (TPD, TPre) by using a method of introducing sequentially the reactants to the catalyst. Indications were found that two different mechanisms exist on the dissociation of ammonia dependent on the catalyst pretreatment. Also, effects of competitive adsorption between desired product and the reactant ammonia were found. Chapter 4 describes the structure-activity relationship for various γ -Al₂O₃ supported molybdenum catalyst after different pretreatments and time on stream. It also shows the results of a number of characterisation techniques, such as XRD, HREM, IR, LEIS and XPS, applied to fresh and spent catalysts, which led finally to a good understanding in the relation between catalytic activity and the surface structure present. In Chapter 5, a number of promoted molybdenum catalysts are investigated with respect to their catalytic activity and compared to the unpromoted catalyst. In case of better performance by

adding the promoter, further characterisation was undertaken. Also, an attempt was made to explain the positive or negative effect of the promoter added. Finally, the most important conclusions are summarised in Chapter 6.

Literature cited

- 1 Grasselli, R.K., *J. Chem. Educ.* **63**(3) (1986) 216
- 2 Haber, J. in "New Developments in Selective Oxidation by Heterogeneous Catalysis." Ruiz, P., Delmon, B. (Eds.), Elsevier Science Pub. Amsterdam, (1992) 259
- 3 Centi, G., Trifirò, F., *Appl. Catal.*, **12** (1984) 1
- 4 Thomas, C.L. in "Catalytic Processes and Proven Catalysts.", Academic Press, New York, (1970)
- 5 van Santen, R.A., Kuipers, H.C.P.E., *Adv. Catal.* **35** (1988) 265
- 6 van Helden, R., Kohll, C.F., Medema, D., Verberg, G., Jonkhoff, T., *Recueil* **87** (1968) 961
- 7 Henry, P.M., *J. Am. Chem. Soc.* **94** (1972) 7305
- 8 Teter, J.W., Olson, L.E., *US Patent 2 658 041* (1953)
- Denton, W.I., Bishop, R.B., *Ind. Eng. Chem.* **45** (1953) 282
- Kominami, N., Hori, H., *Kogyo Kagaku Zasshi* **61** (1958) 1312
- Plate, A.F., Volpin, M.E., *Dokl. Akad. Nauk* **89** (1953) 491
- Ozaki, A., Miyazaki, Y., Sato, Y., Ohki, K., *Kogyo Kagaku Zasshi* **69** (1966) 59
- 9 Olivé, G., Olivé, S., *US-Patent 4 179 462* (1979)
- 10 Aliev, S.M., Ph. D. thesis, Inst. Katal., Novosibirsk (1979)
- 11 Takahashi, N., Minoshima, H. Iwadera, H., *Chem.Lett.* (1994) 1323
- 12 Xu, B.-Q., Yamaguchi, T., Tanabe, K., *Chem. Lett.* (1988) 281
- Xu, B.-Q., Yamaguchi, T., Tanabe, K., *Chem. Lett.* (1987) 1053
- Olivé, G., Olivé, S *US Patent 4 058 548* (1977)
- Catani, R., Centi, G., *J. Chem. Soc., Chem. Commun.* (1991) 1081
- Reddy, B.M., Manohar, B., *J. Chem. Soc., Chem. Commun.* (1993) 234
- Encyclopedia of Chemical Technology, Nitriles*, 3rd ed., **15** (1978) 888
- 13 Hummel, A.A., Badani, M.V., Hummel, K.E., Delgass, W.N., *J.Catal.* **139** (1993) 392
- Auvil, S.R., Penquite, C.R., *US-Patent 4 272 452* (1981)
- Hamada, H., Kuwahara, Y., Matsuno, Y., Wakabayashi, K., *Sekiyu Gakkaishi* **30** (3) (1987) 188
- Gambell, J.W., Auvil, S.R., *US-Patent 4 272 451* (1981)
- Tatsumi, T., Kunitomi, S., Yoshiwara, J., Muramatsu, A., Tominaga, H., *Catal. Lett.* (1989) 223
- Badani, L.M., Eshelman, L.M., Delgass, W.N., "Proceedings of the 10th International Congress on Catalysis" (1992), Budapest, Hungary, Elsevier Science Publ. B.V.
- Eshelman, L.M., Delgass, W.N., *Catal. Today* **21** (1994) 229
- 14 *Ullmann's Encyclopedia of Industrial Chemistry, Nitriles*, 5th ed., **A17** (1991) 363
- 15 Grasselli, R.K., Burrington, J.D., *Adv. Catal.*, **30** (1981) 133
- 16 Burrington, J.D., Kartisek, C.T., Grasselli, R.K., *J. Catal.*, **87**(1984) 363
- Allison, J.N., Goddard, W.A. in "Solid State Chemistry in Catalysis." (1985) 23
- Andrushkevich, T.V., *Catal. Rev.-Sci. Eng.* **35** (1993) 213
- Dadyburjor, D.B., Jewur, S.S., Ruckenstein, E., *Catal. Rev.-Sci. Eng.*, **19** (1979) 293
- 17 Burrington, J.D., Kartisek, C.T., Grasselli, R.K., *J. Catal.* **63** (1980) 235
- Burrington, J.D., Kartisek, C.T., Grasselli, R.K., *J. Catal.* **75** (1982) 225
- 18 Geus, J.W., van Veen, J.A.R., "Catalysis: an Integrated Approach to Homogeneous, Heterogeneous and Industrial Catalysis", (J.A. Moulijn, P.W.N.M. van Leeuwen, R.A. van Santen, Eds.) Elsevier, Amsterdam (1993) 339
- 19 van Veen, J.A.R., Hendriks, P.A.J.M. *Polyhedron* **5** (1986) 75
- 20 van Veen, J.A.R., de Wit, H., Emeis, C.A., Hendriks, P.A.J.M., *J. Catal.* **107** (1987) 579
- 21 van Veen, J.A.R., *J. Colloid Interface Sci.* **121** (1988) 214

- 22 Mensch, C.T.J., van Veen, J.A.R., van Wingerden, B., van Dijk, M.P., *J. Phys. Chem.* **92** (1988) 4961
- 23 van Veen, J.A.R., Hendriks, P.A.J. M., Romers, E.J.G.M., Andréa, R.R., *J. Phys. Chem.* **94** (1990) 5275
- 24 Kasztelan, S., Grimblot, J., Bonnelle, J.P., Payen, E., Toulhoat, H., Jacquin, Y., *Appl. Catal.* **7** (1983) 91
- 25 Wang, L., Hall, W.K., *J. Catal.* **77** (1982) 232
- 26 Spanos, N., Vordonis, L., Kordulis, Ch., Lycourghiotis, *J. Catal.* **124** (1990) 301
Spanos, N., Vordonis, L., Kordulis, Ch., Koutsoukos, P.G., Lycourghiotis, A., *J. Catal.* **124** (1990) 315
Spanos, N., Lycourghiotis, A., *J. Catal.* **147** (1994) 57
- 27 Aveston, J., Anacker, E.W., Johnson, J.S., *Inorg. Chem.* **3** (1964) 735
- 28 Honig, D.S., Kustin, K., *Inorg. Chem.* **11** (1972) 65
- 29 Hall, W.K., Massoth, F.E., *J. Catal.* **34** (1974) 41
- 30 Massoth, F.E., *J. Catal.* **36** (1975) 164
- 31 Schuit, G.C.A., Gates, B.C., *AIChE J.* **19** (1973) 417
- 32 Ratnasamy, P., Knözinger, H., *J. Catal.* **54** (1978) 155
- 33 Knözinger, H., Jeziorowski, H., *J. Phys. Chem.* **82** (1978) 2002
- 34 Krylov, O.V., Margolis, L.Y., *Kinet. Katal.* **11** (1970) 358
Asmolov, G.N., Krylov, O.V., *Kinet. Katal.* **11** (1970) 847
Asmolov, G.N., Krylov, O.V., *Kinet. Katal.* **12** (1971) 1117
Stork, W.H.J., Coolegem, J.G.F., Pott, G.T., *J. Catal.* **32** (1974) 497
Stork, W.H.J., Pott, G.T., *Recl. Trav. Chim. Pays-Bas* **96** (1977) M105
- 35 Sonnemans, J., Mars, P., *J. Catal.* **31** (1973) 209
- 36 Wang, L., Hall, W.K., *J. Catal.* **66** (1980) 251
- 37 Leyrer, J., Mey, D., Knözinger, H., *J. Catal.* **124** (1990) 349
- 38 Margraf, R., Leyrer, J., Knözinger, H., Taglauer, E., *Surf. Sci.* **189/190** (1987) 842
Margraf, R., Leyrer, Taglauer, E., J., Knözinger, H., *React. Kinet. Catal. Lett.* **35** (1987) 261
Leyrer, J., Margraf, R., Taglauer, E., Knözinger, H., *Surf. Sci.* **201** (1988) 603
- 39 Leyrer, J., Zaki, M.I., Knözinger, H., *J. Phys. Chem.* **90** (1986) 4775
- 40 Stencil, J.M., Diehl, J.R., D'Este, J.R., Makovsky, L.E., Rodrigo, L., Marcinkowska, K., Adnot, A., Roberge, P.C., Kaliaguine, S., *J. Phys. Chem.* **90** (1986) 4739
- 41 Brongersma, H.H., van Leerdam, G.C., *Fundamental Aspects of Heterogeneous Catalysis Studied by Particle Beams*, (H.H. Brongersma, R.A. van Santen, Eds.) Plenum press, New York **NATO ASI series B265** (1991) 283
Brongersma, H.H., Jacobs, J.-P., *Appl. Surf. Sci.* **75** (1994) 133
- 42 Liu, D., Zhang, L., Yang, B., Li, J., *Appl. Catal.* **105** (1993) 185
- 43 Haber, J., Marczewski, W., Stoch, J., Ungier, L., *Ber. Bunsen-Gesellschaft* **79(11)** (1975) 970
- 44 Segawa, K., Hall, W.K., *J. Catal.* **76** (1982) 133
- 45 Millman, W.S., Hall, W.K., *J. Phys. Chem.* **83** (1979) 427
- 46 Millman, W.S., Hall, W.K., in "Proceedings of the 7th International Congress on Catalysis", Tokyo (1980) (T. Seiyama and K. Tanabe, Eds.), Kodansha Ltd., Tokyo (1981) Part B, 1304
- 47 Cirillo, A.C., Jr., Dereppe, J.M., Hall, W.K., *J. Catal.* **61** (1980) 170
- 48 Segawa, K., Hall, W.K., *J. Catal.* **77** (1982) 221
- 49 Grünert, W., Stakheev, A.Yu, Mörke, W., Feldhaus, R., Anders, K., Shpiro, E.S., Minachev, Kh.M., *J. Catal.* **135** (1992) 269

2

CATALYST PREPARATION AND CHARACTERISATION

1 Introduction.

In most academic and many industrial laboratories the aim of catalyst characterisation is to understand the mechanism by which the catalyst operates. Catalyst characterisation is also useful in optimisation of a new catalyst formulation, which is the aim in many industrial studies. A detailed description of the catalyst will assist in determining the best composition and the most suitable preparation method for the new catalyst. Characterisation evidence can also be of immense value where it is necessary to diagnose catalyst failure. The range of techniques applied in catalyst characterisation is extremely wide. A reliable rule that should be kept in mind is very simple: never rely on only one technique. Each technique imposes its own perspective on the problem, which can be misleading in some situations, so careful choice is important. The guideline is to choose in-situ techniques where possible. The highest aim of catalyst characterisation is to establish the relationship between the electronic and geometric structure of the catalyst and its performance.

In order to prevent duplicate descriptions, all experimental procedures are described in detail in this chapter. Only specific procedures of testing catalytic performance and TPD experiments are described in other relevant chapters. This resulted in the subdivision of this chapter into three parts. First the catalyst preparation is described, concerning alumina and silica supported molybdenum and alumina supported molybdenum promoted with various transition metals. The second part concerns physical methods for the characterisation of freshly prepared and spent catalysts, with corresponding procedures of sample preparation. The third part contains a detailed description of the apparatus used for TPD experiments and catalytic performance tests.

2 Preparation of various catalysts.

2.1 Alumina supported molybdenum oxide catalysts.

Batches of 5 g of catalyst with various molybdenum content were prepared by incipient wetness impregnation of a commercial γ - Al_2O_3 (Akzo/Ketjen 000 1.5E) with a specific surface area of 205 m^2/g and a BET pore volume of 0.55 ml/g. A sieve fraction of 250-500 μm was used. Molybdenum was added from an aqueous solution of ammonium heptamolybdate-tetrahydrate (AHM, $(\text{NH}_4)_6\text{Mo}_7\text{O}_{24}\cdot 4 \text{H}_2\text{O}$ obtained from Merck), which had a pH of approximately 5, followed by slowly heating in air to 110 $^\circ\text{C}$ overnight. Subsequently, the batch was heated in a flow of 20 Nml/min of artificial air to 500 $^\circ\text{C}$ and held there for 1h. An isothermal period of 15 min at 130 $^\circ\text{C}$ was applied in order to remove water slowly and the heating rate was kept at 5 $^\circ\text{C}/\text{min}$. Batches containing 3, 5, 10 and 15 wt% molybdenum were prepared. Due to the limited solubility of AHM, the batches of 10 and 15 wt% were prepared by two sequential impregnation steps, as described above, for 5 and 7.5 wt% Mo, respectively.

2.2 Silica supported molybdenum oxide catalysts.

For comparison with the alumina support, a 5 wt% Mo/ SiO_2 catalyst was prepared by incipient wetness impregnation of pre-shaped Grace 332 type silica, with specific surface area of 300 m^2/g and specific pore volume of 1.6 ml/g. This silica contained 0.02% Na, 0.0005% K and 0.044% Fe. An aqueous solution of AHM was added to the sieve fraction of 125-200 μm of the support, followed by slowly drying in air at 110 $^\circ\text{C}$ overnight. Subsequently, the batch was heated in a flow of 20 Nml/min of artificial air to 500 $^\circ\text{C}$ and held there for 1h, with an isothermal period for 15 min at 130 $^\circ\text{C}$.

2.3 Alumina supported mixed oxide catalysts containing molybdenum.

An extended motivation for the choice of the set of secondary components added to a supported molybdenum catalyst is given in Chapter 5. All secondary compounds were transition metals of all series of the periodic system, and, except for chromium, are known for their application in supported molybdenum catalysts for the synthesis of acetonitrile from syngas and ammonia, and for (amm)oxidation reactions of hydrocarbons. At an early stage of this surveying study, the promoted catalysts were prepared by sequential impregnation, with a hydrogen pretreated 5 wt% Mo/ γ - Al_2O_3 serving as a precursor. Various ratios of platinum over molybdenum and manganese over molybdenum were tested. After impregnation, the

catalysts were dried slowly in air at 110 °C overnight, followed by heating in a flow of 10 vol% hydrogen in nitrogen to 600 °C. An isothermal period of 15 min at 130 °C was applied in order to remove water slowly, and the heating rate was kept at 5 °C/min. The catalysts prepared are listed in Table 2.1.

★ **Table 2.1** Catalysts prepared containing a secondary compound with a hydrogen pretreated 5 wt% Mo/ γ -Al₂O₃ as a precursor.

Catalysts	Catalyst code	Atomic ratio	Precursor salt
Mo:Pt	MoPt1	1 : 0.003	H ₂ PtCl ₆
	MoPt2	1 : 0.03	H ₂ PtCl ₆
	MoPt3	1 : 0.1	H ₂ PtCl ₆
Mo:Mn	MoMn1	1 : 0.2	MnBr ₂ ·4 H ₂ O
	MoMn2	1 : 0.35	MnBr ₂ ·4 H ₂ O
	MoMn3	1 : 1	MnBr ₂ ·4 H ₂ O
	MoMn4	1 : 2	MnBr ₂ ·4 H ₂ O

Another set of mixed oxide catalysts were prepared by sequential incipient wetness impregnation of a calcined 10 wt% Mo/ γ -Al₂O₃ catalyst, adding an aqueous solution of the desired metal salt. After slowly drying in air at 110 °C overnight, the catalyst was heated in a flow of 20 Nml/min of artificial air to 500 °C and held there for 1 hour. The catalysts prepared are listed in Table 2.2 with the corresponding metal salts used as precursor for the impregnation solution.

★ **Table 2.2** Catalysts prepared containing a secondary compound with a calcined 10 wt% Mo/ γ -Al₂O₃ as a precursor.

Catalysts	Catalyst code	Atomic ratio	Precursor salt
Mo:Ag	MoAg1	10 : 1.8	AgNO ₃
Mo:Ag	MoAg2	10 : 3	AgNO ₃
Mo:Cu	MoCu	10 : 3	Cu(NO ₃) ₂ ·3 H ₂ O
Mo:Mn	MoMn5	10 : 3.45	MnBr ₂ ·4 H ₂ O
Mo:Cr	MoCr	10 : 3.7	Cr(NO ₃) ₃ ·9 H ₂ O
Mo:Ni	MoNi	10 : 3	Ni(NO ₃) ₂ ·6 H ₂ O
Mo:Rh	MoRh	10 : 3	RhCl ₃ ·3 H ₂ O

3 Catalyst characterisation.

3.1 Atomic Absorption Spectroscopy.

The chemical analyses were done by means of Atomic Absorption Spectroscopy (AAS) using a Perkin Elmer 3030 Atomic Absorption Spectrophotometer. Prior to analysis, the sample was crushed and dried at 110 °C for 2 h. The protocol was to heat approximately 40 or 100 mg of a sample with 1 g of potassium-peroxo-disulfate, until a clear melt was obtained. After cooling, the melt was dissolved in 5 ml 2.5 M H₂SO₄ and diluted with water to 100 ml. The samples were measured by the method of standard addition. The results are summarised in Table 2.3, and show that the molybdenum content aimed for during impregnation is achieved within reasonable accuracy. Also, after submitting the catalyst several times to severe reaction conditions did not result in a considerable loss of the active component (approximately 5%).

★ Table 2.3 AAS analysis of various Mo/ γ -Al₂O₃ catalysts after different treatment.

Catalyst	wt% Mo according to AAS ^a
3 wt% Mo, calcined	3.2
5 wt% Mo, calcined	5.2
10 wt% Mo, calcined	9.8
15 wt% Mo, calcined	14.9
reduced 15 min at 700 °C	14.8
spent	14.1

^a AAS accuracy of +/- 0.1 wt%

3.2 BET surface area and pore volume by N₂-adsorption.

The BET measurements were performed on a Sorptomatic 1900 of Carlo-Erba Instruments. To remove water and adsorbed gases, the sample was heated in vacuum for 3 hours at 200 °C. This was followed by cooling to 77 K (temperature of liquid nitrogen) and addition of small doses of N₂ until the pressure of saturation was reached (1 atm). From the adsorption curve the micro pore volume and BET area were calculated, based on a multi-layer adsorption. From the desorption curve (hysteresis) the distribution of the pore radius was determined. The results for various

pretreated γ -Al₂O₃ and Mo/ γ -Al₂O₃ catalysts are listed in Table 2.4. The mean pore radius was 40-50 Å.

★ **Table 2.4** Specific surface area and pore volume according to BET measurements for various pretreated γ -Al₂O₃ and Mo/ γ -Al₂O₃ catalysts.

Sample	Surface area [m ² /g]	Pore volume [ml/g]
γ -Al ₂ O ₃	205	0.55
0.5h at 700 °C in H ₂ ; 5 °C/min	187	0.58
3 times 0.5h at 700 °C in H ₂ ; 5 °C/min	183	0.46
1h at 875 °C	159	0.53
3 wt% Mo, calcined	197	0.54
5 wt% Mo, calcined	204	0.50
10 wt% Mo, calcined	168	0.46
15 wt% Mo, calcined	173	0.44
Al ₂ (MoO ₄) ₃	< 1	n.d. ^a

^a n.d.: not determined

From Table 2.4 it can be concluded that only severe conditions can influence the surface area and pore size of the alumina significantly. Also, the addition of molybdenum does not change these parameters to a large extent. At high molybdenum content (10 and 15 wt% Mo) the surface area dropped sharply, due to the presence of Al₂(MoO₄)₃ (see Chapter 4, section 3.2-1 and 3.2-2), which possesses a lower surface area.

3.3 Temperature Programmed Reduction/Oxidation.

Temperature programmed reduction (TPR) is an indirect method to discriminate between different metal oxide phases which differ in reduction characteristics. For example, Roozeboom *et al.* [1] attributed the two reduction peaks to the two-dimensional metal oxide overlayer and the crystallites (the high and low temperature peak, respectively).

The TPR program consisted of heating a 100 mg sample in a flow of 5 ml/min 5 vol% hydrogen in argon to 700°C and held there for 10 min. The TPO program consisted of heating in a flow of 5 ml/min with 5% oxygen in helium to 500 °C and held there for 1 h. The heating rate

was kept at 5 °C/min. The TPR/TPO apparatus has been described elsewhere [2], the results of the different catalysts are given in Table 2.5.

Since the heating rate was kept constant, it was not possible to determine the activation energy of the reduction according to the theoretical treatment of the TPR as given by Hurst *et al.* [3]

★ **Table 2.5** Peak maximum and peak area of temperature programmed oxidation and reduction for various calcined catalysts.

Catalyst	TPR		TPO	
	T _{max} [°C]	Peak area [a.u.]	T _{max} [°C]	Peak area [a.u.]
3 wt%	470	0.8	^a	^a
5 wt%	415	2.1	160	1.8
10 wt%	390, 495	5.9	156	7.1
15 wt%	430, 520	8.4	176	8.5
MoO ₃	740	n.d. ^c	-	-
Al ₂ (MoO ₄) ₃	(330, 570, 685) 725 ^b	n.d. ^c	-	-

^a insufficient signal to noise. ^b numbers between brackets represent the positions of shoulders preceding to the main signal. ^c n.d.: not determined.

and Wimmers *et al.* [4] The reduction band shifted to a lower temperature with increasing Mo content, implying an increase in the reducibility. At 3 wt%, the main molybdenum species present are monomeric and tetrahedrally coordinated, which are difficult to reduce. At 5 wt%, the aggregated octahedrally coordinated Mo species are present and are easier to reduce, resulting in a reduction band at lower temperature. Apparently, TPR cannot distinguish between these species, due to the broad signal. At 10 and 15 wt% Mo, two reduction bands appeared, indicating that more than one molybdenum species is present. The reduction temperature increased at 15 wt% Mo, indicating an increase in particle size. Reducing bulk structures, such as MoO₃ and Al₂(MoO₄)₃ requires higher temperatures.

3.4 Fourier-Transform Infrared Spectroscopy.

Infrared transmission spectroscopy is a bulk rather than a surface specific technique. It is therefore necessary to prove for any detected species that it is a surface group. This can be realised in many cases by following changes in band position on exposure of the solid adsorbent to a suitable

adsorptive or by isotopic exchange experiments. The sensitivity is dependent on the extinction coefficient of the surface groups. Data can be obtained on the composition and structure of surface compounds, the nature of the bonds formed between adsorbed molecules and the surface, the existence of various types of surface compounds and active surface centres. As the vibrational spectrum reflects both the properties of the molecule as a whole and the characteristic features of separate chemical bonds, this method offers the fullest possible data on the perturbation experienced by the molecule on contact with the solid surface, and easily determines the structure and properties of adsorption complexes and surface compounds.

Infrared spectra were recorded on a Bruker IFS 113v FTIR spectrometer, equipped with a heatable vacuum cell. All measurements were performed in transmission mode. The spectra were recorded by adding at least 500 scans at a resolution of 1 cm^{-1} , using a standard DTGS detector. A self-supported disc was prepared of 15 mg of ground sample, and pretreated in 10 % H_2 in N_2 for 10 hours at $550\text{ }^\circ\text{C}$, followed by evacuation for 2 h at $550\text{ }^\circ\text{C}$, or in oxygen at $500\text{ }^\circ\text{C}$, followed by evacuation at $450\text{ }^\circ\text{C}$ for 1 h. All heating rates were kept at $5\text{ }^\circ\text{C}/\text{min}$, and an isothermal period was applied of 30 min at $100\text{ }^\circ\text{C}$.

3.5 X-Ray Photoelectron Spectroscopy.

XPS is based on the photoelectric effect: an atom absorbs a photon of certain energy, which ejects a core or valence electron of a specific binding energy with kinetic energy. Because a set of binding energies is characteristic for an element, XPS can be used to analyse the composition of samples. Almost all photoelectrons used in XPS have kinetic energies in the range of 0.2 to 1.5 keV. According to the inelastic mean free path of a photoelectron in solids, the probing depth varies between 1.5 and 6 nm, depending on its kinetic energy. Since the probing depth differs upon the element present, this must be accounted for when determining concentrations. Binding energies are not only element specific but contain chemical information as well, because the energy levels of core electrons depend slightly on the chemical state of the atom. Chemical shifts are typically in the range of 0 - 3 eV. In favourable cases, XPS can recognise how well particles are dispersed over a support. When the particles are small, almost all atoms are at the surface, while the support is covered to a large extent. In this case, XPS measures a high intensity from the particles (I_p), but a relatively low intensity for the support (I_s), resulting in a high ratio I_p/I_s . For poorly dispersed particles, on the other hand, this ratio is low. Thus the XPS intensity ratio I_p/I_s reflects the dispersion of a catalyst.

The XP spectra were recorded on a VG ESCALAB 200 spectrometer equipped with a standard dual X-ray source, of which the Al $K\alpha$ part was used, and a hemispherical analyser, connected to a five-channel detector. Measurements were done at 20 eV pass energy, and

charging was corrected for using the C *1s* signal at 84.5 eV as a reference. Since also spent catalysts were submitted to XPS analysis, charging was also corrected for using the Al *2p* and O *1s* signal, which binding energies were at 74 and 531 eV (± 0.2 eV), respectively, to check for differences in the carbon present on the surface. Spectra were fitted with the VGS program fit routine. A Shirley background subtraction was applied and Gauss-Lorentz curves were used for the fits. The samples were prepared by shutting the reactor after flushing and cooling the catalyst in a helium flow. Subsequently, the reactor was introduced into a nitrogen-filled glove box. The catalyst was crushed and mounted on an iron stub carrying an indium film. The sample was placed in a vessel filled with nitrogen for transport to the spectrometer.

3.6 Low Energy Ion Scattering.

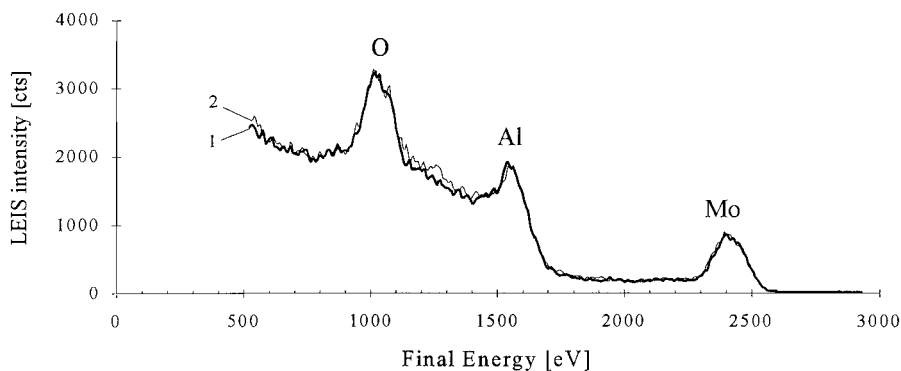
Low Energy Ion Scattering (LEIS) is a surface analysis technique that probes only the outermost atomic layer of a material. A beam of inert low energy ions, such as $^4\text{He}^+$ or $^{10}\text{Ne}^+$ (0.5 to 10 keV), collides with the surface layer of the sample and is elastically scattered. The incident ions lose kinetic energy in essentially two-body collisions, in which the energy loss depends on the energy and the mass of the primary ion, the scattering angle and the mass of the surface atom. The technique provides information about the surface composition, but is rather insensitive to the chemical state of the surface atoms [5, 6]. Analysis of the outermost layer can be of great importance in catalysis, since it concerns the layer which is in direct contact with reactants during a heterogeneous catalytic reaction.

The LEIS experiments were performed in co-operation with Dr. A.W. Denier van der Gon of the Surface and Interface Physics Group at the Eindhoven University of Technology. The newly developed ERISS was used as the ion scattering apparatus. The analyser of the ERISS is approximately 1000 times more sensitive than a conventional one. In this apparatus ion doses can be reduced to such a low level that the damage of the surface is negligible, thus enabling the performance of static LEIS. By scanning the manipulator under the beam while measuring, the effective beam spot was increased from 0.3 mm^2 (the typical cross-section of a focused ion beam) to a square of $3 \times 3 \text{ mm}$. Under these conditions it is possible to obtain spectra with ion doses less than 10^{12} ions/cm² using a beam current of typically 1 nA. The time needed for a full energy spectrum is typically 6 minutes. The ERISS is equipped with a Beam Profile Analyser to optimise the beam current and shape, which improves the reproducibility to a great extent. To prevent charging of insulating materials, a neutraliser is available to spray low energy electrons to the sample.

Samples were prepared by pressing an amount of ground sample with a load of 1600 kg into a tantalum cup ($\varnothing 1 \text{ cm}$) and subsequently loaded into the pretreatment chamber, which

is connected to the main UHV chamber. Pretreatment of fresh catalysts consisted of heating overnight in either 0.5 bar of oxygen to 275 °C, or in 0.5 bar of hydrogen to 240 °C. The spent catalyst and pure MoO₂ were heated in 0.5 bar of hydrogen to 100 °C for 2 hours. Pure MoO₃ and Al₂(MoO₄)₃ were heated in 0.5 bar of oxygen to 160 °C for 2 hours. After evacuating (until $p < 10^{-6}$ mbar) and some cooling, the sample was transported to the main chamber.

Successive spectra were obtained from scattering 3 keV He⁺ with an ion current of 5, 25 or 75 nA. The scan area was 3 x 3 mm and the measurement time was 7.2 min resulting in ion doses of 10¹⁴, 7.5·10¹⁴ or 2.5·10¹⁵ ions/cm². Assuming an atomic density on the surface of 10¹⁵ atoms/cm², this implied that at the smallest dose at a sputter yield of 10%, which is typical for heavier components, only 1% of the surface is removed by sputtering. Figure 2.1 shows two subsequent LEIS spectra of a calcined 5 wt% Mo catalyst obtained with ion doses of 1.3·10¹⁴ ions/cm². Clearly, the difference between the two spectra is negligible, which guarantees that the LEIS analysis under these conditions is representative of the undamaged surface.



★ **Figure 2.1** Two subsequent LEIS spectra of a calcined 5 wt% Mo catalyst obtained with an ion dose of 1.3·10¹⁴ ions/cm².

The possibility of using low ion doses also implies that light elements, such as adsorbed hydrogen, carbon and nitrogen, are not easily removed from the surface. Hydrogen, due to its lower mass than the primary ion, can not be detected by LEIS, and the detection of nitrogen and carbon is difficult, due to low sensitivity. Also, these lighter elements, especially hydrogen, may obscure other elements. This can cause problems with quantification by using the absolute signals. To avoid this, the samples were transported to the main chamber while still hot after a heat treatment with hydrogen.

3.7 X-ray Diffraction.

XRD is used to identify bulk phases. It is based on the elastic scattering of X-ray photons by atoms in a periodic lattice. The scattered monochromatic X-rays that are inphase give constructive interference. So, XRD is limited to crystalline particles which are not too small (> 4 nm).

Powder diffraction patterns were collected on a Philips PW 7200 X-ray powder diffractometer using Cu-K α radiation. A step scan mode was applied of $1^\circ/1000$ sec. The catalyst was crushed and kept in a nitrogen atmosphere before pressing an amount in a sample holder.

3.8 High Resolution Transmission Electron Microscopy.

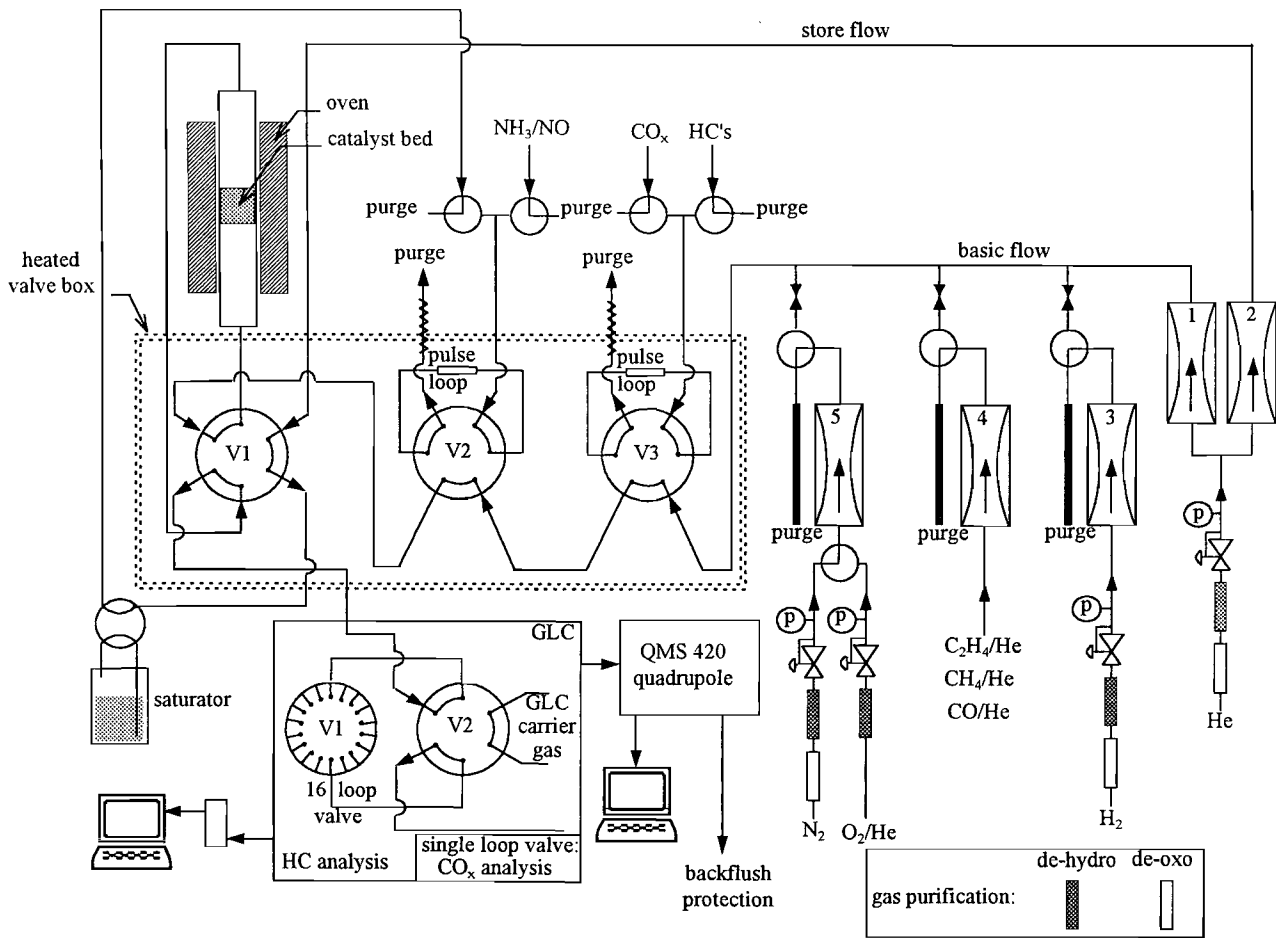
It is of crucial importance to know whether the active material is distributed uniformly on the support and the overall sample is homogeneous. HR-TEM is a very powerful technique to probe for uniformity of finely dispersed solids.

HR-TEM was performed by Dr. P.J. Kooyman of the National Centre for High Resolution Electron Microscopy at the Delft University of Technology, using a Philips CM 30 ST electron microscope with a field emission gun as the source of electrons, operated at 300 kV. Samples were mounted on a microgrid carbon polymer supported on a copper grid by placing a few droplets of a suspension of ground sample in ethanol on the grid, followed by drying at ambient conditions.

4 Outline of the TPD and TPre apparatus.

The apparatus used for temperature programmed desorption (TPD) and reaction (TPRe) experiments operated under atmospheric pressure and is shown schematically in Figure 2.2. The catalyst bed was fixed between quartz wool plugs, and the remaining empty space in the reactor was filled with splinters of quartz to enhance plug flow. The reactor, consisting of a quartz tube, was heated by a furnace which was temperature controlled by a Eurotherm. The gas flows were controlled by mass flow controllers and purified by molsieves to remove water and by BTS catalysts to remove oxygen. The helium carrier gas was splitted in a basic and a store flow, in order to prevent back diffusion of air by introducing an inert gas flow to the reactor while quantifying the reaction stream in the by-pass mode.

Pulse valve 1 served as a switch for the reactor between basic and store flow. Pulse valve 2 was used for introducing corrosive components, such as ammonia and acetonitrile and pulse valve 3 for introducing hydrocarbons (HC's) and carbon oxides (CO $_x$). The volume of all pulse loops was 100 μ l, which corresponded with 3.2 μ mol including the connection vol-



★ Figure 2.2 Schematic presentation of the TPD and TPRe apparatus.

ume. The pulse valves were placed in a furnace and kept at 125 °C to avoid hold-up by adsorption, and the tubing was also heated to 125 °C for that reason. All gasses were obtained from Hoekloos and used without further purification. The saturator was used for introducing liquid components to the gas stream for calibration purposes.

The reactor effluent was monitored on-line by a quadrupole mass spectrometer (Balzers QMG-420) which operated at ionisation potential of 70 eV and inlet pressure of $5.0 \cdot 10^{-6}$ mBar. The Balzers software program "Quadstar 420 v3.05" was used in the multiple ion detection mode, where 16 different masses could be selected. Organic compounds were analysed by introducing a sample into a Hewlett Packard 5890A gas liquid chromatograph equipped with a Poraplot Q column, 10 m * 0.32 mm i.d., and flame ionisation detector (FID). Besides on-line sampling, off-line analysis could be performed by storing 15 samples in a 16 loop valve. Inorganic compounds, such as CO_x, were analysed by introducing a sample into a Porapak N column, 6 ft * 3x2mm (e.d. x i.d.) 80/100 mesh equipped with a thermal conductivity detector (TCD). The GLC was connected to a Nelson interface and a computer for spectra assimilation.

Literature cited

- 1 Roozeboom, F., Mittelmijer-Hazeleger, M.C., Moulijn, J.A., Medema, J., de Beer, V.H.J., Gellings, P.J., *J. Phys. Chem.* **84** (1980) 2783
- 2 Wagstaff, N., Prins, R., *J. Catal.* **59** (1979) 434
- 3 Hurst, N.W., Gentry, S.J., Jones, A., McNicol, B.D., *Catal. Rev.-Sci. Eng.* **24** (1982) 233
- 4 Wimmers, O.J., Arnoldy, P., Moulijn, J.A., *J. Phys. Chem.* **90** (1986) 1331
- 5 Van Leerdam, G.C., *Ph.D. thesis*, Eindhoven University of Technology, (1991)
- 6 Brongersma, H.H., Van Leerdam, G.C., "*Fundamental Aspects of Heterogeneous Catalysis Studied by Particle Beams*" (H.H. Brongersma, R.A. van Santen, Eds.) Plenum Press, New York, (1991)

3

SUPPORTED MOLYBDENUM OXIDE CATALYSTS.

TEMPERATURE PROGRAMMED TECHNIQUES

Abstract.

The reaction of ethylene with ammonia to acetonitrile over supported molybdenum catalysts in the absence of gaseous oxygen was studied with temperature programmed desorption and reaction techniques (TPD and TPRE). Ammonia TPD experiments showed that dissociative adsorption started at 300-350 °C. The temperature where dissociative adsorption of ammonia occurred decreased with increasing molybdenum content, indicating that larger molybdenum clusters are more active towards ammonia dissociation.

It was concluded that the dissociation can occur via two mechanisms, dependent on the catalyst pretreatment. On oxygen pretreated catalysts ammonia reacted according to a condensation reaction, forming water and NH_x surface species. When pretreated in hydrogen, dissociation proceeded via the formation of hydrogen and NH_x surface species. Despite the different mechanisms of formation, the same surface species is suggested for N-insertion.

The effects of various molybdenum loading and catalyst pretreatment on the reaction of ammonia with ethylene were investigated. Using a method of sequentially introducing the reactants, it was concluded that only adding ethylene to a catalyst pre-adsorbed with ammonia led to the formation of acetonitrile. Acetonitrile formation started at temperatures exceeding 300-350 °C, similar to the temperature region of dissociative adsorption of ammonia, indicating that dissociation is needed for N-inserting surface species.

Also with this method, it was observed that competitive adsorption exists between ammonia and acetonitrile. This phenomenon revealed the existence of two sites for acetonitrile formation. One, whose concentration appeared to be independent of the Mo content, released acetonitrile at reaction temperature. The other, whose concentration increased with increasing Mo content, adsorbed strongly the acetonitrile formed at reaction temperature, which could only be removed from the catalyst surface by annealing or by competitive adsorption of ammonia.

1 Introduction.

Molybdenum oxide based catalysts can be applied in many reactions, such as methathesis, dehydrogenation, reforming and selective (amm)oxidation. In order to explain the catalytic properties of these catalysts, it is of great interest to gain insight into the relationship between structure and activity. The high dispersion, the heterogeneity and the absence of crystalline material, typical for molybdenum containing catalysts, are the main reasons that some characterisation techniques, spectroscopic or other such as XRD, can only provide limited information. The abundance of different oxidic species and the variation of the strength of the Mo-support interaction as a function of Mo content can have great influence on the catalytic activity. Temperature programmed techniques can provide useful information about these characteristics.

The temperature programmed desorption (TPD) technique was developed in 1963 by Amenomiya and Cvetanovic [1] in order to adapt the flash-filament desorption method. This technique was widely applied to study adsorption on metals, powders and particles, so materials of great interest in catalysis. An overview of this technique has been published by Amenomiya [2]. By controlled heating of the sample in time, desorption of adsorbed species will occur. Analysis of these desorbed products can lead to identification of various adsorption sites, their populations and the strength of adsorption. The TPD technique only can not distinguish the molecular nature of the adsorption site. Only the combination of TPD with other techniques, such as FTIR can achieve this.

Temperature programmed reaction (TPRe) methods have the advantage that they are applicable to real catalysts, single crystals and model catalysts and are experimentally simple and inexpensive. The method of introducing a reactant to a catalyst pre-adsorbed with the other reactant can demonstrate that the catalytic behaviour of a surface does not depend only on the presence of a particular surface configuration or structure, but also on the nature of the changes in the surface reactivity induced by adsorption of the reactants. Introducing the reactants sequentially can give for example information about the reactivity of one reactant towards the other adsorbed and/or activated reactant. By varying the temperature the region of activity of adsorbed species can be determined. In this way, the importance of co-adsorption, dissociative adsorption or a rate determining step can be determined. Also, the surface situation can be varied by varying the amount of adsorbed species. Changes in activity and selectivity can give insights in some aspects of the reaction mechanism, such as competitive adsorption effects, inhibition effects, which sites are active for side reactions, the occurrence of a dual site mechanism or poisoning.

The literature contains a number of examples where the method of introducing components sequentially has led to insight in the reaction mechanism. The study on the oxidative dehydrogenation of butene of Kung *et al.* [3] showed by adsorption of butene and butadiene sequentially on $\alpha\text{-Fe}_2\text{O}_3$ that adsorption took place on the same type of sites. By combination with TPD experiments it was suggested that combustion occurred on different sites. A study of Yang *et al.* [4] on the same system showed that pre-adsorption of oxygen had no effect on the catalytic performance, whereas the presence of gaseous oxygen drastically changed the product distribution. This indicated that adsorbed alkenes or alkene precursors must be very sensitive to attack by weakly adsorbed oxygen. An IR study on the ammoxidation of propylene over $(\text{VO})_2\text{P}_2\text{O}_7$ catalysts by Centi *et al.* [5] showed no difference between spectra of co-adsorbed propylene and ammonia, propylene and pre-adsorbed ammonia and ammonia and pre-adsorbed propylene. They concluded that a reaction between both adsorbed species occurred activated by the temperature.

This chapter describes ammonia TPD experiments on supported molybdenum catalysts and TPRE experiments with ammonia and ethylene by a sequential pulse method. The influence of the molybdenum content and different catalyst pretreatment on the activity was studied. The TPD experiments with ammonia proved the existence of two mechanisms of dissociative adsorption, dependent on the catalyst pretreatment. The TPRE technique showed the effect of competitive adsorption between acetonitrile and ammonia on the formation of acetonitrile.

2 Temperature programmed desorption of ammonia.

2.1 Introduction.

Ammonia is a relatively strongly basic molecule due to its lone pair of electrons at the nitrogen atom, which are available for donation to coordinately unsaturated sites or for accepting a proton from proton donating sites of an oxide surface. It can non-dissociatively interact with the surface in three different ways. The first involves the transfer of a proton from Brønsted acid sites of the oxide, yielding ammonium ions. The second involves the coordination of ammonia through the lone pair of electrons to co-ordinately unsaturated sites, *i.e.* to Lewis acid sites. The third possible interaction is via hydrogen bonding, which may involve the interaction of the nitrogen with the hydroxyl groups on the surface or of the hydrogen with the surface oxygen or the surface oxygen atom of hydroxyl groups. Also dissociative adsorption is known to occur on some M_xO_y surfaces [6], yielding surface M-NH_2 and M-OH species. In the ammoxidation mechanism of propylene over bismuth

molybdate catalysts proposed by Grasselli [7] ammonia is suggested to adsorb dissociatively according to a condensation reaction forming M=N-H surface species, while water desorbs.

2.2 Experimental procedure.

The preparation of supported molybdenum catalysts is described in chapter 2, section 2.1 and 2.2, and the apparatus used for TPD experiments is described in section 4. Prior to the adsorption of ammonia, an exact amount of 0.2 g catalyst was heated in a flow of 10 vol% oxygen in helium to 550 °C and held there for 10 h, or in a flow of 10 vol% hydrogen in helium to 650 °C and held there for 10 h. To remove water slowly, an isothermal period of 30 min at 130 °C was applied and the heating rate was kept at 5 °C/min. The support was heated in a flow of 10 vol% oxygen in helium to 400 °C and held there for 1 h. Adsorption was at 50 °C on the support, and at 350 °C on the catalysts. Ammonia was introduced by pulses until an increase of the $m/e = 17$ was observed by the mass spectrometer, implying saturation of the catalyst, followed by flushing with helium for 1 h. Subsequently, a TPD with 5 °C/min to 650 °C in a helium flow of 20 Nml/min was performed.

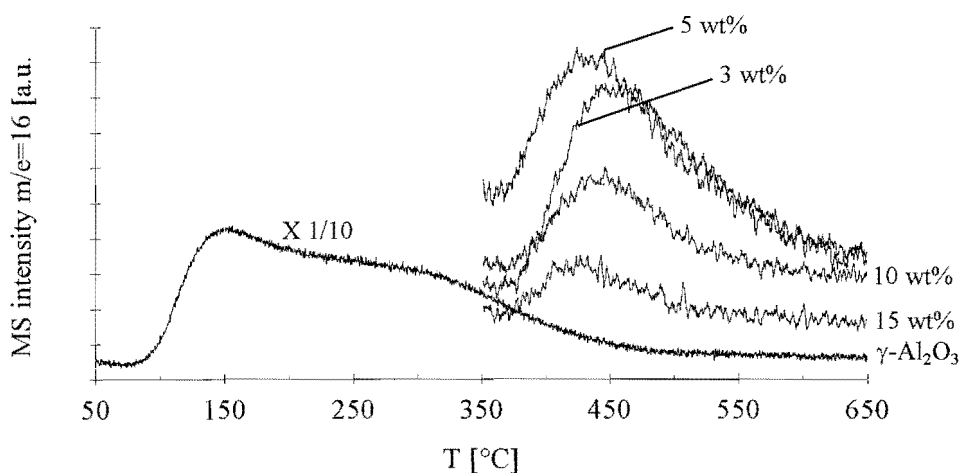
2.3 Results and discussion.

Alumina, due to its acidity, is known to adsorb a large amount of ammonia. Adsorption at 50 °C resulted in a characteristic, asymmetric desorption pattern with an extended tail, which is well-known for energetically heterogeneous surfaces. Two TPD peaks were observed: a low temperature peak at 150 °C and a high temperature peak at 320 °C (see Figure 3.1 and 3.2). This indicates that ammonia can adsorb on alumina sites with a different activation energy for desorption, where the low temperature peak corresponds with a weakly acid site. The presence of different sites was already observed by Amenomiya *et al.* [1] by TPD experiments of ethylene on alumina. Also IR spectra of CO adsorption showed the presence of different sites on γ -Al₂O₃ which were described as co-ordinately unsaturated aluminium ions [8]. These sites can be generated by removal of one oxygen ion from the coordination sphere of a tetrahedron or an octahedron, resulting in Lewis acid centres of different strength.

When ammonia was adsorbed on the molybdenum catalysts at temperatures up to 300 °C, the adsorption on the support interfered significantly with adsorption on the molybdenum. For this reason the adsorption temperature for the catalysts was kept at 350 °C. Another argument for applying a high adsorption temperature is that this temperature is in the temperature region of 300-460 °C applied in ammoxidation reactions [9]. So it is in

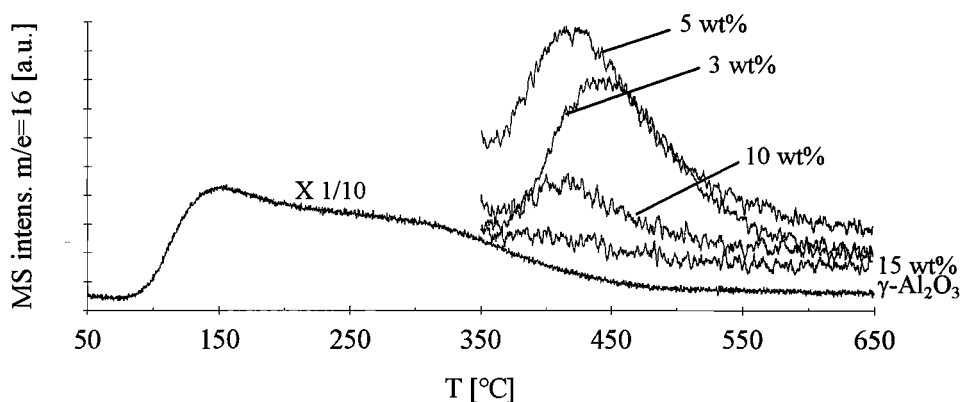
principle possible to find correlations between TPD experiments and the activity of various catalysts towards ammonia activation.

Although the amount of ammonia added until saturation, to oxygen pretreated catalysts at 350 °C, was of the same order of magnitude ($\sim 30 \mu\text{mol/g}$ catalyst), the amount of ammonia desorbed during TPD decreased with increasing molybdenum content (see Figure 3.1). Since the fraction of alumina decreases with increasing Mo content and at 350 °C the TPD curve of $\gamma\text{-Al}_2\text{O}_3$ still showed some tail of ammonia desorption, it is likely that the ammonia desorption originated from the uncovered alumina surface.



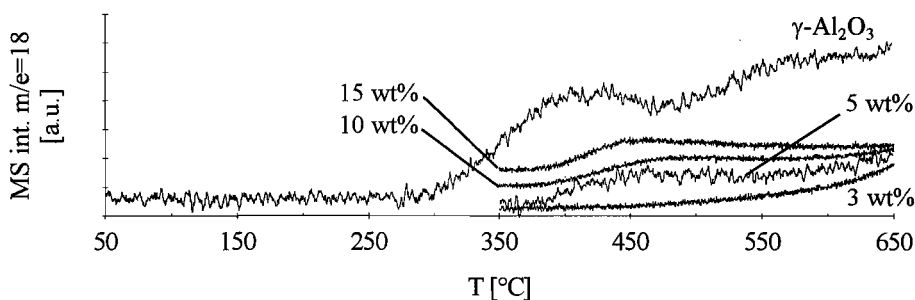
★ **Figure 3.1** TPD of ammonia after adsorption at 50 °C on $\gamma\text{-Al}_2\text{O}_3$ and at 350 °C on various oxygen pretreated Mo/ $\gamma\text{-Al}_2\text{O}_3$ catalysts.

Although the amount of ammonia added until saturation at 350 °C was higher when pretreated in hydrogen and increased with increasing Mo content (60–90 μmol), the same trend was observed (see Figure 3.2). Also a decrease in the amount of ammonia desorption was observed with increasing molybdenum content, although the differences were more conspicuous, considering the gap between 3, 5 and 10, 15 wt% Mo. The 15 wt% Mo even showed almost no ammonia desorption during TPD, suggesting that this catalyst did not adsorb ammonia at all, and that the maximum temperature of desorption is below 350 °C.



★ **Figure 3.2** TPD of ammonia after adsorption at 50 °C on $\gamma\text{-Al}_2\text{O}_3$ and at 350 °C on various hydrogen pretreated $\text{Mo}/\gamma\text{-Al}_2\text{O}_3$ catalysts.

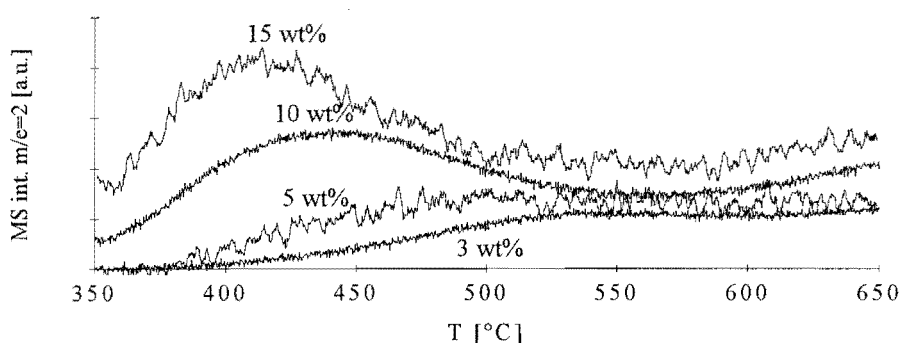
Considering the TPD of other species after ammonia adsorption, striking differences between both pretreatments were observed. When pretreated in oxygen, water desorbed during TPD, suggesting dissociative adsorption (see Figure 3.3). Water was already observed during ammonia adsorption at molybdenum content exceeding 5 wt%, and increased with increasing Mo content. The support showed also desorption of water via two maxima (at 400 and 600 °C), but these maxima did not coincide with the catalysts. At low molybdenum content (3 wt%) no maximum in water desorption is seen, indicating that, if water is formed while adsorbing ammonia, it is strongly adsorbed. At higher molybdenum content, clear



★ **Figure 3.3** TPD of water after adsorption of ammonia at 50 °C on $\gamma\text{-Al}_2\text{O}_3$ and at 350 °C on various oxygen pretreated $\text{Mo}/\gamma\text{-Al}_2\text{O}_3$ catalysts.

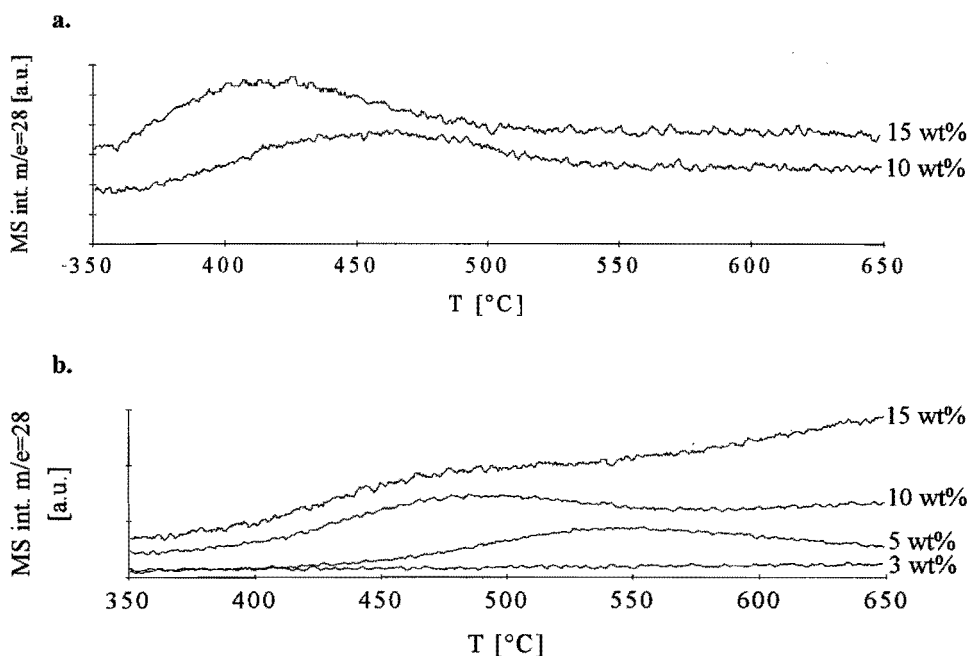
maxima were observed shifting from 490 to 440 °C at increasing molybdenum content. The 15 wt% Mo catalyst was coloured blue at the end of the TPD experiment, which can be ascribed to the formation of $\text{Mo}_2\text{O}_5 \cdot \text{H}_2\text{O}$. This indicates that some reduction of Mo(VI) to Mo(V) occurred.

When pretreated in hydrogen, no desorption of water was observed at all, but instead hydrogen desorbed during TPD (see Figure 3.4). The amount increased with increasing molybdenum content, while the peak maximum shifted to a lower temperature. An increasing amount of hydrogen at increasing molybdenum content was also observed during ammonia adsorption. It is likely to originate from the dissociation of ammonia, but it cannot be excluded that it originates from the catalyst pretreatment.



★ **Figure 3.4** TPD of hydrogen after adsorption of ammonia at 350 °C on various hydrogen pretreated Mo/ γ - Al_2O_3 catalysts.

The desorption of nitrogen forms the best indication that ammonia dissociation had occurred. This was not only observed on all hydrogen pretreated but also on oxygen pretreated catalysts with 10 and 15 wt% Mo (see Figure 3.5a and b). Also, the peak maximum shifted to a lower temperature with increasing molybdenum content. At lower molybdenum content, the molybdenum is supposed to be present as isolated, tetrahedrally coordinated species, whereas at higher loading octahedrally coordinated polymeric species are formed. Apparently, the isolated tetrahedrally coordinated molybdenum is less active for the dissociation of ammonia (a peak maximum at a higher temperature) than the octahedrally coordinated polymeric species, which have less interaction with the support. The octahedrally coordinated molybdenum species present at higher molybdenum content are more active towards dissociation and this effect is more dominant on hydrogen pretreated than on oxygen



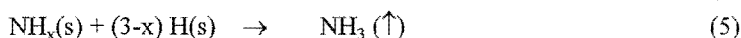
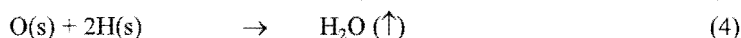
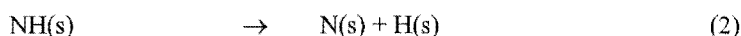
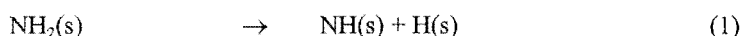
★ **Figure 3.5** TPD of nitrogen after adsorption of ammonia 350 °C on oxygen pretreated (a) and hydrogen pretreated (b) Mo/ γ -Al₂O₃ catalysts.

pretreated catalysts. It is likely that the increasing recombination probability also plays an important role, as proposed by de Boer *et al.* [10] When it is assumed that agglomeration occurs upon hydrogen pretreatment, it is also explained that hydrogen pretreated catalysts are more active towards the dissociation of ammonia. Only, nitrogen is more strongly adsorbed on hydrogen pretreated catalysts, considering the higher desorption temperature.

We thus propose that dissociative adsorption of ammonia takes place via different mechanisms dependent on the catalyst pretreatment. When oxygen pretreated, dissociation proceeds through a condensation reaction, forming water, surface NH_x (x = 1,2) and probably surface OH. This is conform the first step in the ammoxidation mechanism of propylene proposed by Grasselli *et al.* [7] During TPD, water and nitrogen desorbed almost simultaneously, suggesting that the surface NH_x dissociates into N(s) and OH(s) (where (s) stands for surface species). When pretreated with hydrogen, the ammonia is dissociated into H(s) and NH_x (x = 0-2), where a part of H(s) recombines to hydrogen. Nitrogen desorbs at a higher temperature than hydrogen. This indicates that when these NH_x species dissociate (when x ≠ 0), the nitrogen is bonded more strongly to a reduced molybdenum surface. The increasing recombination possibility with increasing Mo content causes the shift in

desorption temperature to a lower value. When $x = 0$, a surface nitride is formed, where the hydrogen desorbs at two temperatures.

These observations are in agreement with the mechanism proposed by Aruga *et al.* [11], derived from a TPD and a LEED study on the adsorption and reaction of ammonia on clean and oxygen-precovered Mo(112) surfaces. On a clean Mo surface ammonia dissociated immediately to form N(s) and H(s) at the adsorption temperature of 57 °C. At high exposures desorption of hydrogen was observed. The hydrogen that remained on the surface (H(s)) desorbed at 157 °C. No desorption of ammonia was observed at any NH₃ exposures and nitrogen desorbed at high temperatures (767 °C). On surfaces precovered with oxygen a different behaviour was observed. Although the formation of NH_x ($x = 1,2$) or OH could not be excluded, it was suggested that in the region of $\theta_O \leq 0.8$ also complete dissociation of ammonia occurred. It was also shown that N and O atoms competed with each other to occupy the same or neighbouring adsorption sites. At $\theta_O \geq 0.8$, besides ammonia desorption, the desorption of hydrogen and water was observed simultaneously at 377 °C. From this it was concluded that NH_x ($x = 1-3$) species were present on the surface. Although it could not be established whether the surface species were composed of a mixture of NH(s), NH₂(s) and NH₃(s) or mainly NH₂(s), the latter was suggested to be correct. The following scheme was proposed to occur at 377 °C at $\theta_O \geq 0.8$, where NH₂ species are presumed to be formed immediately after NH₃ adsorption at 57 °C or during the annealing to below 177 °C (see Scheme 3.1):



★ **Scheme 3.1** Proposed surface reactions of ammonia on a Mo(112) surface precovered with oxygen; $\theta_O \geq 0.8$ [11].

Also mentioned by the authors was the possibility of the formation of an OH(s) intermediate by the reaction of NH_x(s) with and O(s) during the annealing to 377 °C. At high oxygen precoverage, the strong interaction of the oxygen atoms results in MoO₂ chains, which can be compared to the hydrogen pretreated supported molybdenum studied in this work. So, it is possible that reactions (1), (2) and (3) can also occur on the catalyst surface, because hydrogen desorbed at lower temperature than nitrogen. This leads to the same conclusion drawn by Aruga [11], that the N-containing surface species are very stable, which makes

them suitable to participate in a variety of catalytic reaction pathways with co-adsorbed species. The formation of surface hydroxyls is also very likely for oxygen pretreated catalysts. Although desorption of NH_3 is observed from the catalyst surface, it is dubious to ascribe this to reaction (5). The question is, if different surface species exist on oxygen and hydrogen pretreated catalysts, which species is active as an N-inserting one.

Ammonia TPD after adsorption at 350 °C on the oxygen pretreated 5 wt% Mo/SiO₂ showed different behaviour from its $\gamma\text{-Al}_2\text{O}_3$ supported analogue. The temperature at which maximum desorption of hydrogen and nitrogen occurred was 480 and 520 °C respectively. This indicates that dissociation of ammonia occurred, which was not observed on the 5 wt% Mo/ $\gamma\text{-Al}_2\text{O}_3$. It was already concluded that particle size and activity towards complete NH_3 dissociation are related. Apparently, the molybdenum is better dispersed on alumina, which is extensively described in the literature [12]. The poor dispersion of MoO₃/SiO₂ catalysts is caused by a lack of adsorption of Mo(VI) on SiO₂ during impregnation [13, 14], resulting in precipitation of crystallites while drying.

When the 5 wt% Mo/SiO₂ is submitted to TPSR after ammonia adsorption, only desorption of nitrogen and water occurred. Apparently, on molybdenum the dissociated ammonia can not be hydrogenated to ammonia, due to the high stability of the NH_x species on a molybdate surface. Although, it cannot be excluded that, due to a surface that is fully covered with NH_x , the catalyst is not capable of dissociating hydrogen, which is a necessary step in the hydrogenation mechanism.

3 Temperature programmed reaction of ethylene and ammonia: the method of sequentially introducing of the reactants.

3.1 Experimental procedure.

The preparation of the supported molybdenum catalysts is described in chapter 2, section 2.1 and 2.2. The apparatus used for the TPRE experiments is described in section 4. An exact amount of 1.0 gram catalyst was placed in the reactor. Prior to reaction, the catalyst was subjected to an oxidative treatment, consisting of heating in a flow of 5 vol% oxygen in helium to 500 °C and held there for 1 h, or reductive treatment, consisting of heating in a flow of 10 vol% hydrogen in helium to 700 °C and held there for 5 min. In order to remove water slowly, an isothermal period was applied at 130 °C for 15 min. The total flow was kept at 20 Nml/min and the heating rate at 5 °C/min. After cooling in helium to reaction temperature, the reactants were sequentially introduced by pulses to the total helium flow of

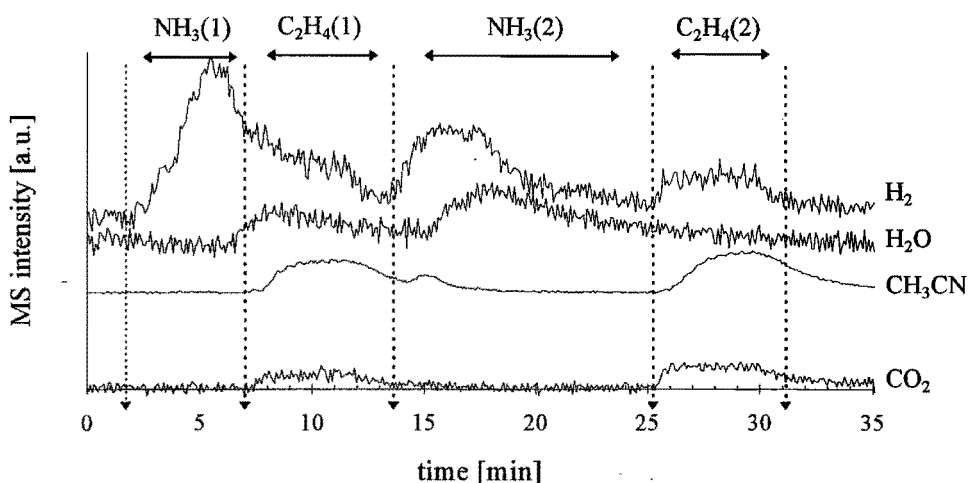
23 Nml/min (~ 3 pulses/min; volume of one pulse: 3.2 μ mol). First, ammonia was introduced at reaction temperature until an increase was observed of the mass spectrometer signal $m/e=17$, indicating that the catalyst was saturated, followed by flushing in helium for 1 h, removing all gaseous and weakly adsorbed ammonia. Subsequently, 25 pulses of ethylene (total amount of 80 μ mol) were introduced at the same temperature. After flushing in helium for 10 minutes a temperature programmed desorption (TPD) was performed to 700 °C with a heating rate of 10 °C/min. The reaction temperature window applied was 300-550 °C and the catalysts with molybdenum content 3, 5, 15 wt% were submitted to this procedure. For comparison a 5 wt% Mo on SiO₂ catalyst was tested under the same conditions. The conversion of ethylene, selectivities and the yield of acetonitrile were calculated using the MS and GC data during the period of introducing ethylene. Since no TCD was available at that time, no accurate amount of CO could be determined.

3.2 Results and discussion.

3.2-1 The influence of the sequence of introducing reactants.

When the method of pulsing was applied by introducing ammonia and ethylene at various conditions, some interesting trends were observed. Starting at room temperature with only ethylene, no detectable interaction with the catalyst surface was observed. At temperatures exceeding 300 °C, the calcined catalysts started with some combustion, whereas on hydrogen pretreated catalysts hydrogenation started to occur. Reduced molybdenum catalysts are known for their hydrogenation capacity. According to Lombardo *et al.* [15] two types of adsorbed hydrogen can exist on the surface: a weak reversible and a strong irreversible one. Since our catalysts were flushed with helium at high temperature after hydrogen treatment, it is likely that only the strong irreversible type was present, obviously resulting in hydrogenation at higher temperatures.

On a catalyst pre-adsorbed with ammonia, no N-containing organic compounds were detected while pulsing ethylene up to 300-350 °C. In this temperature region ammonia starts to adsorb dissociatively on the molybdenum surface (*vide supra*), indicating that dissociative adsorption is necessary for the N-insertion, which is known in ammoxidation reactions [7]. In Figure 3.6 the formation of acetonitrile, water, hydrogen and CO₂ is plotted as a function of reactant pulsed at 425 °C. Starting with introducing ammonia to a fresh catalyst, a large amount of hydrogen desorbed, suggesting dissociative adsorption. Clearly it can be seen that only a significant amount of acetonitrile was formed while pulsing ethylene. After switching back to pulses of ammonia, a little acetonitrile was formed only in the beginning of period



★ **Figure 3.6** The formation of acetonitrile ($m/e=41$), water ($m/e=18$), hydrogen ($m/e=2$) and CO_2 ($m/e=44$) during subsequent periods of reactant pulsed to a hydrogen pretreated 5 wt% Mo/SiO_2 catalyst at 425°C .

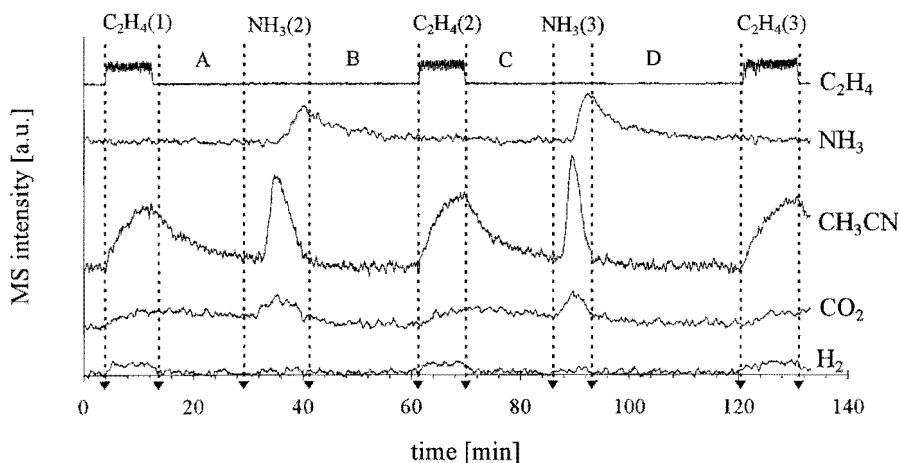
$\text{NH}_3(2)$, indicating that acetonitrile was pushed from the catalyst surface by ammonia due to competitive adsorption.

Water was released only during the first period of ethylene and the second period of ammonia pulses. Previously it was concluded that the activation of ammonia can proceed via both the release of hydrogen and water. Apparently, after a reductive treatment the two mechanisms can operate simultaneously, when an amount of removable lattice oxygen is still present. Clearly, the formation of CO_2 also indicated that the removable lattice oxygen was not depleted completely during the reductive pretreatment.

When ethylene was introduced to a fresh catalyst at a temperature where N-insertion was expected, followed by pulses of ammonia, *no* acetonitrile was formed. Apparently, due to a low interaction with the catalyst surface (*vide supra*), ethylene desorbed before it could react with the activated ammonia.

When the experimental procedure mentioned above was applied to the hydrogen pretreated 5 wt% $\text{Mo}/\gamma\text{-Al}_2\text{O}_3$ catalyst at 460°C , similarities to its SiO_2 counterpart were observed (see Figure 3.7). Again, the sequence of pulsing ammonia prior to ethylene appeared to be crucial for the formation of acetonitrile. When the pulses of ethylene were discontinued, the acetonitrile formation dropped sharply (see Figure 3.7; period A and C). When the switch was made from ethylene to ammonia, a sharp peak was observed in the

acetonitrile formation (see period $\text{NH}_3(2)$ and $\text{NH}_3(3)$). The maximum of acetonitrile coincided with the sharp increase of the ammonia signal, suggesting again that competitive adsorption exists between acetonitrile and ammonia. In contrast with the silica supported catalyst, ammonia showed also competitive adsorption with CO_2 , which is known to have a stronger interaction with alumina, forming surface carbonates. The amount of acetonitrile in these periods was much larger for the alumina supported catalyst, indicating that the acetonitrile formed is adsorbed more strongly on the surface. This is again an indication that the molybdenum is better dispersed on the alumina (*vide supra*). No water formation was observed, suggesting that the dissociation of ammonia occurred only via the release of hydrogen.

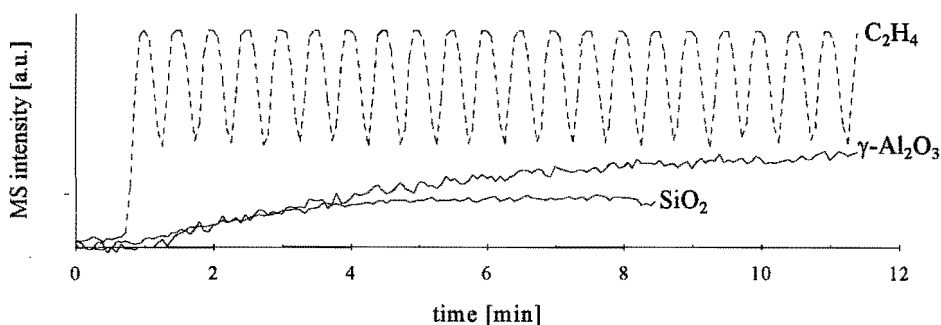


★ **Figure 3.7** The formation of acetonitrile ($m/e=41$), hydrogen ($m/e=2$) and CO_2 ($m/e=44$) as during subsequent periods of reactant pulsed at 460°C on a hydrogen pretreated 5 wt% $\text{Mo}/\gamma\text{-Al}_2\text{O}_3$ catalyst. Ammonia was pre-adsorbed (" $\text{NH}_3(1)$ " not shown). Periods A-D: only a He flow is introduced to the catalyst.

Since the sequence of introducing ammonia first, followed by ethylene is crucial for the formation of acetonitrile, this sequence is applied to all following pulse experiments.

3.2-2 Silica versus alumina support.

When the 5 wt% Mo/SiO_2 is compared to its $\gamma\text{-Al}_2\text{O}_3$ supported counterpart, similarities are found in the reactivity. Figure 3.8 shows the formation of acetonitrile on a silica and alumina supported molybdenum catalyst under identical reaction conditions of pulsing ethylene to a catalyst pre-adsorbed with ammonia at 425°C . On the $\gamma\text{-Al}_2\text{O}_3$ supported molybdenum catalyst more acetonitrile was formed, compared to its SiO_2 supported counterpart.

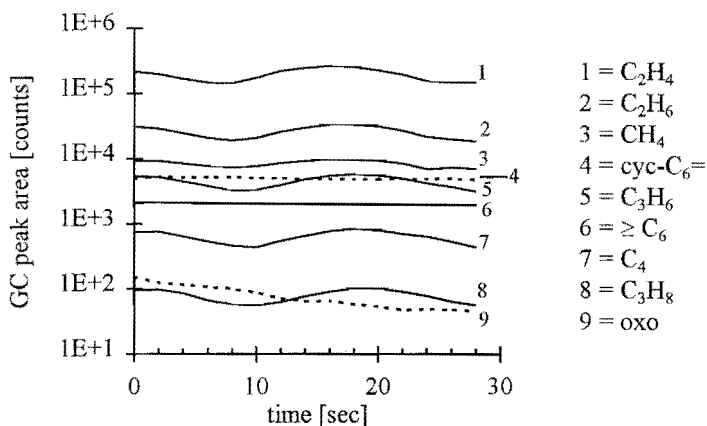


★ **Figure 3.8** The formation of acetonitrile ($m/e=41$, solid lines) on hydrogen pretreated 5 wt% Mo on $\gamma\text{-Al}_2\text{O}_3$ and SiO_2 catalysts while pulsing ethylene ($m/e=28$, dashed line) after adsorption of NH_3 at 425°C .

It was already stated that the molybdenum is better dispersed on alumina. Obviously, this has great consequences for the catalytic performance. Because of the poor catalytic performance of the silica supported catalyst, and the preparation of highly dispersed molybdenum on silica is a complicated project [14], only $\gamma\text{-Al}_2\text{O}_3$ supported molybdenum catalysts will be considered after this section.

3.2-3 Formation of organic products during a pulse of ethylene.

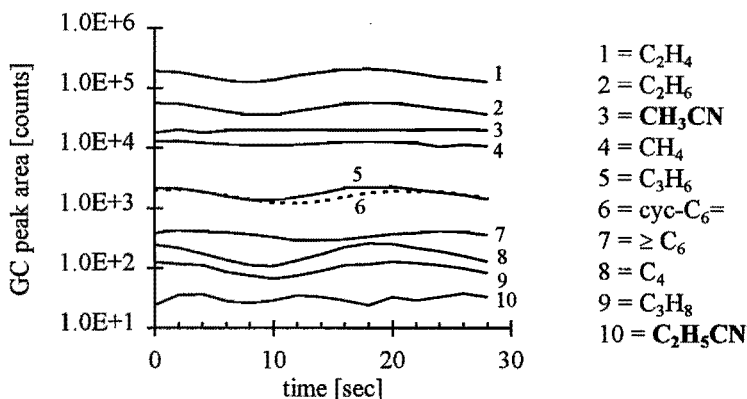
While introducing a pulse of ethylene, the formation of organic compounds at higher temperatures could be monitored more closely. The effect of pre-adsorbing ammonia was studied by comparing the product distribution of a fresh catalyst and a catalyst pre-adsorbed with ammonia. By taking a GC sample every 2 seconds the profile of 1.5 pulse of ethylene with corresponding products could be determined. Figure 3.9 and 3.10 show this profile of a hydrogen pretreated 5 wt% Mo/ $\gamma\text{-Al}_2\text{O}_3$ catalyst at 460°C without and with pre-adsorbed ammonia. Without ammonia pre-adsorption, ethylene was converted into a variety of products (see Figure 3.9). Both hydrogenation and oligomerization were predominating. In literature reduced molybdenum catalysts are known for their hydrogenation, homologation and metathesis capacity of olefines [15,16]. All hydrocarbons up to C_4 followed the pattern of the ethylene pulse exactly with only little delay, indicating that the formation and desorption of these components is fast. The higher hydrocarbons showed no pulse profile, so formation and/or desorption is slower. The cyclic C_6 compound is most likely cyclohexadiene. Only some oxidation was observed, producing CO (not shown in Figure 3.9)



★ **Figure 3.9** The profile of 1.5 pulse of ethylene with corresponding organic products for the hydrogen pretreated 5 wt% Mo catalyst at 460 °C without pre-adsorbing ammonia. All areas are relative to the intensity of ethylene.

and an unknown product, probably acrolein or propanal. The oxygen containing component showed a slow decrease in formation, indicating that the amount of removable lattice oxygen was limited, which is expected, since the catalyst was submitted to a reductive pretreatment.

When ammonia was pre-adsorbed, no oxygen containing organic products were observed (see Figure 3.10), only some CO (not shown in Figure 3.10). This implies that after a hydrogen pretreatment still lattice oxygen can be removed by ammonia. Instead, besides acetonitrile, acrylonitrile or propionitrile was detected, indicating that O-inserting species were replaced by N-inserting species. No pulse profile was observed due to slow desorption and/or formation of the product. In contrast with the pulse experiment where ethylene was introduced to a fresh catalyst, all hydrocarbons showed a pulse profile when ammonia was pre-adsorbed. The delay increased with increasing molecular weight. Besides hydrogenation, the nitrile formation dominated over oligomerization. This indicates that a part of the sites used for the oligomerization of ethylene are now occupied by N-inserting species. In both cases the formation of propylene and cyclohexadiene seem to be related, suggesting that the latter is formed out of two propylene molecules. This was confirmed by similar experiments repeated at increasing temperature, where clearly the formation of propylene went through a maximum which coincided with a strong increase of the amount of cyclohexadiene. The amount of both components is less when ammonia is pre-adsorbed, probably due to the formation of propionitrile out of propylene.



★ **Figure 3.10** The profile of 1.5 pulse of ethylene with corresponding organic products for the hydrogen pretreated 5 wt% Mo catalyst at 460 °C pre-adsorbed with ammonia. All areas are relative to the intensity of ethylene.

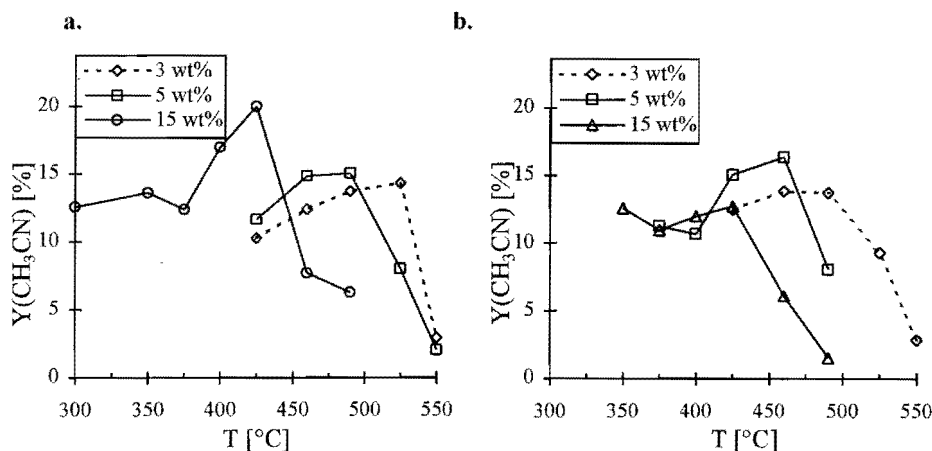
The two experiments described in this section show clearly the possibility that both primary and secondary reactions can occur on the reduced molybdenum surface, yielding a rather complex product distribution. Considered that various catalytic sites are present on these catalysts, one might understand the enormous amount of research done on molybdenum containing catalysts, due to the wide variety of reactions they catalyze.

3.2-4 γ -Al₂O₃ supported Mo catalysts with various loading.

Different pretreated catalysts with various molybdenum content were submitted to the sequential pulse method at different reaction temperatures. Ammonia was pre-adsorbed at the same temperature at which ethylene was introduced. Only the catalytic activity during the period of ethylene pulses was considered. All catalysts showed an increase in conversion of ethylene at increasing reaction temperature, while the selectivity towards acetonitrile decreased. At temperatures exceeding the optimum, the complete dissociation of ammonia started to dominate, resulting in the desorption and nitrogen, this way terminating the N-insertion. Consequently, a strong increase of the formation of hydrocarbons and CO_x occurred, resulting in an optimum of the yield versus reaction temperature, which is shown in Figure 3.11 a and b.

The 3 wt% Mo catalyst (dashed line in Figure 3.11 a and b) showed a catalytic activity which was independent of the pretreatment. At higher molybdenum content, the conversion

of ethylene for the hydrogen pretreated catalysts was significantly higher than for the oxygen pretreated ones. Nevertheless, the yield of acetonitrile did not increase on the hydrogen pretreated catalysts, as the selectivity decreased sharply.



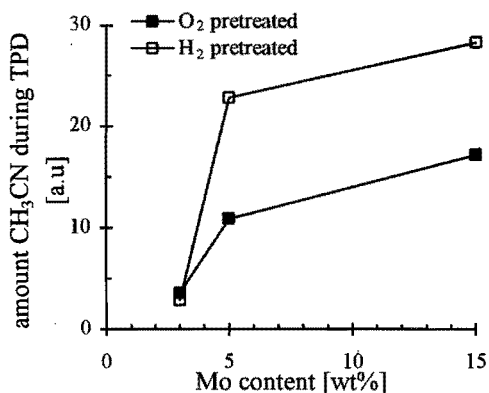
★ **Figure 3.11** The yield of acetonitrile versus reaction temperature for oxygen (a) and hydrogen (b) pretreated catalysts with various molybdenum content pre-adsorbed with NH_3 while pulsing ethylene.

Considering the temperature at which an optimum yield of acetonitrile is obtained, a shift to a lower value is observed at increasing molybdenum content, similar to the dissociative adsorption of ammonia, discussed in section 2.3. Overall, the optimum temperature for hydrogen pretreated catalysts is lower than when pretreated with oxygen, but the shift in optimum temperature with increasing Mo content is of the same magnitude: 490-400 °C and 525-425 °C (see Figure 3.11a and b) for hydrogen and oxygen pretreated catalysts respectively. As concluded earlier, large molybdenum clusters are more active towards ammonia dissociation, resulting in a N-insertion at a lower temperature. It was found that this effect was more conspicuous for hydrogen pretreated catalysts, due to the agglomeration induced by the hydrogen pretreatment.

Most remarkable is the fact that this maximum yield did not increase at increasing molybdenum content. Apparently a limiting step in the formation of acetonitrile is operative, which is independent of the molybdenum content. The experiment where the pulse profile of the reaction stream was monitored (see section 3.2-3) already showed that the formation or the desorption of acetonitrile is slow. Also from the experiments, where alternatively ammonia and ethylene was pulsed (see section 3.2-1) it was suggested that NH_3 displaces

acetonitrile from the catalyst surface. So, it is likely that desorption of acetonitrile is very slow, and from the acetonitrile formed, a large part will remain on the surface. But if desorption of acetonitrile is the rate determining step, still an increase of the acetonitrile formation with increasing molybdenum content is to be expected. This suggests that two sites are responsible for acetonitrile formation: one whose concentration is independent of the molybdenum content and slowly releases acetonitrile, and a second, whose concentration increases at increasing molybdenum content, and only releases acetonitrile by annealing or by competitive adsorption with ammonia. This is made plausible when the amounts of acetonitrile that desorbed during the TPD performed after pulsing ethylene at the optimum temperature are compared at various molybdenum content, which is shown in Figure 3.12. Clearly it can be seen that the amount increased with increasing molybdenum content, indicating that indeed more N-inserting sites were generated, but a part of the desired product remained adsorbed more strongly.

Competitive adsorption phenomena are known to influence ammoxidation reactions. Centi *et al.* [17] observed with the ammoxidation of propane over $(VO)_2P_2O_7$ catalysts competitive adsorption between ammonia and oxygen and their contemporaneous presence is required for the formation of acrylonitrile. So, an optimum will exist between oxygen and ammonia coverage distribution and selectivity. Under flow conditions, a high coverage of ammonia suppressed combustion, this way increasing the selectivity towards products of partial oxidation.



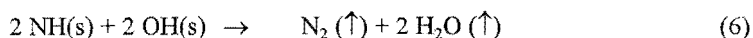
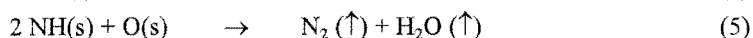
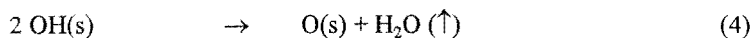
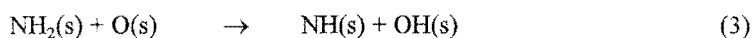
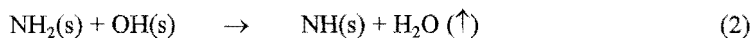
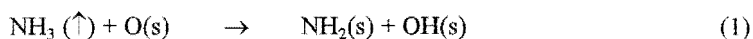
★ Figure 3.12 The amount of acetonitrile desorbing from various Mo/ γ -Al₂O₃ catalysts during TPD after pulsing ammonia, followed by ethylene pulses at the optimum temperature, derived from Figure 3.11a and b.

4 Proposed N-containing (reactive) surface species.

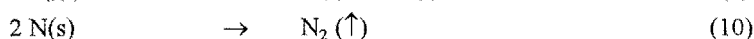
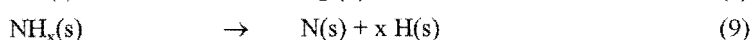
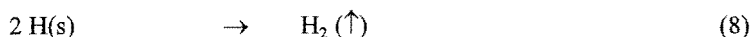
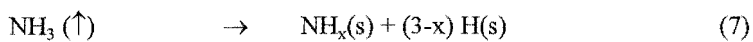
From the ammonia TPD experiments it was concluded that ammonia can dissociatively adsorb on a molybdenum oxide surface via two mechanisms, dependent on the catalyst pretreatment. On oxygen pretreated catalysts the dissociation occurs according to a condensation reaction, forming water and NH_x (x = 1,2) surface species. Since during TPD

besides nitrogen, water desorbed simultaneously, surface hydroxyl groups were also expected to be present or to be formed while annealing. When pretreated with hydrogen, ammonia is dissociated into hydrogen and NH_x ($x = 0-2$) surface species. During TPD, the nitrogen desorbed at higher temperature than hydrogen, indicating that after dissociation of NH_x (if $x \neq 0$) the nitrogen is more strongly bonded to the surface, or, if $x=0$, the H(s) recombines and desorbs at a lower temperature. For both pretreatments the following reaction schemes are proposed (see Scheme 3.2):

Calcined catalysts:



Reduced catalysts:



★ **Scheme 3.2** Proposed surface reactions of ammonia at elevated temperatures on calcined and reduced supported molybdenum catalysts

At intermediate adsorption temperatures (300-350 °C), both NH_2 and NH species can be present on calcined catalysts. At lower molybdenum content (< 5 wt%) no desorption of water and nitrogen was observed, so reactions (1) and (3) of Scheme 3.2 are suggested to occur. At higher molybdenum content both water and nitrogen adsorb, which can be ascribed to reactions (2), (4)-(6), thus decreasing, perhaps to zero, the amount of NH_2 species. During TPD still water and nitrogen desorbed simultaneously, so NH surface species dissociated according to reaction (5) and/or (6). The unknown factor in this scheme for calcined catalysts is the role of OH(s) and O(s) . Also the number of Mo centres involved in this scheme will not be limited to one.

For hydrogen pretreated catalysts, Scheme 3.2 is based on the assumption that no surface OH is formed, due to the absence of water desorption. But it can not be excluded that surface

OH may also play a role when pretreated with hydrogen. At both intermediate adsorption temperatures and molybdenum content (5 wt%) hydrogen desorbed already, suggesting reaction (7) and (8) to occur. Reaction (9) is suggested to occur during TPD prior to reaction (10), which proceeds at a higher temperature than reaction (8).

Applying the method of sequentially introducing ammonia and ethylene, the sequence was found to be crucial for the formation of acetonitrile. Only ammonia followed by ethylene will produce acetonitrile, for both pretreatments applied. The temperature where a maximum yield was obtained shifted to a lower value at increasing molybdenum content, due a higher activity towards complete ammonia dissociation at higher molybdenum content. The maximum yield of acetonitrile was fixed to an upper limit independent of the molybdenum content, due to strong adsorption on the catalyst surface. This upper limit is attributed to an active site whose concentration is independent of the molybdenum content. The presence of a second site for acetonitrile formation was suggested, whose concentration increased at increasing molybdenum content, but a release of the desired product only occurred at annealing or when ammonia was present in the reaction stream.

Both pretreatments yielded acetonitrile in the same order of magnitude, but in a slightly different temperature region. For calcined catalysts the temperature where maximum yield is obtained coincides with the temperature region where water and nitrogen desorb during ammonia TPD. For hydrogen pretreated catalysts with molybdenum content exceeding 3 wt%, the optimum temperature for reaction coincides with the temperature region of hydrogen desorption during ammonia TPD. So, where N(s) is suggested to be most abundant on this surface, the rate of N-insertion has decreased sharply. Considering again Scheme 3.2, it is likely that NH is the main N-inserting species for both pretreatments. It was already suggested in 1982 by Grasselli *et al.* [18] that surface NH₂ can exist at lower temperatures (< 400 °C) via the formation of coordinately saturated molybdenum. However, these species were considered to be a poison for the active sites. Since at lower temperatures still N-insertion occurred, reaction (3) of Scheme 3.2 might be an equilibrium, or NH₂ species can also serve as N-inserting species for ethylene.

5 Conclusions.

The dissociative adsorption of ammonia on supported molybdenum catalysts was proposed to proceed via two mechanisms, dependent on the pretreatment. When adsorbing ammonia at higher temperatures on oxygen pretreated catalysts, ammonia dissociated according to a condensation reaction, forming water and NH_x surface species. When

pretreated with hydrogen, the dissociation occurred by the release of hydrogen and forming surface NH_x . Although different surface species are present, the N-inserting species is considered most likely to be $=\text{NH}$ for both pretreatments. The molybdenum content is an important parameter for the dissociative adsorption of ammonia. Catalysts with a higher Mo content are more active towards dissociation, which can be attributed to the polymeric octahedrally coordinated Mo species known to be present at higher coverage. This effect is more dominant for hydrogen pretreated catalysts, which can be attributed to the agglomeration of these polymeric octahedral coordinated Mo species induced by the reductive treatment. When NH_x dissociates while annealing, the nitrogen is more strongly bonded to a reduced molybdenum structure than on a calcined one. This suggests that the different pretreatments applied result in a different surface structure present on the alumina.

Two sites were suggested to be present for the formation of acetonitrile. One site, whose concentration appeared to be independent of the molybdenum content, releases slowly the acetonitrile formed, resulting in an upper limit of the yield. The other site, whose concentration increased at increasing molybdenum content, strongly adsorbed the acetonitrile formed, which was only removed by annealing or by competitive adsorption of ammonia.

Literature cited

- 1 Amenomiya, Y., Cvetanovic, R.J., *J. Phys. Chem.* **67** (1963) 144
- 2 Amenomiya, Y., *Chem. Technol.* **6** (1976) 128
- 3 Kung, M.C., Cheng, W.H., Kung, H.H., *J. Phys. Chem.* **83** (1979) 1737
- 4 Yang, B.L., Kung, H.H., *J. Catal.* **77** (1982) 410
- 5 Centi, G., Perathoner, S., *J. Catal.* **142** (1993) 84
- 6 Morrow, B.A., Cody, I.A., *J. Phys. Chem.* **80** (1976) 1988
- 7 Grasselli, R.K., Burrington, J.D., *Adv. Catal.* **87** (1987) 363.
- 8 Gordymova, T.A., Davydov, A.A., *Kinet.Katal.* **20** (1979) 727
- 9 Grasselli, R.K., Burrington, J.D., *Adv. Catal.* **30** (1981) 133
- 10 de Boer, M., Huisman, H.M., Mos, R.J.M., Leliveld, R.G., van Dillen, A.J., Geus, J.W., *Catal. Today* **17** (1993) 189
- 11 Aruga, T., Tateno, K., Fukui, K., Iwasawa, Y., *Surf. Sci.* **324** (1995) 17
- 12 Cheng, C.P., Schrader, G.L., *J. Catal.* **60** (1979) 276
Sarrazin, P., Mouchel, B., Kasztelan, S., *J. Phys. Chem.* **93** (1989) 904
Stampfl, S.R., Chen, Y., Dumesic, J.A., Niu, C., Hill, C.G., *J. Catal.* **105** (1987) 445
Ismail, H.M., Theocharis, C.M., Waters, D.N., Zaki, M.I., Fahim, R.B., *J. Chem. Soc., Faraday Trans. I* **83** (1987) 1601
Kakuta, N., Tohji, K., Udagawa, Y., *J. Phys. Chem.* **92** (1988) 2583
Kasztelan, S., Payen, E., Moffat, J.B., *J. Catal.* **31** (1979) 209
- 13 Van Veen, J.A.R., Hendriks, P.A.J.M., *Polyhedron* **5** (1/2) (1986) 1166
- 14 De Boer, M., Ph.D. thesis, Univ. Utrecht, (1992) Chapter 3
- 15 Lombardo, E.A., Houalla, M., Hall, W.K., *J. Catal.* **51** (1978) 256
- 16 Mol, J.C., Moulijn, J.A., *Adv. Catal.* **24** (1975) 131
Lombardo, E.A., Lo Jacono, M., Hall, W.K., *J. Catal.* **64** (1980) 150
Tanaka, K., Tanaka, K., *J. Chem. Soc., Faraday Trans. I* **83** (1987) 1859

Grünert, W., Stakeev, A.Y., Mörke, W., Feldhaus, R., Anders, K., Shpiro, E.S., Minachev, K.M. *J. Catal.* **135** (1992) 269

Grünert, W., Stakeev, A.Y., Feldhaus, R., Anders, K., Shpiro, E.S., Minachev, K.M. *J. Catal.* **135** (1992) 287

17 Centi, G., Tosarelli, T., Trifirò, F., *J. Catal.* **142** (1993) 70

18 Grasselli, R.K., Burrington, J.D., Brazdil, J.F., *Faraday Discuss. Chem. Soc.* **72** (1982) 203

4

γ -Al₂O₃ SUPPORTED MOLYBDENUM CATALYSTS.

STRUCTURE-ACTIVITY RELATIONSHIPS

Abstract.

The reaction of ethylene with ammonia to acetonitrile over γ -Al₂O₃ supported molybdenum catalysts was studied in the absence of gaseous oxygen. The effects of various molybdenum content and catalyst pretreatments on the reactivity were investigated.

While introducing the reactants under semi-flow conditions, an unusual activity profile was observed as a function of time on stream, where three regions of interest could be distinguished: a semi-steady-state, a transition period and a real-steady-state. Experiments showed that the activity at the semi-steady-state is highly structure sensitive. Pretreated with oxygen, the catalyst is highly selective towards CH₃CN, with CO_x as main side product. Pretreated with hydrogen, the catalyst is more active but less selective, with ethane as main side product. From this, two mechanisms for acetonitrile formation were deduced:

- 1) based on the ammoxidation mechanism with the consumption of lattice oxygen.
- 2) based on the co-production of ethane, without lattice oxygen consumption.

The product distribution at the steady-state showed no oxygen containing components and was independent of the pretreatment. This indicates that mechanism 1) can gradually change into 2) when removable lattice oxygen becomes depleted. From the product distribution it was also derived that the mechanisms can be active simultaneously. Mechanism 1) is active on freshly calcined catalysts, where the molybdenum is present in a highly dispersed Al₂(MoO₄)₃-like structure. Mechanism 2) is suggested to be operational on a highly dispersed MoO₂-like structure, which has reached a structural and chemical equilibrium.

1 Introduction.

Catalysts based upon Mo/Al₂O₃ are remarkable for the variety of reactions they promote. In spite of the numerous investigations, the nature of their catalytic performance is still unclear. The activity of those catalysts is determined from their chemical and phase composition, the preparation mode and activation procedure.

In catalytic (amm)oxidation, one of the most important questions of the reaction mechanism is the participation of the lattice oxygen in the formation of reaction products, implying a structure sensitive aspect. The concepts of structure-insensitive (*facile*) and structure-sensitive (*demanding*) reactions were introduced by Boudard [1]. It was believed that in the rate-determining step of a *facile* reaction only one surface atom took part, and consequently little change of activity with structure could be expected in this case. On the other hand, in a *demanding* reaction several adjacent atoms were thought to be required, thus leading to a distinct change of activity with structure [2]. Although the background for these concepts was found in results for hydrogen-hydrocarbon reactions over metals, the same concepts appeared in principle also to be valid for oxidation reactions over metal oxides. However, oxides are in some respects more complicated than metals. At the surfaces of metal oxides both metal and oxygen ions are exposed. These ions can exist at several crystallographically non-equivalent positions, and even the valences of the cations may differ. At surfaces, oxygen species can exist in various forms, such as O⁻, O²⁻ and -OH.

Concerning oxidation reactions over oxides, published results can be classified according to two types of structure sensitivity. The first is where the turnover frequency of a specific species, on a specific face, depends on its environment. The second type is where activity and selectivity for various products are related to the distribution of crystal planes at the oxide surface [3]. The study of the so-called oxidative ammonolysis, *i.e.*, ammoxidation with the absence of molecular oxygen, is a suitable reaction with which the occurrence of the second type of structure sensitivity can be studied. Only lattice oxygen takes part in the formation of products.

In ammoxidation reactions usually higher olefines or alkanes and aromatics are involved. Lower hydrocarbons, such as methane and ethylene are mainly used in selective oxidation reactions [4]. Only few investigations are known involving the ammoxidation of ethylene [5], probably due to a lack of industrial interest.

A fundamental understanding of the structure-activity relationships observed in heterogeneous catalytic oxidation, is of basic importance for the development of new catalytic materials and for the decision about possible actions to be taken in order to improve the performance of existing catalysts. This chapter describes the study of the structure-

activity relationships for the oxidative ammonolysis of ethylene to acetonitrile over γ -Al₂O₃ supported molybdenum catalysts. Various characterisation techniques, such as XPS, XRD, LEIS, HREM and IR, were applied on freshly pretreated and spent catalysts, in order to find a correlation between the presence of particular molybdenum structures and catalytic performance. Also an attempt was made to elucidate some aspects of the reaction mechanism operating on different molybdenum structures found to be present.

2 Experimental procedure.

The catalyst preparation and the apparatus used for reactivity experiments is described in chapter 2, sections 2.1 and 4, respectively. Experiments were done with an exact amount of 1.0 gram catalyst containing 3, 5, 10 or 15 wt% molybdenum. Prior to reaction a reductive or an oxidative treatment was applied. The reductive treatment consisted of heating the catalyst in a 10 vol% hydrogen in helium flow to 650 °C and held there for 24 hours, whereas oxidative treatment consisted of heating in a 10 vol% oxygen in helium flow to 550 °C and held there for 24 hours. The reactants were introduced simultaneously to the catalyst by introducing pulses of ammonia to a flow of 1 vol% ethylene in helium (provided by Hoekloos), which was diluted with helium to 0.8 vol%, resulting in 1 vol% of NH₃. The total flow was kept at 20 Nml/min and the reaction temperature window applied was 350-550 °C.

As reference compounds, pure MoO₂ and Al₂(MoO₄)₃ were obtained from Johnson Matthey, and MoO₃ was obtained from Merck.

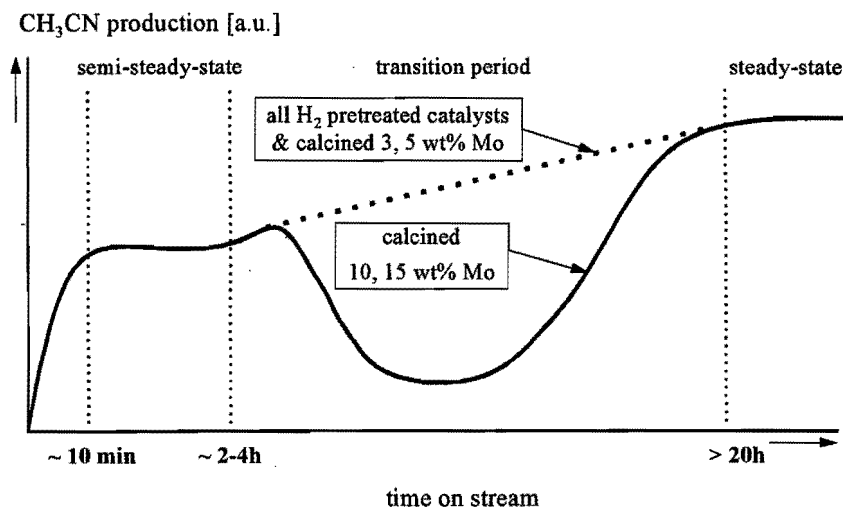
The experimental procedures for IR, XPS, LEIS, XRD and HREM are described in chapter 2, section 3.

3 Results and discussion.

3.1 Characteristic regions of the activity profile.

Activity measurements were performed on catalysts with various molybdenum content after an oxidative or a reductive pretreatment. Monitoring more than 20 hours on stream, an unusual profile of acetonitrile formation was observed. This is schematically shown in Figure 4.1.

Three regions of interest can be distinguished: a semi-steady-state, a transition period and a steady-state. Characteristic for the semi-steady-state was a constant formation of acetonitrile, whereas the selectivity to other products was changing. The semi-steady-state



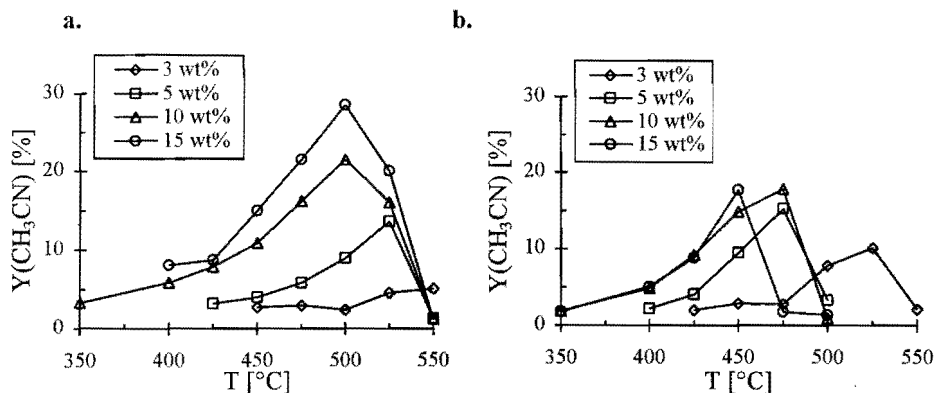
★ **Figure 4.1** Schematic profile of the formation of acetonitrile on various Mo/ γ -Al₂O₃ catalysts as a function of time on stream.

was reached after approximately 10 minutes, and lasted about 2 to 4 hours on stream, dependent on the molybdenum content. The performance during the transition period appeared to be highly dependent on the Mo content and catalyst pretreatment. Oxygen pretreated catalysts with molybdenum content of 5 wt% or less and all catalysts pretreated in hydrogen showed a gradual increase in activity and acetonitrile production (see Figure 4.1; dotted line). However, the calcined 10 and 15 wt% Mo catalysts showed a non-gradual increase in both acetonitrile formation (see Figure 4.1; solid line) and activity. The conversion of ammonia and ethylene went through a maximum, while the acetonitrile formation went through a minimum. When reaching the steady-state, the amount of acetonitrile had increased 2 to 3 times for all catalysts, compared to the semi-steady-state.

3.1-1 The Semi-Steady-State Period.

All catalysts showed a period of semi-steady-state, which was characterised by the constant formation of acetonitrile, while the selectivity to other products was changing. The conversion increased at increasing temperature, whereas the selectivity decreased, resulting in an optimum curve of the yield versus temperature, which is shown in Figure 4.2a and b.

The calcined catalysts showed clearly an increase of the yield at increasing molybdenum content (see Figure 4.2a). Previous experiments [6] revealed that the yield of acetonitrile was

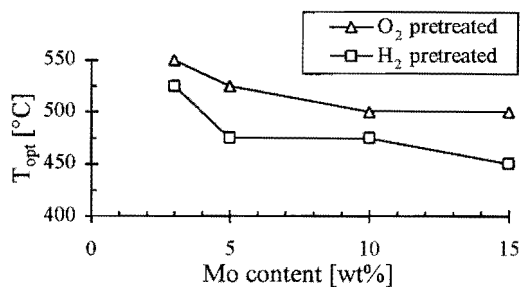


★ **Figure 4.2** The yield of acetonitrile versus reaction temperature in the semi-steady-state period for oxygen pretreated (a) and hydrogen pretreated catalysts with various molybdenum content.

fixed to an upper limit, when ethylene was introduced to a catalyst pre-adsorbed with ammonia. This upper limit was ascribed to an active site, whose concentration was independent of the Mo content. A second site for acetonitrile formation was suggested, whose concentration increased at increasing Mo content, but desorption only occurred by annealing or by competitive adsorption of ammonia. The fact that under flow conditions, where both ethylene and ammonia were present, an increase of the yield at increasing Mo content was observed implies that both active sites are responsible for acetonitrile formation. When pretreated with hydrogen, the variation of the yield with Mo content was much less (see Figure 4.2b). Also, except for the 3 wt% catalyst, the yield is lower in the whole temperature range considered, when compared to the oxygen pretreated ones.

When plotting the temperature where the optimum yield was obtained (T_{opt}) versus the molybdenum content, it is clear that both series showed a shift in T_{opt} to a lower value at increasing Mo content (see Figure 4.3).

At temperatures exceeding T_{opt} , the complete dissociation of ammonia started to dominate, resulting in the desorption of nitrogen and thereby suppressing the desired reaction. Also, the conversion of ethylene increased to side products, causing the curves in Figure 4.2 to drop very sharply after reaching the maximum. The T_{opt} for



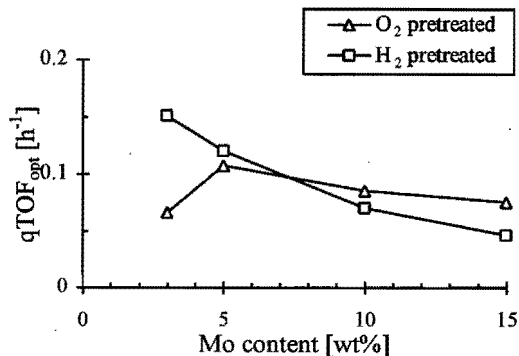
★ **Figure 4.3** The temperature where optimum yield of CH₃CN is obtained versus Mo content.

hydrogen pretreated catalysts is lower for all Mo loadings considered. Recent ammonia TPD and TPRE experiments [6] showed that the activity towards ammonia dissociation increased at increasing Mo content. Also, when pretreated with hydrogen, the catalysts appeared to be more active towards ammonia dissociation than when pretreated with oxygen. This observation is confirmed in the literature which states that molybdenum is better dispersed after calcination than after a heat treatment in hydrogen [7]. Considering that larger molybdenum clusters are more active towards complete ammonia dissociation, it is explicable that this reaction starts to dominate at lower temperatures, shifting T_{opt} to a lower value with increasing molybdenum loading. It also follows that, for hydrogen pretreated catalysts T_{opt} is lower for the whole range considered.

When the optimum quasi turnover frequency versus molybdenum content is plotted, a remarkable trend is observed (see Figure 4.4). Both the hydrogen pretreated 3 and 5 wt% Mo catalyst gave a better performance than the oxygen pretreated analogues. The curves suggest an intersection at approximately 7.5 wt% Mo, where the catalytic performance should not be influenced by the pretreatment. This observation can be related to the LEIS study by Van Leerdaam *et al.* [8] on γ - Al_2O_3 supported molybdenum catalysts. It was suggested that the E-layer of the (100)-face was the most probable crystallographic surface plane of $Mo/\gamma-Al_2O_3$ at a calcination temperature of 500 °C.

This E-layer contains sites at which Mo can be accommodated without shielding surface Al atoms, which are well-separated, resulting in monomeric oxomolybdenum. This site occupation corresponds with epitaxial growth of Mo on the support lattice, which is possible for a coverage ≤ 8 wt% MoO_3 (≤ 5.3 wt% Mo). At MoO_3 contents exceeding 8 wt%, other sites of the support are occupied, forming polymeric oxomolybdenum species up to a mono layer coverage of 19 wt% MoO_3 (12.5 wt% Mo). It is intelligible that the isolated tetrahedral Mo-species, present at a low coverage, are resistant to reduction and aggregation. However, when partly reduced, a better catalyst is obtained, probably due to a decrease in interaction between molybdenum and alumina.

The oxygen pretreated catalysts were less strongly affected by variation of the molybdenum content, and the $qTOF$ decreased slightly at molybdenum contents exceeding

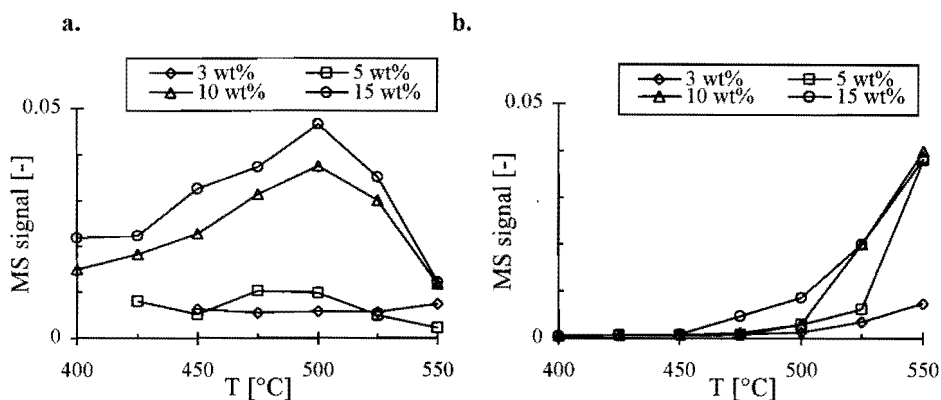


★ Figure 4.4 The optimum quasi turnover frequency versus molybdenum content.

10 wt% (see Figure 4.4; triangles). This indicates that the molybdenum added is indeed well-spread on the alumina surface and accessible for reaction. Seemingly, the influence of dispersion effects starts to dominate at higher molybdenum content. The hydrogen pretreated catalysts with low molybdenum content initially had the best performance among all catalysts tested. At higher molybdenum content the $qTOF_{opt}$ decreased sharply (see Figure 4.4; squares), due to a decrease in the dispersion induced by the hydrogen pretreatment. These observations are in agreement with the effects on the T_{opt} , as discussed earlier.

Although the hydrogen pretreated catalysts showed a higher activity, the selectivity to acetonitrile is lower than when pretreated in oxygen (see Appendix I, Tables I.1-8). The side reactions that occurred, had overlapping temperature regions and depended on catalyst morphology. On oxygen pretreated catalysts, combustion was the main side reaction. At temperatures exceeding the optimum for acetonitrile, the formation of CO_2 decreased, while the formation of CO , CH_4 and C_2H_6 increased. At higher molybdenum content, the formation of C_2H_6 went through a maximum, while high amounts of CO and CH_4 were detected. When pretreated in hydrogen, hydrogenation was the main side reaction. At higher temperatures, the increase of CO and CH_4 coincided with the decrease in C_2H_6 . The formation of some CO_2 proved that still removable lattice oxygen was present on the catalyst surface, despite the reductive treatment.

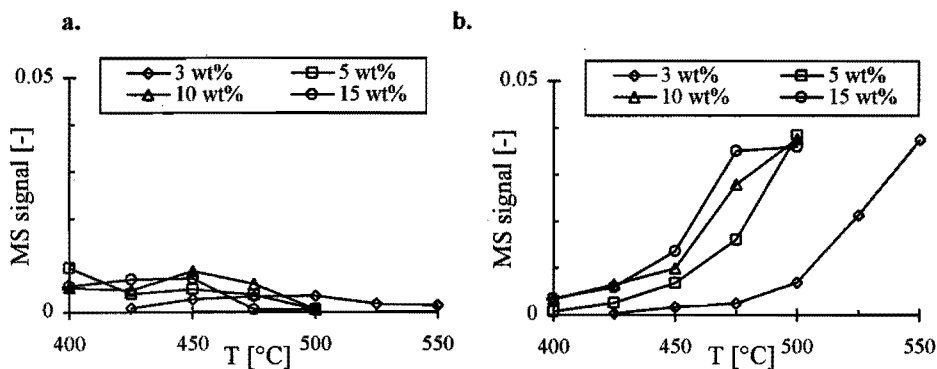
Conform the traditional ammoxidation reactions, the nitrile is formed with the release of water [9]. Figure 4.5a and b show the formation of water and hydrogen during the semi-steady-state period for oxygen pretreated catalysts. Indeed the water formation seems to be related to the formation of acetonitrile (see Figure 4.5a). The amount of water increased with



★ **Figure 4.5** The formation of water (a) and hydrogen (b) during the semi-steady-state of oxygen pretreated catalysts with various molybdenum content. The mass spectrometer signal is normalised to the helium internal standard ($S(n/e=18)/S(m/e=4)$).

increasing Mo content, due to the increasing reducibility. The amount of hydrogen can be neglected up to the optimum temperature for the formation of acetonitrile (see Figure 4.5b). Apparently, at higher temperatures (475-500 °C), the high conversion reduced the molybdenum surface significantly, resulting in side reactions.

When pretreated in hydrogen, the pattern is completely different. The amount of water is much less (approximately a factor 2 to 5, dependent on the Mo content), due to the removal of lattice oxygen by the catalyst pretreatment (see Figure 4.6a). If the formation of water and acetonitrile are necessarily related, the catalytic performance of the hydrogen pretreated catalysts for nitrile formation should be very poor. Since this is not the case, it is therefore suggested that two routes exist for the formation of acetonitrile: one with the formation of



★ **Figure 4.6** The formation of water (a) and hydrogen (b) during the semi-steady-state of hydrogen pretreated catalysts with various molybdenum content. The mass spectrometer signal is normalised to the helium internal standard ($S(m/e=18)/S(m/e=4)$).

water, conform the ammoxidation mechanism, and the other with the formation of hydrogen, so without the consumption of lattice oxygen. The amount of hydrogen is of the same magnitude as the water formed on the oxygen pretreated catalysts. Recent ammonia TPD experiments [6] showed two similar mechanisms of dissociative adsorption of ammonia on $\text{Mo}/\gamma\text{-Al}_2\text{O}_3$ catalysts, dependent on the pretreatment. Apparently, both these mechanisms can both produce N-inserting surface species. The first mechanism can be active separately on calcined catalysts, whereas the mechanisms are active simultaneously on hydrogen pretreated catalysts.

All experiments were done in the absence of gaseous oxygen in the reaction stream. The question is whether surface reoxidation is fast enough to regenerate the catalyst surface, to perform ammoxidation instead of oxidative ammonolysis. When gaseous oxygen was added to the reaction stream (the concentration was varied from ppm scale to 10 vol%), the

formation of water and CO_2 increased, while the formation of acetonitrile decreased. This indicates that the oxygen is consumed, but not towards selective oxidation products. The incorporation of oxygen from the gas phase into the lattice is a slow diffusion limited process, this way favouring the non-selective oxidation.

In summary, the semi-steady-state activity is highly structure sensitive. When oxygen pretreated, the catalysts are very selective but not very active and at higher molybdenum a higher yield of acetonitrile was obtained. Hydrogen pretreated catalysts were very active but less selective. Considering the qTOF, the hydrogen pretreated catalysts with low Mo content ($< 5\text{wt}\%$ Mo) performed better, whereas for oxygen pretreated catalysts this is the case for a higher Mo coverage ($> 5\text{wt}\%$ Mo). This causes in Figure 4.4 the point of intersection at approximately $7.5\text{wt}\%$ molybdenum loading. Apparently the complete dissociation of ammonia, resulting in the desorption of nitrogen, is favoured on reduced larger molybdenum clusters.

Although hydrogen pretreated catalysts are more active, the selectivity towards acetonitrile is much lower than for oxygen pretreated catalysts. Since the yield of acetonitrile is not significantly lower than for the oxygen pretreated catalysts, it is suggested that two routes for formation exist: one with the release of water conform the ammoxidation mechanism, and the other with the release of hydrogen, resulting in oxidative ammonolysis.

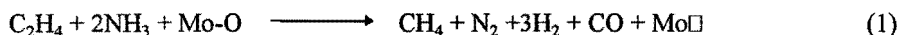
Experiments with molecular oxygen in the feed, showed that incorporation of oxygen into the lattice oxygen vacancies formed by reaction, is too slow, resulting in non-selective oxidation.

3.1-2 Transition Period.

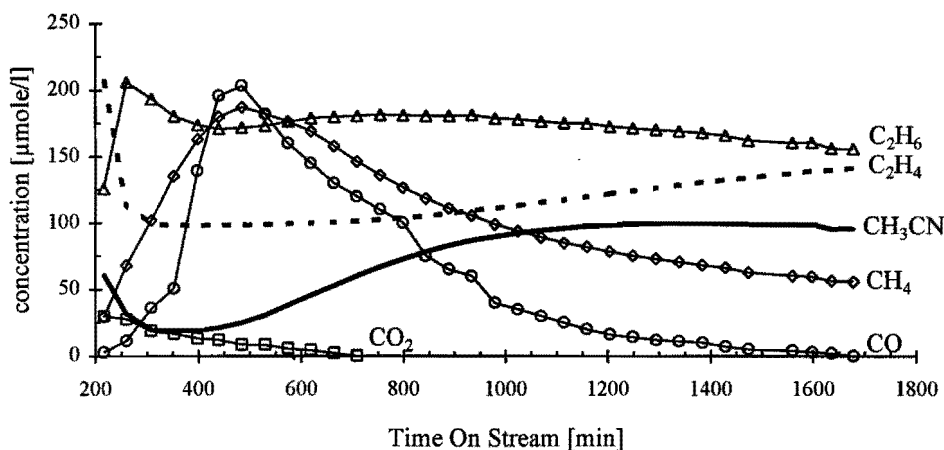
During the transition period strong fluctuations were observed in both activity and selectivity. All hydrogen pretreated catalysts and the oxygen pretreated catalysts with $5\text{wt}\%$ Mo or less showed a gradual increase in the formation of acetonitrile, until an upper limit was reached (see Figure 4.1; dotted line). During this increase, the formation of ethane and hydrogen increased, while the formation of CO_x and water decreased, resulting in an overall increase of the activity.

Only with the $10\text{wt}\%$ and $15\text{wt}\%$ Mo catalysts pretreated with oxygen, a non-gradual increase of the activity and selectivity was observed. Although a strong increase in activity occurred, the selectivity to acetonitrile drops sharply, resulting initially in an overall slight increase of the yield. During the period of low acetonitrile production the conversion of ethylene and ammonia increased to approximately 80% , while products were methane, ethane, nitrogen, hydrogen and carbon monoxide. This is shown for the calcined $15\text{wt}\%$ Mo

catalyst in Figure 4.7. The formation of ethane increased sharply, followed by a slow decrease to finally a steady-state level. The formation of CO_2 showed a decline, while CO went, simultaneously with CH_4 , through a maximum. The overall reaction that dominated in this transition period was (see reaction (1)):



Parallel, the hydrogenation of ethylene continued. Despite the fact that the conversion slowly decreased, the formation of acetonitrile slowly increased, due to the reduction of reaction (1). Apparently, the molybdenum structure is radically changed during the transition period, since the consumption of lattice oxygen is very high in the earlier stages, until eventually terminated by the depletion of the removable lattice oxygen.

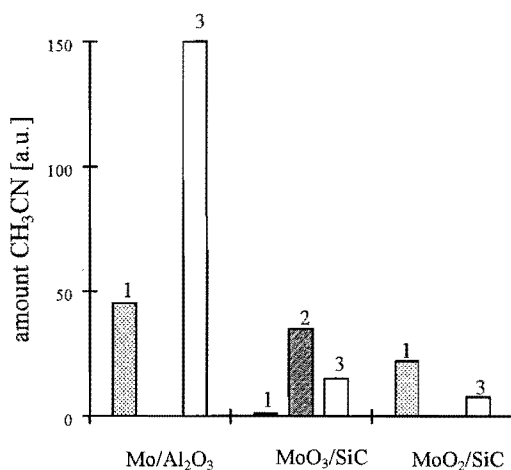


★ **Figure 4.7** The fluctuations in the conversion of ethylene and in the product distribution during the transition period at 450 °C for the calcined 15 wt% Mo/ γ - Al_2O_3 catalyst.

This unusual profile was not observed when the catalysts were pretreated with hydrogen. Also, calcined catalysts with Mo content of 5 wt% or less, showed a gradual change in activity. The factor in control is obviously the amount of removable lattice oxygen. Due to the lower Mo content and the poor reducibility of smaller clusters, these catalysts contain less removable lattice oxygen. Apparently, the reductive treatment of the 10 and 15 wt% Mo catalysts has removed enough lattice oxygen to suppress the reaction (1) partly, resulting in also a gradual increase of the formation of acetonitrile.

3.1-3 Steady-State Period.

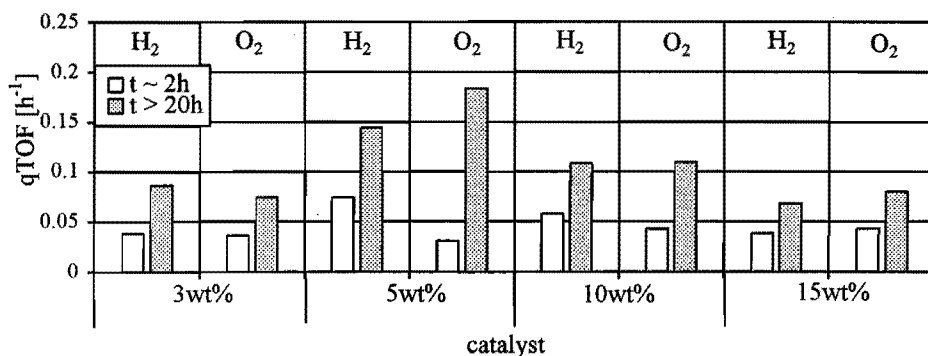
Compared to the semi-steady-state, significant increases in catalytic activity were observed over at least 20 hours on stream at 450 °C. No oxygen containing products were detected in the reaction stream and the product distribution was constant, so a *real* steady-state was reached. This observation is different from the ammoxidation of propylene. Aykan [10] observed a fast decline in catalytic activity with increasing reduction of the catalyst in the absence of gaseous oxygen. When using different ratios of bismuth and molybdenum, the 30% MoO₃ on silica appeared to be a very poor catalyst. Experiments where acrylonitrile was introduced to the catalyst showed that a low activity towards decomposition of this desired product gave a high selectivity to acrylonitrile. Amorphous SiO₂ and MoO₃ were found to be inert with respect to acrylonitrile. Only after complete reduction to MoO₂ the catalyst showed initially a high activity towards conversion of acrylonitrile to CO₂, acetonitrile and propionitrile which decreased very rapidly. It was suggested that this was caused by a large amount of carbon deposition. These observations are in agreement with our experiments of mechanical mixtures of MoO₃ and MoO₂ with SiC. The amount of acetonitrile produced by MoO₃/SiC (based on 10 wt% Mo) was initially very little and increased via a maximum to a level 10 times less than the molybdenum catalyst (see Figure 4.8). The MoO₂/SiC mixture produced initially an amount of acetonitrile 2 times less than the catalyst at semi-steady-state, and slowly decreased to a poor level of 20 times less than the catalyst at steady-state. The mechanical mixtures were highly selective; only traces of methane, ethane and propionitrile were observed. From this it can be concluded that bulk MoO₃ is not the catalytically active phase for the ammoxidation of ethylene. When slightly reduced by reaction, sites were generated that were active in the formation of acetonitrile. However, no real steady-state was reached, because the amount of acetonitrile was still slightly decreasing after 20 hours on stream, probably due to reduction below MoO₂ or carbon deposition. The bulk structure of MoO₂ initially showed clearly the



★ **Figure 4.8** The amount of acetonitrile formed at 450 °C at various time on stream on Mo/ γ -Al₂O₃, MoO₂/SiC and MoO₃/SiC based on 10 wt% Mo. 1: ~2h, 2: ~6h (only shown for MoO₃/SiC) and 3: >20h.

presence of sites responsible for the selective formation of acetonitrile, but deactivated slowly, also due to carbon poisoning. Obviously, the alumina support is needed to obtain a highly dispersed molybdenum phase to make a maximum utilisation of the active material possible and to suppress carbon deposition.

The point where steady-state was reached coincided with the absence of oxygen containing components in the product stream, indicating that the molybdenum structure is not altered further by the reaction. Comparing the qTOF of the semi-steady-state and the steady-state, the largest increase was generally observed when the catalysts were pretreated with oxygen (see Figure 4.9). The best catalytic performance was observed on the calcined 5 wt% Mo catalyst.



★ Figure 4.9 The quasi turnover frequency at semi-steady-state (2h) and at steady-state (> 20h) at 450 °C for different pretreated catalysts with various molybdenum content.

Overall, after reaching the steady-state, the oxygen pretreated catalysts reacted similarly to the hydrogen pretreated ones, considering the qTOF and product distribution. The main side product was ethane for all catalysts (see Figure 4.10). The amount of methane increased up to 5 wt% Mo to remain almost constant at higher Mo content. Also, the amount of ethane increased up to 5 wt% Mo, but was larger for hydrogen pretreated catalysts. Although the selectivity to acetonitrile is poor (25 to 30 %), the amount formed is higher, due to the higher activity of the catalysts. Besides methane and ethane, traces of propylene, cyclopropane, propionitrile and cyclohexadiene were observed. Since the activity profile of the steady-state is almost independent of the catalyst pretreatment, it is suggested that a specific Mo structure is operative, created under the reaction conditions. Since no lattice oxygen is consumed anymore, this structure acts as a real catalyst, instead of as a third reactant, as was occurring in the preceding reaction periods. It is therefore concluded that the two mechanisms suggested in section 3.1-1 operating simultaneously in the semi-steady-state on hydrogen

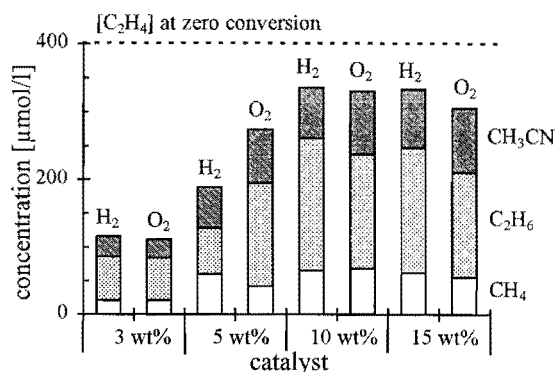
pretreated catalysts, can both operate separately. In the steady-state, acetonitrile is only formed via oxidative ammonolysis independent of the catalyst pretreatment, so by the release of hydrogen.

To obtain more insight in the reaction mechanism, it is important to know what surface species are present on the catalyst surface.

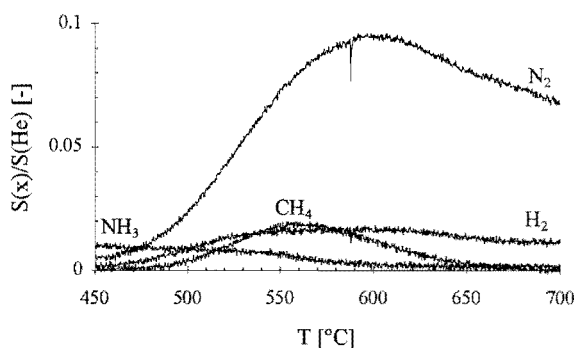
When a catalyst is submitted to TPD after reaching the steady-state, the desorbing components can give

some indications of the surface species present during reaction. This is shown in Figure 4.11 for the calcined 5 wt% Mo catalyst, which had been 24 hours on stream to reach the steady-state. Nitrogen was the main desorbing component, along with smaller amounts of hydrogen and methane and a very small amount of ammonia. During steady-state, only methane, ethane and acetonitrile are formed in significant amounts. Recent TPRE experiments [6] have shown that the formation and desorption of alkanes are fast processes. Also, in the temperature region considered, the presence of large amounts of adsorbed hydrogen can be excluded. So, it is therefore suggested that, even though the catalyst morphology is different, due to a different pretreatment, the =NH species are responsible for the formation of acetonitrile and =CH₂ and/or =CH-CH₃ species are responsible for the formation of hydrocarbons.

The ammoxidation of propylene is an example of N-insertion at an allylic carbon. In the case of ethylene this concerns a vinylic carbon, obviously due to the lack of choice. When the feed was switched from ethylene to propylene, indeed some acrylonitrile was formed on



★ Figure 4.11 The product distribution in the steady-state at 450 °C for different pretreated catalysts with various molybdenum content.



★ Figure 4.10 A TPD performed on a calcined 5 wt% Mo/ γ -Al₂O₃ catalyst after 24 h on stream at 450 °C. The mass spectrometer signals are normalised to the He internal standard.

calcined catalysts during the period of semi-steady-state. However, in the steady-state period this amount was much less and propionitrile was, besides acetonitrile and propane, the main product. The ratio propionitrile/acrylonitrile was approximately 25/1. This confirms the idea that in the steady-state the mechanism of the ammoxidation on our catalysts differs from the conventional ammoxidation mechanism. The difference is not believed to be in the nature of N-inserting species, but in the interaction of the hydrocarbon with a different molybdenum surface. -

3.2 Characterisation of Mo/ γ -Al₂O₃ catalysts.

The characterisation of supported metal oxide catalysts requires the use of several techniques because no one technique can provide all the information needed.

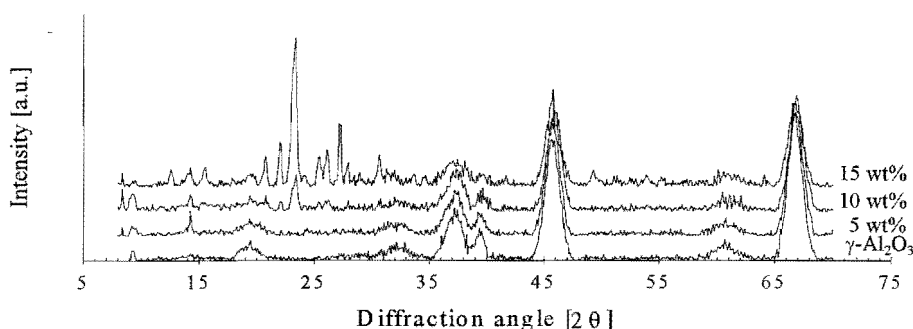
The different pretreatments were applied in order to examine the influence of different concentrations of lattice oxygen on the catalytic activity. Undoubtedly, besides different concentrations of lattice oxygen, also different structures of molybdenum on the alumina surface will be induced. To investigate this, different physical characterisation techniques, such as LEIS, XRD, HREM, IR and XPS were applied on both fresh and various spent catalysts. An attempt was made to correlate the identified different molybdenum structures with the varying catalytic activity described in the previous sections.

3.2-1 X-ray Diffraction.

X-ray Diffraction (XRD) is a characterisation technique that can identify large three-dimensional crystallites. Although it is a very powerful tool to probe the presence of crystalline phases, the detection is limited to a crystal size of approximately 4 nm [11] and two-dimensional metal oxide overlayers cannot be detected by XRD. Thus, when applied to a catalytic system, the absence of an XRD signal may be due to highly dispersed small crystallites, a low concentration of crystallites, or to the presence of a two-dimensional metal oxide overlayer, which is usually the case for catalysts with low coverage. However, the presence of an XRD signal confirms only that large crystallites are present and does not provide any information about the presence or absence of a two-dimensional metal oxide overlayer.

When the molybdenum content increases, it is expected that the particle size increases. The maximum adsorption capacity of the alumina used in this study is approximately 8-9 wt% Mo [12]. At molybdenum content exceeding this maximum, larger crystals are expected to be formed. This is shown for the calcined catalysts in Figure 4.12, where the 3 wt% Mo catalyst is not shown because the spectrum was similar to the support and the 5 wt%

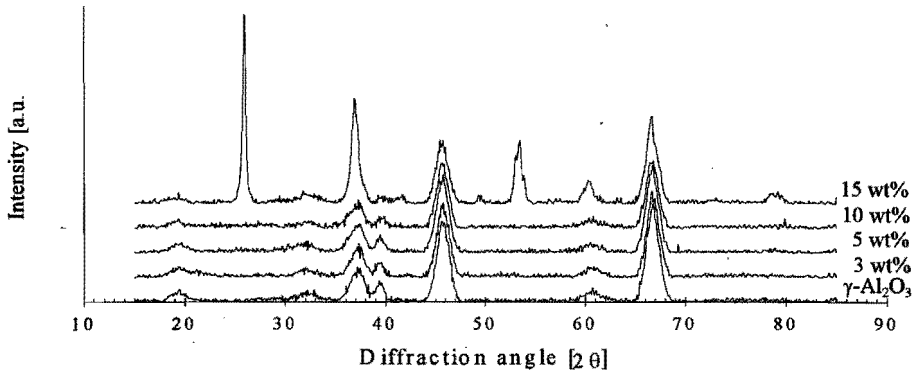
Mo. Apparently, these catalysts contained very small crystallites or the molybdenum phase is amorphous, resulting in only the signals of the poly-crystalline γ - Al_2O_3 . At 10 wt% Mo, little traces of a crystalline phase were observed, whereas clear crystalline signals appeared at 15 wt% Mo. However, these signals could not be ascribed to any form of pure molybdenum oxide, but to a mixed compound, namely $\text{Al}_2(\text{MoO}_4)_3$ [13]. This observation of chemical



★ **Figure 4.12** XRD spectra of γ - Al_2O_3 without any treatment and catalysts calcined at 550 °C with various molybdenum content.

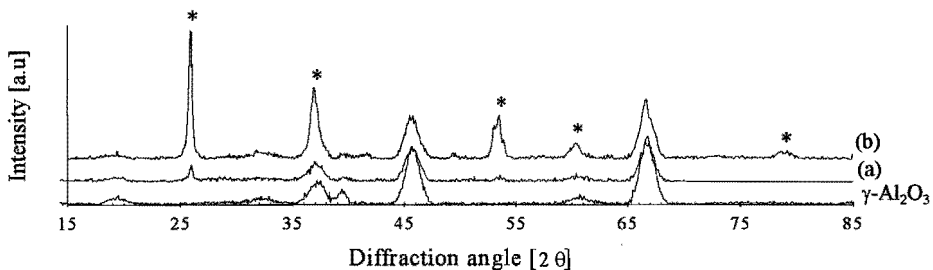
interaction of alumina and molybdate is in agreement with Giordano *et al.* [14] where $\text{Al}_2(\text{MoO}_4)_3$ was observed on MoO_3/γ - Al_2O_3 catalysts with more than 20 wt% MoO_3 and all samples calcined at 700 °C. The aggregation of free MoO_3 was excluded, except for the 30 wt% MoO_3/γ - Al_2O_3 catalyst. It was concluded that $[\text{MoO}_6]$ in the octahedral vacancies are the precursor of $\text{Al}_2(\text{MoO}_4)_3$, and that the formation of this stable phase is slow. The formation of $\text{Al}_2(\text{MoO}_4)_3$ was already observed by Sonnemans and Mars [15] and Asmolov and Krylov [16].

It was suggested that a change in molybdenum structure occurred during hydrogen pretreatment and reaction. When all oxygen pretreated catalysts were analysed by XRD after reaching the steady-state, remarkable trends were observed. This is shown in Figure 4.13. Again, at molybdenum content of 5 wt% or less, the spectrum is similar to the support. However, this is also the case for the 10 wt% Mo catalyst. This implies that the small amount of $\text{Al}_2(\text{MoO}_4)_3$ present in a fresh calcined catalyst was removed at least to the amount beyond the detection limit of XRD. This was most conspicuous for the 15 wt% Mo catalyst. Not only did the signals of $\text{Al}_2(\text{MoO}_4)_3$ disappear completely, a new crystalline phase appeared as well. The diffraction pattern is that of MoO_2 [17]. The presence of large $\text{Al}_2(\text{MoO}_4)_3$ crystals in calcined catalysts with high Mo content can explain the unusual catalytic profile of these catalysts, where during the transition period of high activity and low selectivity the structure is converted to large MoO_2 crystals.



★ **Figure 4.13** XRD spectra of oxygen pretreated catalysts with various molybdenum content after reaching the steady-state at 450 °C.

The question is whether this MoO₂ phase can already be formed by the hydrogen pretreatment. In Figure 4.14 it can be seen that indeed the hydrogen pretreated 15 wt% Mo catalyst contained MoO₂, but its presence is much less conspicuous in the XRD pattern than in the case of the steady-state catalyst. This indicates that even after a vigorous reductive treatment, the catalyst morphology is altered further under reaction conditions. The absence of large Al₂(MoO₄)₃ crystals in freshly reduced catalysts explains their gradual catalytic behaviour.



★ **Figure 4.14** XRD spectra of γ-Al₂O₃, a 15 wt% Mo/γ-Al₂O₃ catalyst after hydrogen treatment at 650 °C for 24 hours (a) and after oxygen treatment, followed by 24 hours on stream at 450 °C (b). The (*) indicate typical MoO₂ lines [17].

Although catalyst characterisation by XRD has answered some important questions concerning the different morphology present in differently pretreated fresh and spent catalysts, the exact nature of the active phase is still open for discussion, since XRD is not suitable for identifying small surface species.

3.2-2 High Resolution Transmission Electron Microscopy.

A powerful technique to estimate particle size is High Resolution Electron Microscopy (HREM). Combined with Energy Dispersive X-ray spectroscopy (EDX), which can determine the bulk composition of a restricted area, important parameters, such as impurities, dispersion and morphology of the active phase can be determined.

In this study, bright field Transmission Electron Microscopy (TEM) was applied to estimate the particle size of the molybdenum phase and to probe for crystallinity. Although Figure 4.15 shows a calcined 5 wt% Mo catalyst after reaching the steady-state, this picture is



★ Figure 4.15 HREM picture of a calcined 5 wt% Mo catalyst after 24 h on stream at 450 °C.

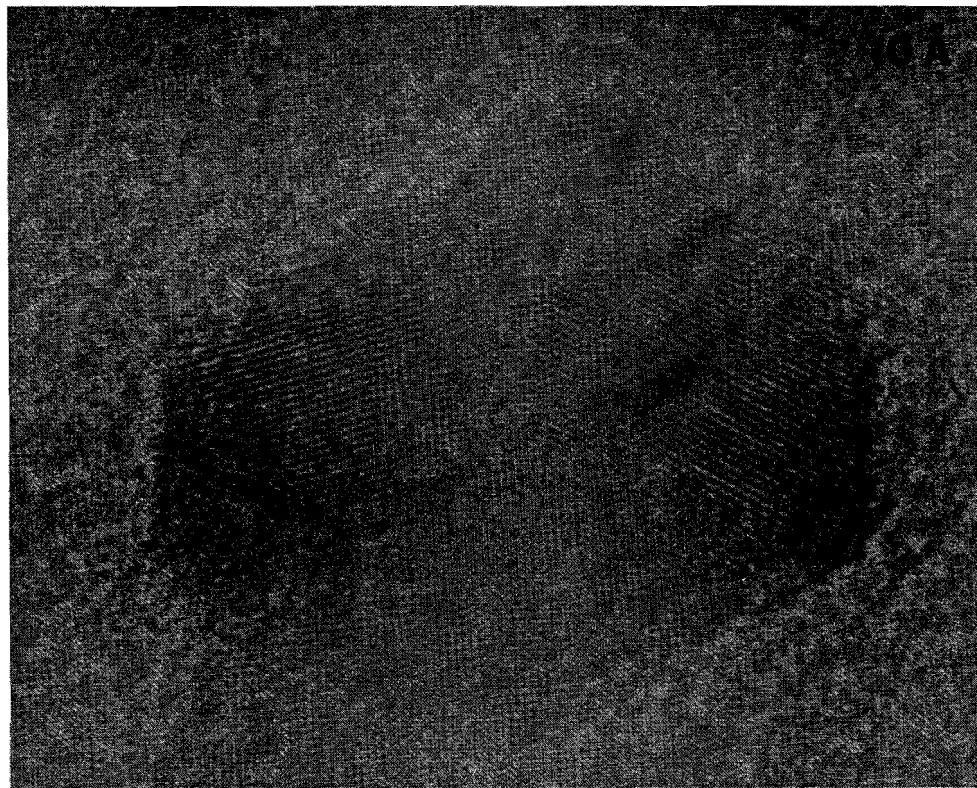
representative for all fresh and spent catalysts. The poly-crystalline phase correlated with γ - Al_2O_3 . No small molybdenum oxide particles were visible on the alumina surface, implying that the particle size was less than the detection limit of 5 Å. EDX analysis showed a molybdenum and a aluminium signal, which ratio did not deviate significantly over different areas in one sample but increased at increasing molybdenum content. This also implies a highly dispersed molybdenum phase on the alumina surface.

However, at molybdenum content exceeding 5 wt% Mo, when freshly calcined, large crystalline particles with a different structure and composition appeared (see Figure 4.16). The size of these crystals (> 200 Å) indicates obviously that they were not adsorbed inside the alumina pores, but outside the support or exist separate from the support. Of the spacings determined, 5.4 and 8.2 Å, only the first could be assigned to $\text{Al}_2(\text{MoO}_4)_3$. No Mo_xO_y structure, as well as ammonium molybdates are known to contain these spacings. EDX analysis showed a large excess of molybdenum. Since XRD indicated very clearly the presence of this component, it is likely that these large crystals are $\text{Al}_2(\text{MoO}_4)_3$.



★ Figure 4.16 HREM picture of a calcined 15 wt% Mo catalyst.

When the calcined catalysts containing a high amount of molybdenum, were submitted to reaction, it was suggested that a MoO_2 structure was formed. As XRD already indicated, also with HR-TEM large crystals were observed. The size of the dark crystalline particle in Figure 4.17 is approximately $165 \times 225 \text{ \AA}$. Again, the size is of an order of magnitude that it must concern precipitates outside the support. The spacings measured (3.42 and 2.42 \AA) coincided with those for MoO_2 .



★ Figure 4.17 HREM picture of a calcined 15 wt% Mo catalyst after 24 h on stream at $450 \text{ }^\circ\text{C}$.

In summary, it was concluded that when calcined, the molybdenum is present as highly dispersed particles ($< 5 \text{ \AA}$) and that at higher molybdenum content a chemical interaction occurred between alumina and molybdena, forming large crystals of $\text{Al}_2(\text{MoO}_4)_3$. Both a hydrogen pretreatment and reaction conditions were capable of destroying this crystalline structure, converting it to large MoO_2 crystals. Still, a highly dispersed reduced molybdenum structure remained on the alumina surface, which is suggested to be the active phase.

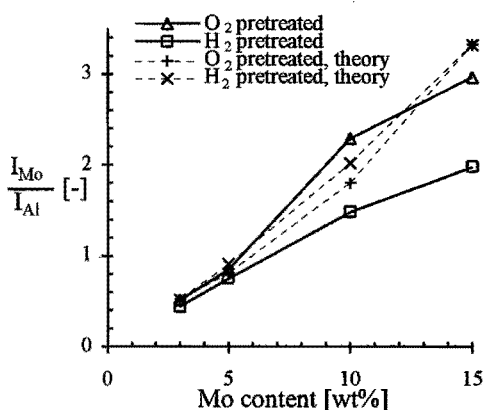
3.2-3 X-ray Photoelectron Spectroscopy.

X-ray Photoelectron Spectroscopy (XPS) supplies information on the elements present in the sample, as well as on their valency and chemical environment. Its analysis depth is about 50 Å, so several atomic layers are involved rather than only the surface atoms. In order to obtain quantitative information on the concentration profile of the active phase in the catalyst or the particle size of the deposited material, a number of models have been proposed to predict XPS intensities for catalysts [18, 19].

In this study, the ratio of the molybdenum and aluminium signal is used qualitatively as an indicator for changes in the dispersion of molybdenum. Figure 4.18 shows the ratio of the intensity of the XPS signals of Mo 3d and Al 2p for fresh catalysts (solid lines). Obviously,

the ratio increases with increasing molybdenum content. Overall, the ratio is higher for the oxygen pretreated catalysts than for the ones after a reductive treatment. Up to 5 wt% Mo, a similar increase was observed independent of the pretreatment applied. This supports the idea of the presence of isolated Mo species, with their resistance to reduction and aggregation. At higher molybdenum content, however, the ratio for oxygen pretreated catalysts is substantially higher than of the hydrogen pretreated ones, which showed a linear behaviour. A theoretical $I_{\text{Mo}}/I_{\text{Al}}$ was calculated by using

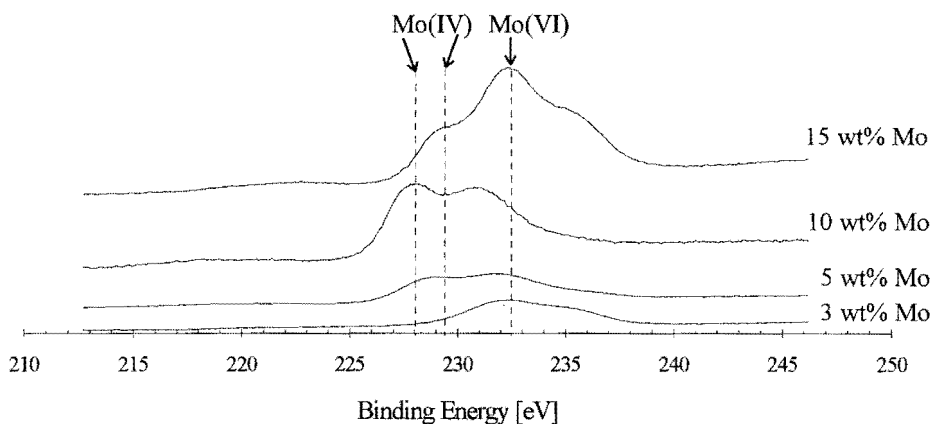
Kuipers model [19], in which the catalyst is represented by small surface elements with a random orientation to the analyser. The model predicts an equivalent layer thickness from the XPS intensity ratio of the dispersed phase to the support. This thickness can be translated to a particle size, since systems with randomly orientated particles of the same surface to volume ratio appear to yield nearly the same intensity ratios. The physical upper limit of the intensity of the molybdenum signal was calculated, using the bulk density (3 g/cm³) and specific area of the support, the bulk density of the molybdenum phase (4.7-6.5 g/cm³ for MoO₃ and MoO₂, respectively) the concentration of the dispersed compound (g/100 g catalyst) and the intensities and binding energies of aluminium (74 eV) and molybdenum (230 eV). The photoelectric cross-sections were estimated according to Scofield [20] and a Seah factor for inorganic compounds of 0.72 [21] was applied. A theoretical $I_{\text{Mo}}/I_{\text{Al}}$ was calculated from the



★ Figure 4.18 Intensity ratio of the XPS signals of Mo 3d and Al 2p as a function of Mo content and catalyst pretreatment.

calculated physical upper limit of the molybdenum signal and the aluminium signal and is represented by the dotted lines in Figure 4.18. The calculated lines for the fresh hydrogen pretreated catalysts and the spent catalysts coincided, due to the same assumed morphology of MoO_2 present. For the freshly calcined catalysts, the theoretical line and the measured line agree well up to 10 wt% Mo, indicating an optimum dispersion of the molybdenum. When pretreated with hydrogen, these lines agree up to 5 wt%, which implies a highly dispersed molybdenum phase which aggregates to larger particles at higher Mo content upon reduction.

Besides changes in dispersion, also changes in the valence state of molybdenum are expected upon hydrogen pretreatment. When pretreated in oxygen, only hexavalent molybdenum was detected. Figure 4.19 depicts the Mo $3d$ signals for hydrogen pretreated catalysts. Indeed, after hydrogen pretreatment, besides hexavalent (Mo(VI)), other valence states of molybdenum were present. At Mo content exceeding 5 wt%, Mo(IV) was present, whose amount increased with increasing Mo content. The 3 wt% Mo catalyst showed very little reduction. The line broadening suggests the presence of Mo(V) species, but it was very difficult to deconvolute the signal. The 5 wt% Mo catalyst contained about 70% Mo(IV), whereas on the 10 wt% Mo catalyst even 80% Mo(IV) was observed. The position of these



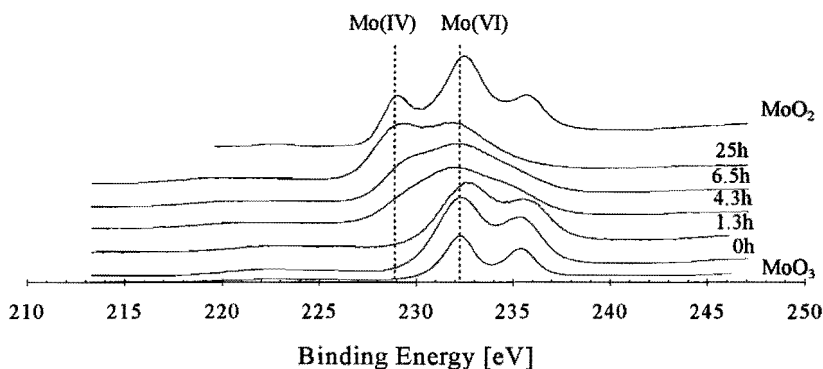
★ **Figure 4.19** XP spectra of the Mo $3d$ signal of catalysts with various molybdenum content after hydrogen pretreatment for 24h at 650 °C. The dotted lines indicate the position of the Mo $3d_{3/2}$ signal.

Mo $3d_{3/2}$ signals was at 228.4 and 228.8 eV, respectively, implying a further reduction of the molybdenum surface than MoO_2 . In the literature, the Mo(IV) $3d_{3/2}$ signal at 229.5 eV is ascribed to Mo(IV) in a MoO_2 structure [22]. Although the presence of lower valence states than 4+ could not be determined, the position of the Mo $3d_{3/2}$ signal at 228.4 eV can very

well be attributed to Mo(II). According to Haber et al. [23] Mo(IV) can exist in two forms: (I) represents isolated Mo^{4+} ions, whereas (II) constitutes Mo^{4+} ions forming pairs in clusters of edge-sharing octahedra, which may be considered as nuclei of a MoO_2 phase. The binding energy of Mo(IV) in form I is typical for Mo(IV) in MoO_2 , whereas the binding energy of Mo(IV) in form II is Mo(II)-like. Since divalent molybdenum ions are known to be very unstable in oxide systems, the appearance of the apparent oxidation number of 2+ must originate from Mo(IV) in form II.

The amount of Mo(IV) in the 15 wt% Mo catalyst was only 45%, whereas the position of the $3d_{3/2}$ signal was at 229.6 eV. This clearly indicates the presence of MoO_2 in this catalyst, which was already confirmed by XRD in section 3.2-1.

For quasi *in-situ* XPS analysis the reaction was quenched at various time on stream. The different spectra for the calcined 10 wt% Mo catalyst are shown in Figure 4.20. For comparison, the spectra of pure MoO_2 and MoO_3 are included. Clearly an increase of the Mo(IV) fraction was observed. A fresh catalyst, containing 100% Mo(VI), was not very

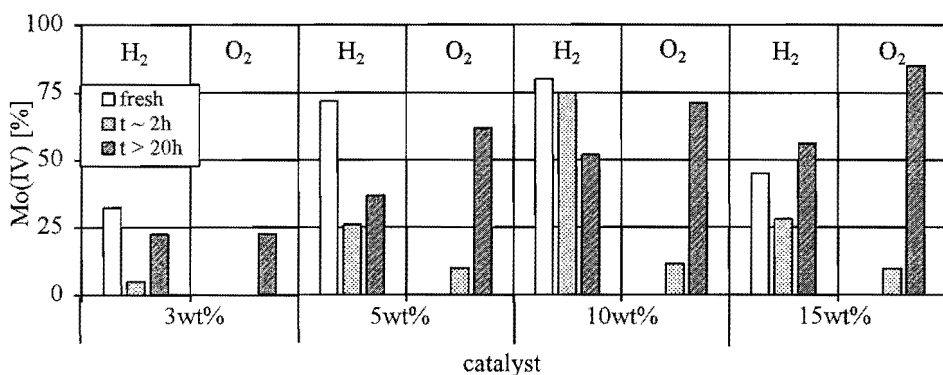


★ **Figure 4.20** XP spectra of the Mo $3d$ signal of pure MoO_2 , MoO_3 , and a calcined 10 wt% Mo catalyst at various time on stream at 450 °C.

active, but highly selective to acetonitrile (see Figure 4.20; after ~ 1.3 h). Before the yield started to decrease, little reduction of molybdenum was observed with XPS (after ~ 2.5 h, not shown in Figure 4.20). Evidently, due to the higher molybdenum content, the presence of a large amount of still removable surface oxygen in a partly reduced catalyst (due to reaction) leads to a very high activity, but only towards the formation of methane and CO (see page 60; reaction (1)) and hydrogenation. This side reaction is terminated at depletion of removable lattice oxygen. The position of the Mo $3d_{3/2}$ signal for Mo(IV) for all catalysts was about 229.5 eV after reaching the steady-state, indicating that a MoO_2 -like surface

structure is formed under reaction conditions. Apart from the fact that the start of the decrease of the yield of acetonitrile occurred several hours later, the oxygen pretreated 15 wt% Mo catalyst evolved similarly to its 10 wt% analogue: 4.3h and 6.5h in Figure 4.20 represent 8.5h and 11.5h on stream, respectively.

By deconvoluting the Mo $3d_{5/2}$ curve, a ratio of Mo(IV)/Mo(VI) could be determined. Figure 4.21 depicts the percentage of Mo(IV) of fresh catalysts, in the period of semi-steady-state and in the steady-state of the reaction for the different pretreated catalysts with various molybdenum content. Again, it can be seen that the reducibility increased with increasing Mo content, because the fraction of Mo(IV) increased, except for the hydrogen pretreated 15 wt% Mo catalyst, due to the presence of larger crystalline particles. Remarkable is the fact that the amount of Mo(IV) decreased for hydrogen pretreated catalysts in the semi-steady-state, suggesting that the diffusion of lattice oxygen to the surface is accelerated under reaction conditions. Although the hydrogen pretreatment induced a highly reduced molybdenum surface, not all reactive lattice oxygen was removed, since in all cases the oxygen containing products were formed prior to the steady-state. It can be concluded from the higher amounts of Mo(IV) on the calcined catalysts at steady-state, that by starting with a highly dispersed calcined precursor, the catalyst surface can be further reduced by reaction than with a hydrogen pretreated catalyst as starting material. The increase of the yield of acetonitrile can not be attributed only to the increase of the amount of Mo(IV). Although the oxygen pretreated 5 wt% Mo catalyst yielded the highest qTOF at steady-state (see Figure 4.9), the largest amount of Mo(IV) was observed on the oxygen pretreated 15 wt% Mo catalyst.



★ **Figure 4.21** Fraction Mo(IV) calculated from deconvolution of the Mo $3d$ signal of fresh catalysts and at the semi-steady-state (2h) and the steady-state (> 20h) period at 450 °C.

Evidently, a well-dispersed calcined precursor is needed to obtain the best performance in the steady-state, where both Mo(IV) and Mo(VI) species are present. At higher molybdenum loading the activity in the steady-state becomes independent of the pretreatment. This suggests the formation of a stable molybdenum structure during reaction, which was previously suggested to be MoO₂.

When submitted to reaction, an increase of the C 1s peak was observed, compared to the fresh catalyst, suggesting that coke formation occurred. Since the catalytic activity showed no indications of deactivation, this carbon could be removed by the reaction stream, or even act as a reaction intermediate. Also, coke deposition on the alumina cannot be excluded. Nitrogen containing species are very difficult to detect by XPS, because of the low sensitivity towards nitrogen and the interference of the Mo 3p_{3/2} signal of Mo(VI), which is always present. Only at higher molybdenum content and after long time on stream, the N 1s signal could be distinguished. From the binding energy (~398 eV) it is concluded that atomic nitrogen is involved and the formation of molybdenum nitrides is therefore excluded. Also, the large amount of nitrogen desorbing during the TPD performed after reaching the steady-state (see Figure 4.11) is an indication that the formation of nitrides is very unlikely, since they are too stable to desorb nitrogen at the temperatures applied.

In summary, the molybdenum phase on the calcined catalysts appeared to be highly dispersed up to approximately 10 wt% Mo. When pretreated with hydrogen, the dispersion started to decrease significantly at Mo contents exceeding 5 wt% Mo. The reducibility increases at increasing molybdenum content up to 10 wt% Mo, where the molybdenum surface seemed further reduced than Mo(IV) in MoO₂. This was ascribed to pairs of Mo(IV) ions in clusters of edge-sharing octahedra, which may be considered as nuclei of a MoO₂ phase. Overall, the dispersion of hydrogen pretreated catalysts is lower than when calcined.

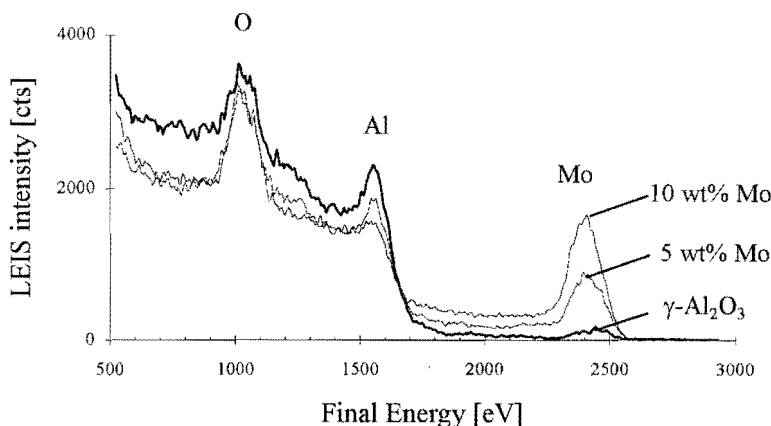
Under reaction conditions molybdenum is converted into a MoO₂ surface structure containing both Mo(IV) and Mo(VI) ions. The formation of nitrides is excluded, whereas the deposition of carbon is negligible.

3.2-4 Low Energy Ion Scattering.

Low Energy Ion Scattering (LEIS) is an extremely surface sensitive technique, enabling the selective analysis of the outermost atomic layer. In catalysis, the analysis of this layer can be of great importance, since it is precisely this layer which is directly involved with the catalytic reaction. When applied to "real" catalysts, LEIS can supply information on structure, composition and dispersion of the active material. Also effects of thermal treatment, adsorption/desorption and reduction/oxidation can be studied [24].

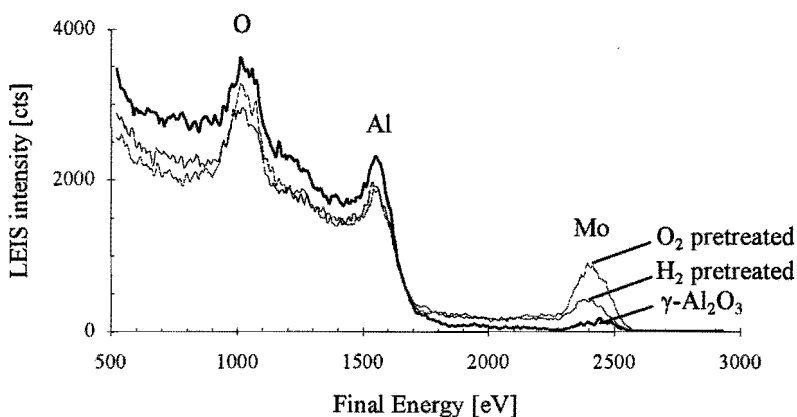
As already shown in chapter 2, section 3.6, it was possible to perform static LEIS, which implies that damage caused by the ion bombardment is negligible. It also implies that light elements, such as adsorbed hydrogen, carbon and nitrogen species, are not very easily removed by sputtering. The calcined catalysts showed constant signals already after a low ion dose, indicating that the surface was not covered significantly by light elements. When a sample is pretreated with hydrogen, careful sputtering is necessary, until the signals present are constant.

Figure 4.22 shows the LEIS spectra of γ - Al_2O_3 and calcined catalysts with 5 and 10 wt% Mo. It appeared that the support already contained a little amount of molybdenum corresponding to less than 1 wt%. It is uncertain whether this concerned an impurity already present in the γ - Al_2O_3 , or a contamination caused by the sample preparation. The 5 wt% Mo catalyst showed a clear signal of molybdenum. At 5 wt% Mo, the amount of one third of a mono layer calculated according to [15] is added, where the area of a Mo cluster is determined at 20 \AA^2 . This implies that the aluminium signal decreased almost proportionally ($\sim 30\%$). The calcined catalyst containing 10 wt% Mo showed an increase of the Mo signal by a factor of two, which can be expected when the molybdenum is well-spread on the alumina surface, so very well detectable by LEIS. This is in agreement with the observed larger amount of shielding of the aluminium atoms ($\sim 57\%$).



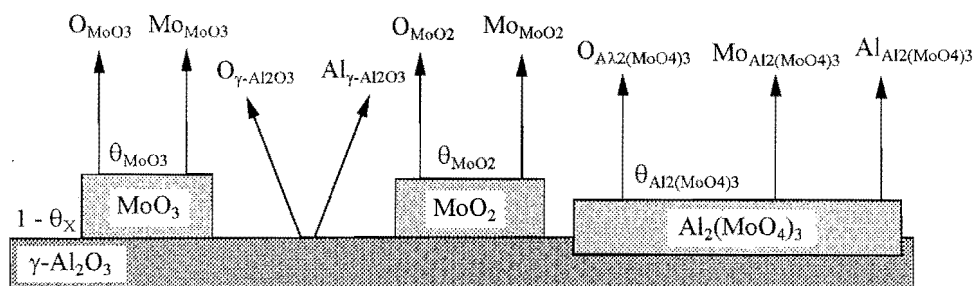
★ **Figure 4.22** LEIS spectra of 3 keV $^4\text{He}^+$ scattering from γ - Al_2O_3 and calcined catalysts with various molybdenum content. All spectra were taken after an ion dose of approximately $5 \cdot 10^{14}$ ions/cm 2 .

It is interesting to know how the surface composition changes upon hydrogen pretreatment. In Figure 4.23 the spectra are shown of a hydrogen and an oxygen pretreated 5 wt% Mo catalyst. The molybdenum signal decreased enormously ($> 50\%$), comparing the hydrogen pretreated with the calcined catalyst, whereas the oxygen signal decreased approximately 30% and the aluminium signal increased with 15%. This suggests a decrease in the dispersion upon hydrogen pretreatment of 50%. If agglomeration occurred, the particles must still be of very small size, considering the high catalytic activity of these catalysts. It is also possible that the decrease of the Mo signal originates from a different shielding by adjacent atoms (O or Al), due to a different structure formed upon hydrogen pretreatment. Since the sample was evacuated and transferred while still hot and a constant spectrum was obtained after a low ion dose, a large amount of adsorbed hydrogen is excluded.



★ **Figure 4.23** LEIS spectra of 3 keV $^4\text{He}^+$ scattering from $\gamma\text{-Al}_2\text{O}_3$, a hydrogen and an oxygen pretreated 5 wt% Mo catalyst. All spectra were taken after an ion dose of approximately $5 \cdot 10^{14}$ ions/cm 2 .

To obtain more specific information about the distribution and nature of the molybdenum phase on the alumina, an attempt was made to use the LEIS data quantitatively. Several compounds which were expected to be present in the catalyst were measured for reference purposes. A model was applied where the alumina surface is covered by different molybdenum structures expected to be present. A schematic representation is shown in Figure 4.24.



★ **Figure 24** Schematic representation of the Mo/ γ -Al₂O₃ surface with corresponding LEIS signals of O, Mo and Al, where θ_{Ξ} is the percentage of alumina covered with molybdenum, where X is MoO₂, MoO₃ or Al₂(MoO₄)₃.

When a combination of reference compounds is present in the catalyst, it must be possible to calculate the LEIS signals of the catalyst by using the composition of the signals of the reference compounds. The percentage of the alumina covered with molybdenum can be calculated according to Equations 4.1-4.4. Subsequently, the oxygen signal can be calculated, using the corresponding reference compound according to Equation 4.5, followed by comparison with the measured value and the conclusion of the best fit. When Al₂(MoO₄)₃ is

$$\theta_{Al} = (1 - ((Al_{cat}/Al_{\gamma-Al_2O_3})) * 100\% \quad \text{Equation 4.1}$$

$$\theta_{MoO_3} = (Mo_{cat}/Mo_{MoO_3}) * 100\% \quad \text{Equation 4.2}$$

$$\theta_{MoO_2} = (Mo_{cat}/Mo_{MoO_2}) * 100\% \quad \text{Equation 4.3}$$

$$\theta_{Al_2(MoO_4)_3} = (Mo_{cat}/Mo_{Al_2(MoO_4)_3}) * 100\% \quad \text{Equation 4.4}$$

$$S_O = \theta_X * O_X + (1 - \theta_X) * O_{\gamma-Al_2O_3} \quad \text{Equation 4.5}$$

$$S_{Al} = Al_{cat} - (\theta_{Al_2(MoO_4)_3}) * Al_{Al_2(MoO_4)_3} \quad \text{Equation 4.6}$$

where θ_X = the percentage of γ -Al₂O₃ covered with molybdenum based on different reference compounds

Mo_{cat}, Al_{cat} = the molybdenum, aluminium signal of the catalyst.

S_O = the oxygen signal calculated from θ_X , O _{γ -Al₂O₃} and the oxygen signal of the reference compound applied (O_X)

S_{Al} = the correct aluminium signal of γ -Al₂O₃ of a catalyst when Al₂(MoO₄)₃ is assumed on the surface

present on the alumina surface, an independent proof can be obtained by calculating the aluminium signal originating from uncovered alumina according to Equation 4.6, which can be implemented in Equation 4.1, resulting in a real θ of $\text{Al}_2(\text{MoO}_4)_3$. The ratios of the signals, as well as the absolute areas of the reference compounds are listed in Table 4.1.

★ Table 4.1 The ratio of LEIS signals of the reference compounds with corresponding absolute areas scaled to the same beam current.

Reference compound	reference code	Al : O : Mo	
		Ratio	Normalised areas [10^3 cts]
MoO_2	1	- : 0.7 : 1	- : 227 : 331
MoO_3	2	- : 0.8 : 1	- : 290 : 374
$\gamma\text{-Al}_2\text{O}_3$	3	1 : 1.1 : -	106 : 120 : -
$\text{Al}_2(\text{MoO}_4)_3$	4	1 : 9.7 : 13.4	20.2 : 195 : 271

Calculations can be done by using the ratios of the signals present and by using the absolute areas, with the measured molybdenum signal as starting point. The measured data and the results of the calculations with corresponding reference compounds are listed in Table 4.2. The calculation is based on the measured Al:Mo ratio of the catalysts with which the ratio of oxygen is calculated by using the ratios of the reference compounds. Although the differences are small, the deviations are in similar direction: when MoO_3 is used as a reference species on the alumina for the calcined catalysts, the calculated oxygen ratio is too

★ Table 4.2 The ratios and areas for various Mo catalysts, calculated ratios with corresponding reference compounds and corresponding coverage θ , using data from Table 4.1 and equations 4.2-4.4.

Catalyst	Measured Al : O : Mo		Calculated ratios	θ [%]	Reference applied; code
	ratios	areas [10^3 cts]			
5 wt% Mo; calcined	1 : 2.1 : 1.4	74.5 : 154 : 105	1 : 2.2 : 1.4	28	2 + 3
			1 : 2.1 : 1.4	39	4 + 3
5 wt% Mo; reduced	1 : 1.4 : 0.5	84.1 : 109 : 45.3	1 : 1.35 : 0.5	14	1 + 3
			1 : 1.50 : 0.5	12	2 + 3
			1 : 1.36 : 0.5	17	4 + 3
10 wt% Mo; calcined	1 : 4.1 : 4.8	43.4 : 180 : 208	1 : 4.8 : 4.8	56	2 + 3
			1 : 4.5 : 4.8	77	4 + 3

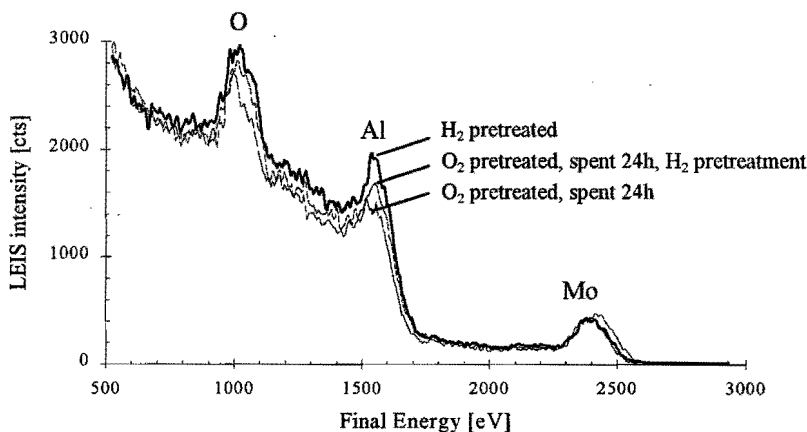
high. When using $\text{Al}_2(\text{MoO}_4)_3$ as a reference, the fit of the oxygen ratio was significantly better. For the reduced 5 wt% Mo catalyst, assuming the presence of MoO_3 resulted also in an oxygen ratio higher than the measured value. When fitting the oxygen signal with MoO_2 or $\text{Al}_2(\text{MoO}_4)_3$, the very small differences made it impossible to find the best fit. But the presence of MoO_2 is most likely to be correct, according to the XPS data as described earlier in section 3.2-3.

Using the absolute areas, the percentage of the alumina covered with molybdenum can be calculated. According to the aluminium signal of the calcined 5 wt% Mo catalyst, 30% of the alumina is covered according to Equation 4.1 $((1-(74.5/106)*100\%))$. Assuming the presence of MoO_3 on the surface, only 28% is covered according to Equation 4.2 $((105/374)*100\%)$, whereas $\text{Al}_2(\text{MoO}_4)_3$ on the surface accounts for 39% coverage of the support (Equation 4.4: $(105/271)*100\%$). These calculations concern only the aluminium and molybdenum signals, which have to be in agreement with the oxygen signal. When the oxygen signal is calculated assuming MoO_3 on the surface, the value of 168 is too high, compared to the measured signal of 154 (Equation 4.5: $0.28*290 + 0.72*120 = 168$). Assuming $\text{Al}_2(\text{MoO}_4)_3$ on the surface, the calculated amount of oxygen fits better the measured value of 154 (Equation 4.5: $0.39*195 + 0.61*120 = 149$). That $\text{Al}_2(\text{MoO}_4)_3$ is the most plausible structure on the alumina is substantiated independently by calculating the aluminium signal of uncovered $\gamma\text{-Al}_2\text{O}_3$ using Equation 4.6 $(74.5-0.39*20.2 = 66.6)$. This value corresponds with a coverage of 37% (Equation 4.1). The same calculations applied to the calcined 10 wt% Mo catalyst yield a coverage of $\gamma\text{-Al}_2\text{O}_3$ of 77 % with $\text{Al}_2(\text{MoO}_4)_3$. Considering the presence of small amounts of bulk $\text{Al}_2(\text{MoO}_4)_3$ in the calcined 10 wt% Mo, as detected by XRD (see section 3.2-1), it can be concluded that at 10 wt% the maximum adsorption capacity of $\gamma\text{-Al}_2\text{O}_3$ is exceeded a little, although only 77% of the alumina is covered. This is in agreement with the observations of van Veen *et al.* [12], where the Mo adsorption levels on $\gamma\text{-Al}_2\text{O}_3$ varied from 8 to 10 wt% Mo, dependent on the pH of adsorption solution, which is approximately 60 to 70% of the calculated maximum coverage.

When hydrogen pretreated, the fit seemed to be more complicated. Still, Equations 4.1-6 can be applied, resulting in a coverage of $\gamma\text{-Al}_2\text{O}_3$ of 21% (Equation 4.1: $1-(84.1/106)$) or 14% (Equation 4.3: $45.3/331$). The fitted oxygen signal is much higher compared to the measured value of 109: 150 (for 14%) or 160 (for 21% coverage). The XPS analysis of the reduced catalysts showed a Mo $3d_{5/2}$ signal at ~ 228.4 eV, whereas this signal for MoO_2 is positioned at ~ 229.5 eV. This suggests that by a hydrogen treatment more oxygen is removed from the surface, resulting in a lower oxygen signal measured with LEIS. So, from the coverage calculated, it is concluded that, when pretreated in hydrogen, approximately

50% less of the alumina is covered with molybdenum than when pretreated in oxygen, so a decrease of the dispersion upon hydrogen pretreatment is estimated at 50%.

It is of great interest to know if changes occur in the surface composition due to reaction, and if adsorbed species are present randomly or on specific positions. An attempt was made to elucidate some of these aspects by LEIS analysis on a spent catalyst. Figure 4.25 shows spectra of the 5 wt% Mo catalyst. A fresh hydrogen pretreated catalyst is compared with a calcined one spent for 24 hours without treatment and a hydrogen treatment prior to the measurement. Clearly, it can be seen that the molybdenum signal was hardly influenced when submitted to the different conditions. Both the oxygen and the aluminium signal were lower compared to the freshly hydrogen pretreated catalyst, and increased little after a hydrogen treatment. This indicates that carbon deposition occurred on the alumina surface and not significantly on the molybdenum. Also, the fact that the spectra are similar when hydrogen pretreated or spent for 24 hours, indicates that the catalyst has reached a similar regarding molybdenum structure during reaction.



★ **Figure 4.25** LEIS spectra of 3 keV $^4\text{He}^+$ scattering from a hydrogen, an oxygen pretreated 5 wt% Mo catalyst after reaching the steady-state without treatment and with hydrogen treatment prior to the analysis. All spectra were taken after an ion dose of approximately $5 \cdot 10^{14}$ ions/cm².

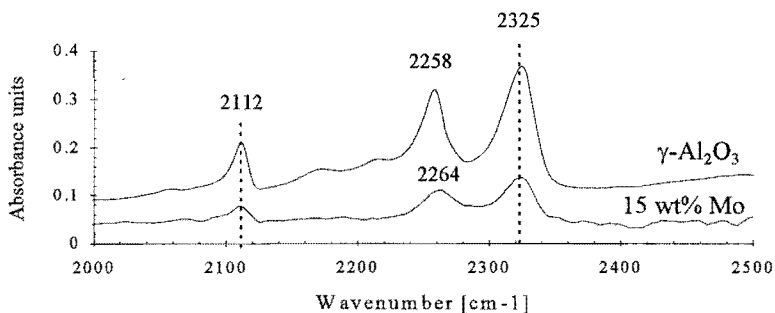
In summary, LEIS has proven to be a powerful tool to estimate quantitatively the coverage of the support with the active material. By applying a model of different reference compounds, it was concluded that for calcined catalysts molybdenum is present as highly dispersed $\text{Al}_2(\text{MoO}_4)_3$ on the $\gamma\text{-Al}_2\text{O}_3$ surface. At a coverage of 10 wt%, where the maximum

adsorption capacity of alumina is little exceeded, only 77% of the $\gamma\text{-Al}_2\text{O}_3$ is covered with $\text{Al}_2(\text{MoO}_4)_3$, indicating that adsorption occurs at specific sites. When hydrogen pretreated, the molybdenum surface species could best be described as MoO_2 -like, although a larger amount of surface oxygen was removed compared to pure MoO_2 . A decrease in dispersion of approximately 50% was found upon hydrogen pretreatment. Carbon deposition was observed only significantly on the alumina surface.

3.2-5 Fourier-Transform Infrared spectroscopy.

Infrared investigations of ammonia adsorption on oxides is now a classical method for detecting Brønsted and Lewis centres on the surface. The criterion for determining their presence is the formation of ammonium ions for Brønsted centres and coordination of ammonia on Lewis centres. When ammonia was adsorbed on $\gamma\text{-Al}_2\text{O}_3$ supported molybdenum catalysts at room temperature (RT), Lewis and Brønsted sites could clearly be determined. Although the differences were small, it was possible to distinguish the adsorption on the support and on the molybdenum phase. On $\gamma\text{-Al}_2\text{O}_3$, bands of coordinated ammonia (Lewis) were observed at 1245 and 1621 cm^{-1} (δ_s and δ_{as} respectively), whereas on the supported molybdenum catalysts these bands were at 1255 and 1612 cm^{-1} . The ammonium (Brønsted) bands for the support were located at 1392 and 1479 cm^{-1} and for the calcined supported molybdenum catalysts at 1440 cm^{-1} . When pretreated with hydrogen, this band shifted to 1470 cm^{-1} , whereas the intensity decreased, indicating that weakening of the Brønsted acid centres had occurred [25]. When ammonia was adsorbed at higher temperatures, the amount of ammonia adsorbed on the Brønsted centres decreased, due to the weaker adsorption strength compared to Lewis sites. No indications were found of the formation of NH_x species.

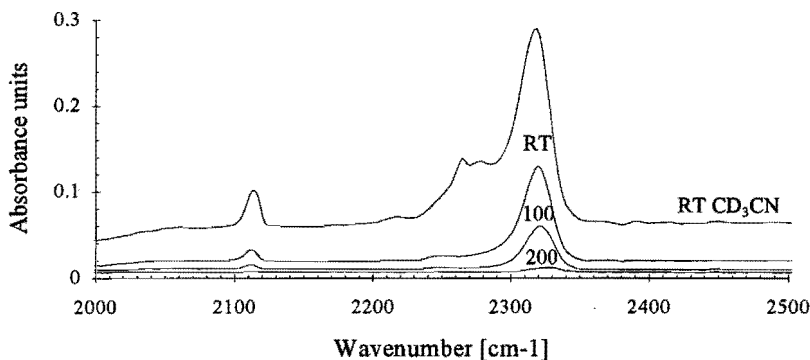
The adsorption of deuterated acetonitrile can also reveal the presence of different sites on the oxidic surface. Figure 4.26 shows IR spectra of CD_3CN adsorption at RT on $\gamma\text{-Al}_2\text{O}_3$



★ **Figure 4.26** IR difference spectra of CD_3CN adsorption at RT on $\gamma\text{-Al}_2\text{O}_3$ and a hydrogen pretreated 15 wt% Mo catalyst.

and a hydrogen pretreated 15 wt% Mo catalyst. The band at 2325 cm^{-1} originates from adsorption on Lewis centres, whereas bands due to physisorbed d_3 -acetonitrile were observed at 2112 and 2264 cm^{-1} . Gas phase CD_3CN was observed at 2258 cm^{-1} [26].

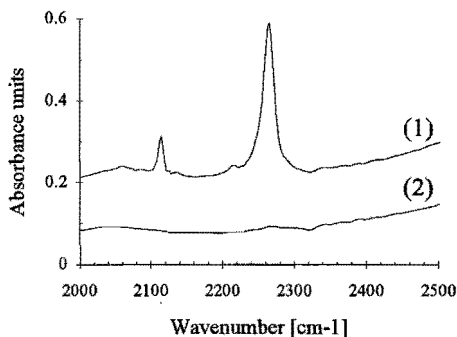
When the desorption behaviour of d_3 -acetonitrile is investigated by IR, the temperature at which the various bands disappear should differ, due to different strength of adsorption. This is shown in Figure 4.27 for the hydrogen pretreated 15 wt% Mo catalyst after adsorption of



★ **Figure 4.27** IR difference spectra of CD_3CN adsorption on a hydrogen pretreated 15 wt% Mo catalyst, after 30 min degassing at RT, after 1 h degassing at 100 and 200 °C.

CD_3CN at RT. After degassing for 30 minutes at RT, the largest amount of the physisorbed CD_3CN had already disappeared. While annealing, almost all acetonitrile had desorbed at 200 °C. This implies that acetonitrile is not strongly adsorbed on the catalyst surface.

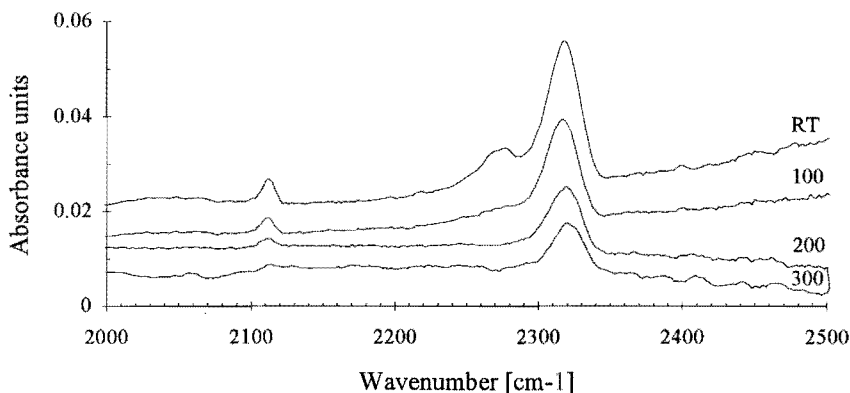
When ammonia was pre-adsorbed at RT on the hydrogen pretreated 15 wt% Mo catalyst, only bands of physisorbed CD_3CN were observed at 2112 and 2265 cm^{-1} (see Figure 4.28; spectrum (1)). After 30 minutes of degassing, all bands of acetonitrile had disappeared (see Figure 4.28; spectrum (2)). This indicates that ammonia is strongly adsorbed on the catalyst surface, and was blocking the sites for acetonitrile. Apparently, acetonitrile is weaker bonded, thus not capable of driving ammonia from the surface. This is similar to



★ **Figure 4.28** IR difference spectra of the adsorption of CD_3CN at RT on a H_2 pretreated 15 wt% Mo catalyst pre-adsorbed with NH_3 (1), after degassing at RT for 30 min (2).

previous TPre experiments [6], where ammonia was necessary to remove acetonitrile formed under reaction conditions on the catalyst surface from ethylene and pre-adsorbed ammonia by competitive adsorption.

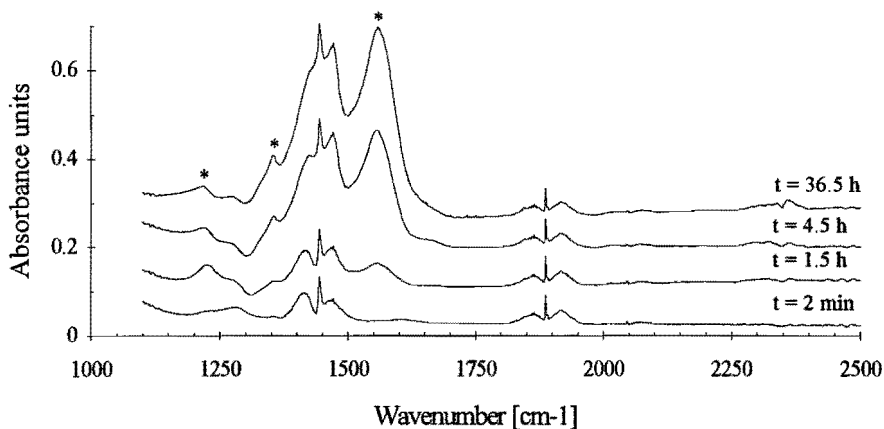
When a similar procedure was repeated at 300 °C, different phenomena were observed. At 300 °C, ammonia was adsorbed, followed by cooling to RT at which d_3 -acetonitrile was introduced. As can be seen in Figure 4.29, 30 minutes evacuating at RT did not remove the bands at 2320, 2274 and 2112 cm^{-1} , which were ascribed previously to Lewis bonded and physisorbed acetonitrile. Even after degassing at 100, 200 and 300 °C for 1 hour did not remove the Lewis bonded acetonitrile. This indicates that by adsorbing ammonia at higher temperature seriously alters the molybdenum surface, resulting in Lewis acid sites of very high strength. Although clearly present when ammonia was adsorbed, no adsorption of acetonitrile at Brønsted sites was observed in all cases considered, which show a typical band in the 2280-2300 cm^{-1} region [26].



★ **Figure 4.29** IR spectra of CD_3CN adsorption at RT on a hydrogen pretreated 15 wt% Mo catalyst pre-adsorbed with NH_3 at 300 °C after 30 min degassing at RT, 1 h degassing at 100, 200, 300 °C.

The detection and identification of surface species under reaction conditions is of great interest, regarding the reaction mechanism. An attempt was made to monitor *in situ* the reaction of ethylene with the catalyst surface pre-adsorbed with ammonia. This is shown in Figure 4.30 for the calcined 15 wt% Mo catalyst pre-adsorbed with NH_3 at 375 °C. As a function of "time on stream" or ethylene exposure, a small amount of gaseous CO_2 was observed at 2350 cm^{-1} (after 36.5 h). No detectable amount of gaseous or adsorbed acetonitrile was formed and a large band emerged at 1560 cm^{-1} , along with small bands at

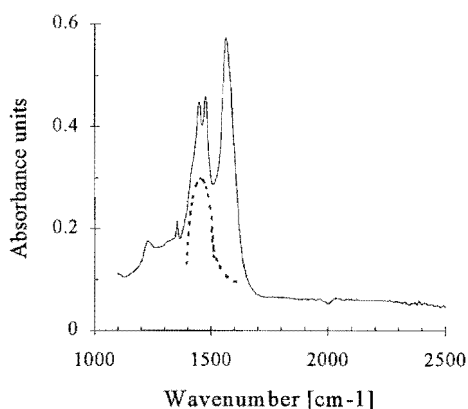
1350 and 1230 cm^{-1} . These bands were not observed when ethylene was introduced to a fresh catalyst. Obviously, the presence of gaseous ethylene obscured a large part of the spectrum, and no clear distinction between adsorbed species and gaseous compounds could be made.



★ **Figure 4.30** IR difference spectra after various time of ethylene exposure on a calcined 15 wt% Mo catalyst at 375 °C pre-adsorbed with NH_3 at 375 °C. The * indicate increasing bands upon exposure with ethylene.

By removing the gaseous compounds, a spectrum can be obtained of the catalyst surface which contains the remaining adsorbed species. After the last spectrum recorded at 36.5 hours of ethylene exposure at 375 °C and evacuation the obtained spectrum is shown in Figure 4.31. Clearly the presence of adsorbed species are visible. Bands at 1227, 1355, 1450, 1470 and 1564 cm^{-1} were present. The shoulder at 1410 cm^{-1} originates from broad a band at approximately 1440 cm^{-1} (dotted line in Figure 4.31) and can be ascribed to non-coordinated carbonate ($\nu_{\text{as}} \text{CO}_3^{2-}$: 1450-1420, $\nu_{\text{s}} \text{CO}_3^{2-}$: 1090-1020 [25]). This species is likely to be the precursor for CO_2 formation. The maxima at 1355 and 1564 cm^{-1} fall inside the frequency range characteristic of formate species. However, the intensity at 1564 cm^{-1} is of the order of magnitude that the presence of ν_{CH} at 2890-2970 cm^{-1} and δ_{CH} at 1380 cm^{-1} should also be detectable. The band at 1355 together with the band at 1450 cm^{-1} are more likely due to methyl bending [27], whereas the band at 1564 cm^{-1} is typical for a C=N stretch frequency [28]. The band at 1478 cm^{-1} can be ascribed to CH_2 bending. The assignment of the band at 1227 cm^{-1} is more complicated. The region for =NH bending is typical at 1150-1180 cm^{-1} on

silicon oxynitrides [29], whereas C-N stretch frequencies are found in the region of 1020-1250 cm^{-1} . When adsorbing ammonia at higher temperatures, also the formation of =NH is to be expected. Since no indications were found of the presence of =NH and the presence of both CH_3 and CH_2 was already suggested, the band at 1227 cm^{-1} originates most likely from a C-N group.



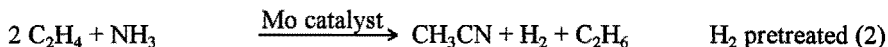
★ **Figure 4.31** IR spectrum of Figure 5.30 after 36.5 h after evacuation and cooling to RT.

In summary, when ammonia is adsorbed on $\gamma\text{-Al}_2\text{O}_3$ and $\text{Mo}/\gamma\text{-Al}_2\text{O}_3$ catalysts, IR clearly shows the presence of Lewis and Brønsted acid sites. The Brønsted acidity of the catalysts decreased upon hydrogen pretreatment, and ammonia adsorption at elevated temperature showed only adsorption at Lewis sites. No NH_x species were detected by IR. By the adsorption of CD_3CN at various conditions it is concluded that by adsorbing ammonia at high temperatures, the surface is modified. Sites are created sites on which acetonitrile is stronger bonded than on a fresh catalyst surface. When exposing the catalyst surface pre-adsorbed with ammonia at 375 °C to ethylene, gaseous CO_2 was detected formed from a non-coordinated carbonate species, also detected by IR. Also, strong indications are found of $\text{CH}_3\text{-CH}_2\text{-N=}$ and $\text{CH}_3\text{-CH=N-}$ surface species. No band frequencies are found of a $\text{C}\equiv\text{N}$ species or gaseous acetonitrile. This is expected, since no gaseous ammonia was present to push the acetonitrile precursor from the catalyst surface by competitive adsorption. If acetonitrile is formed, the concentration will be below the detection limit.

3.3 Proposed reaction mechanisms.

It is expected that the formation of the main side-products is a strong function of the catalyst pretreatment. Water and CO_x were dominant on oxygen pretreated catalysts. Because of the formation of water, the formation of acetonitrile on an oxidic catalyst surface is favoured thermodynamically. Hydrogen pretreated catalysts formed mainly ethane and hydrogen. Only little water and CO and no CO_2 were observed in the semi-steady-state period. It should be remembered that the formation of acetonitrile and hydrogen directly from ethylene and ammonia is thermodynamically unfavourable ($\Delta G^0(427\text{ °C}) \sim 10\text{ kJ/mol}$). This in contrast to

the hydrogenation of ethylene: $\Delta G^0(427\text{ }^\circ\text{C}) \sim -50\text{ kJ/mol}$. Since ethane is always the main side product for hydrogen pretreated catalysts and catalysts in the steady-state period ($\sim 50\%$ selectivity), this exothermic reaction probably delivers the energy needed to drive the reaction. The following two mechanisms are proposed (see Scheme 4.1):



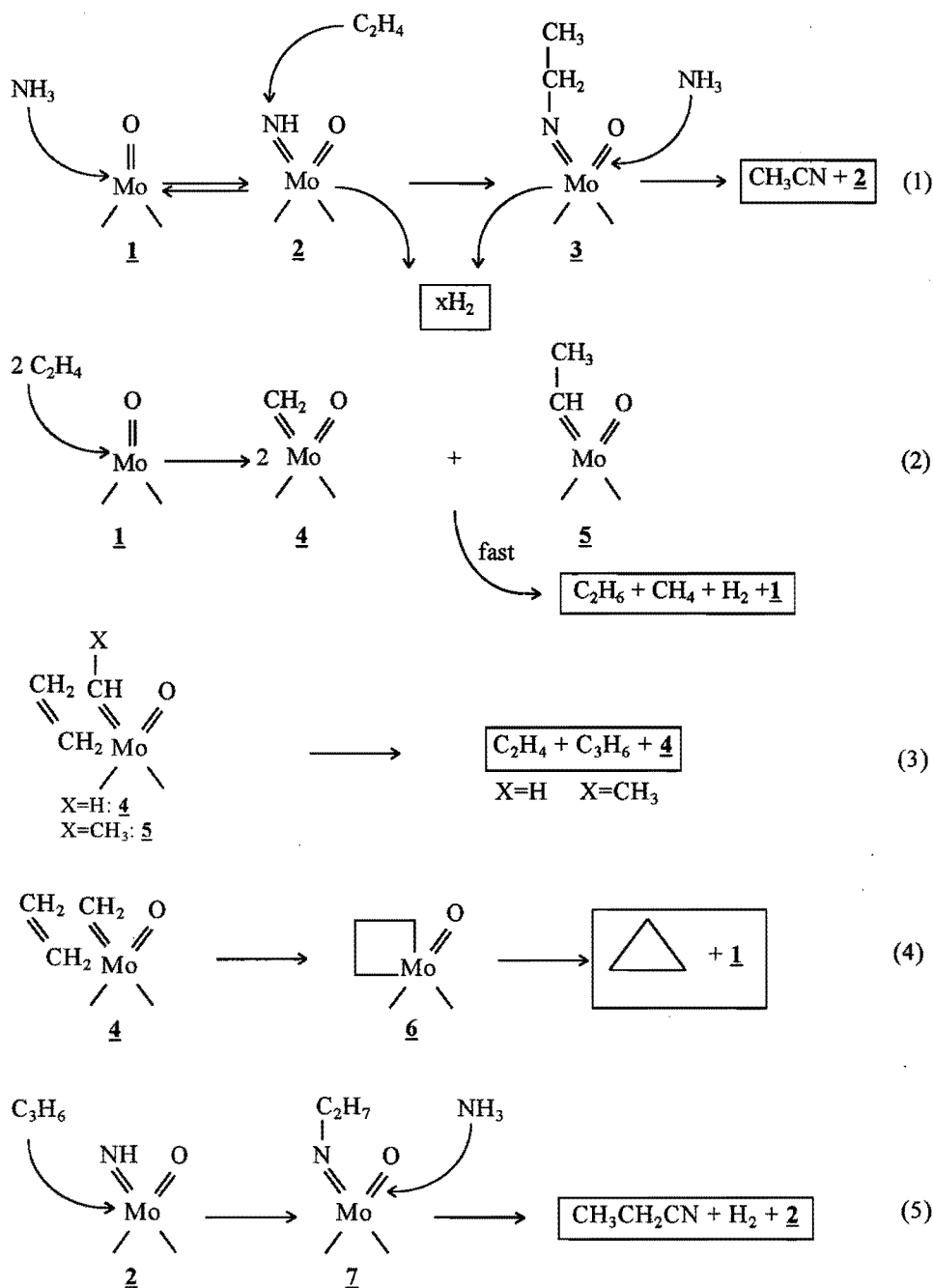
★ **Scheme 4.1** Two mechanisms forming acetonitrile out of ethylene and ammonia over $\text{MoO}_x/\gamma\text{-Al}_2\text{O}_3$ catalysts.

Since no molecular oxygen is present in the feed, it is obvious that deactivation occurs in mechanism (1), because the catalyst acts as a reactant. Apart from the fact that lattice oxygen is not replenished, this mechanism is similar to the ammoxidation mechanism proposed by Grasselli *et al.* [9] In mechanism (2) no deactivation is expected, due to the fact that the catalyst is not altered by reaction. It is therefore suggested that the two mechanisms occur on different sites formed by different molybdenum structures. Since conditions were found where besides acetonitrile, both oxygen containing products (water, CO_x) and non-oxygen containing products (methane, ethane and hydrogen) were formed, it is concluded that the two mechanisms can occur simultaneously. The semi-steady-state condition where this happened showed a strong structure sensitivity.

It appears that during reaction a calcined catalyst, where mechanism (1) is dominant, changes into a catalyst where mechanism (2) dominates after removal of lattice oxygen. This transition proceeds gradually for molybdenum contents of 5 wt% or less. At higher molybdenum contents only after reductive treatment a gradual transition is observed. When calcined, the transition proceeds via a minimum in the formation of acetonitrile, due to a different structure present in these catalysts, namely large $\text{Al}_2(\text{MoO}_4)_3$ crystals. These crystals are destroyed during reaction, resulting in a highly active period where side reactions dominate. The $\text{Al}_2(\text{MoO}_4)_3$ crystals can also be destroyed by a hydrogen pretreatment, resulting in a gradual transition period. Surface oxygen is removed by reaction until depletion, reaching the steady-state. This way the molybdenum phase is converted into a particular stable structure, acting as a real catalyst. This structure is suggested to be a highly dispersed MoO_2 -like species.

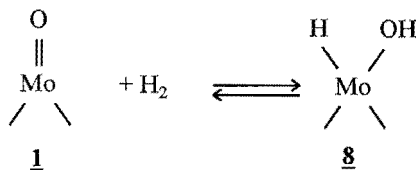
A TPD performed after reaching the steady-state, suggested the presence of =NH and =CH₂ and/or =CH-CH₃ surface species. The formation of =CH₂ species on a photoreduced Mo/SiO₂ catalyst was recognised by Vikulov *et al.* [30] using IR spectroscopy, and was supposed to be a thermally stable complex. This complex was formed on the co-ordinately unsaturated Mo⁴⁺ ions from the interaction with cyclopropane. They also detected a molybdena-cyclobutane intermediate; Mo[□], which was formed after ethylene chemisorption on the Mo=CH₂ complexes. The formation of both Mo=CH₂ and Mo=CH-CH₃ was established by chemisorption of methylcyclopropane, of which the latter was converted fast to the former in the presence of excess gaseous ethylene, forming propylene. In excess of propylene, little conversion of Mo=CH₂ to Mo=CH-CH₃ was observed. At present it is generally accepted that Mo-carbene and Mo-cyclobutane complexes are the active intermediates for olefin methathesis [31].

During the steady-state, the ammonia is dissociated into hydrogen and surface =NH. This hydrogen is partly consumed by ethylene forming ethane, which desorbs fast. The components methane, nitrogen and very little hydrogen desorbing during the TPD, performed after reaching the steady-state, must originate from the active species adsorbed on the catalyst surface. The following reaction mechanism is proposed in Scheme 4.2. Reaction (1) shows the formation of acetonitrile on a coordinately unsaturated Mo⁴⁺ site (Scheme 4.2; complex **1**). Ammonia is activated by the release of hydrogen, forming a =NH species (**2**). The ethylene couples via a π -interaction, followed by a H-shift as a σ -N ethyl species (**3**). By competitive adsorption of ammonia, the σ -N ethyl surface species is pushed from the catalyst surface as acetonitrile, releasing two hydrogen molecules: one from dehydrogenation of the surface species and one from ammonia activation. Ethylene can also interact with the coordinately unsaturated Mo⁴⁺ sites according to reaction (2), forming surface carbene **5**, which can easily be converted to **4**. These surface carbenes can be hydrogenated to methane and ethane, consuming the hydrogen formed by reaction (1). Since these reactions are exothermic and the desorption of products is fast, the reaction (1) will be accelerated, resulting in a higher turnover frequency of the active site **1**. The surface carbenes in **4** and **5** can participate in methathesis according to reaction (3), forming ethylene and propylene. The surface methylene in **4** can also form a molybdena-cyclobutane intermediate (**6**) according to reaction (4), resulting in the formation of cyclopropane. The little amount of propionitrile is believed to be a result of a consecutive reaction of propylene with surface =NH according to reaction (5), which is similar to reaction (1), forming a σ -N propyl species (**7**). In all five reactions, the surface Mo=O species seems to be only a spectator. Obviously, the formation of a surface hydroxyl group to accommodate temporarily a hydrogen atom prior to hydrogen desorption, can not be excluded. The reversible adsorption of hydrogen on coordinately

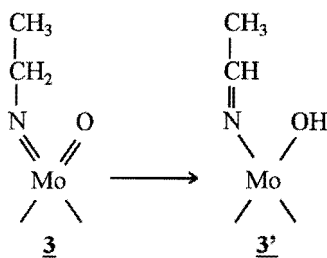


★ Scheme 4.2 Reaction mechanism scheme for various products formed from ethylene and ammonia during steady-state on γ - Al_2O_3 supported molybdenum catalysts.

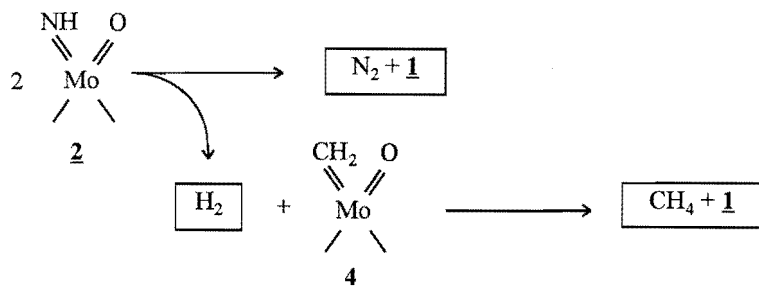
unsaturated Mo⁴⁺ sites was suggested by Lo Jacono and Hall to proceed via the heterolytic cleavage of H₂ [32]:



It is likely that during reactions (1), (2) and (5) the formation of **8** played an important role. However, it is certain that the oxygen is not removed by the formation of water or CO_x. With IR, bands originating from both C-N and C=N were identified, implying that **3** can be converted to **3'** according to:



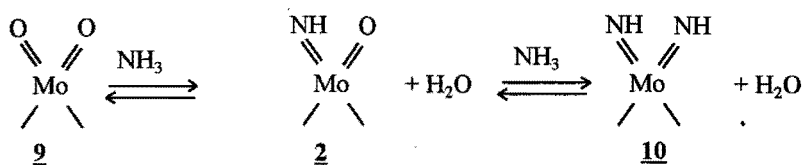
When after quenching the reaction at steady-state a TPD is performed, only the surface imide **2** and the surface methylene **4** were present, considering the desorption products. The dissociation of these species during TPD is suggested to be as follows (see Scheme 4.3):



★ **Scheme 4.3** The dissociation during TPD of the active surface species present at steady-state on γ-Al₂O₃ supported molybdenum catalysts.

Previously, ammonia TPD experiments on hydrogen pretreated Mo/ γ -Al₂O₃ catalysts showed that the adsorbed NH species dissociated to H₂ and N₂, and the hydrogen desorbed at lower temperature [6]. This explains in Figure 4.10 the position of the maximum of CH₄ at lower temperature than the N₂. The hydrogen released by the dissociation of surface NH is used for the hydrogenation of the surface methylene.

On calcined catalysts in the semi-steady-state period, the activation of ammonia proceeds via a condensation reaction (see Scheme 4.4):



★ Scheme 4.4 The activation of ammonia on fresh calcined γ -Al₂O₃ supported molybdenum catalysts [9].

This surface reaction is, besides combustion, the only one possible, resulting in a catalyst that is highly selective. However, it concerns a slow reaction, and the water produced is not consumed, so no acceleration of the equilibrium will occur. So, despite the high selectivity, the catalyst will show a low activity, resulting in a low yield of acetonitrile. The formation of species 10 on hydrogen pretreated catalysts and catalysts at steady-state can not be excluded, and therefore also participate in reaction (1) and (5) of Scheme 4.2.

4 Conclusions.

Two mechanisms are suggested for the formation of acetonitrile: one based on the ammoxidation mechanism with the consumption of lattice oxygen. The other is based on oxidative ammonolysis, i.e. without consumption of lattice oxygen. For thermodynamic considerations a synergetic formation of ethane and acetonitrile is suggested.

The mechanisms can occur separately or simultaneously, depending on the amount of removable lattice oxygen. On freshly calcined catalysts in the semi-steady-state period only the ammoxidation mechanism is active. These catalysts are highly selective but not very active, attributed to Mo(VI) sites present on a Al₂(MoO₄)₃ surface structure, which has a

strong interaction with the support. When pretreated with hydrogen both mechanisms can be active in the semi-steady-state period. The activity is higher, whereas the selectivity to acetonitrile is lower, compared to the calcined catalysts. This is due to Mo(IV) sites present besides Mo(VI), containing one surface Mo=O, which enhance N-H and C-H activation more effectively. On catalysts at steady-state, acetonitrile is only formed via oxidative ammonolysis, independent of the pretreatment or molybdenum content. A reduced molybdenum structure is obtained which is not altered further by reaction, and acts as a real catalyst. This structure is suggested to be MoO₂-like and can only be formed by the removal of lattice oxygen under reaction conditions. The lattice oxygen can be removed by the release of water, forming acetonitrile, or by side reactions forming CO_x, dependent on the concentration. At a high concentration of lattice oxygen (high Mo content), the side reactions are strongly enhanced until depletion.

XPS showed only Mo(IV), Mo(VI) and probably Mo(V) species. The reducibility increases with increasing Mo content, due to presence of polymeric molybdate species which are easier to reduce. When hydrogen pretreated, a decrease in the dispersion of approximately 50% is observed. Since the activity of these catalysts is significantly higher, it is suggested that a decrease in the interaction of molybdenum with the alumina surface has occurred. However, large reduced molybdenum particles are too active towards complete ammonia dissociation, resulting in the termination of the selective reaction and a strong increase in the formation of side products. So, when reduced and with mediate molybdenum content will yield the best catalyst, containing highly dispersed MoO₂ for the formation of acetonitrile from ethylene and ammonia via oxidative ammonolysis.

Literature cited

- 1 Boudard, M., *"Advances in Catalysis"* (D.D. Eley, H. Pines, P.B. Weisz, Eds.), Academic Press, New York, **20** (1969) 153
- 2 Boudart, M., *Proc. 6th ICC*, London, The Chemical Society, **1** (1976) 1
- 3 Andersson, A., Hansen, S., *J. Catal.* **114** (1988) 332 and references herein
- 4 Pitchai, R., Klier, K., *Catal. Rev.-Sci. Eng.*, **28(1)** (1986) 13
Van Santen, R.A., Kuipers, H.P.C.E., *Adv. Catal.*, **35** (1987) 265
Carter, E.A., Goddard III, W.A., *Surf. Sci.*, **220** (1989) 243
- 5 Ozaki, A., Miyazaki, Y., Sato, Y., Ohki, K., *Kogyo Kagaku Zasshi* **69** (1966) 59
Takahashi, N., Minoshima, H., *Chem. Lett.* (1994) 1323
Yamauchi, T., Matsuda, S., *Sekiyu Gakkaishi* **3** (1960) 111
Takahashi, N., Sakagami, H., Kamishima, T., Azuma, S., Matsuda, T., *Catal. Lett.* **36** (1996) 241
Sokolovskii, V.D., Davydov, A.A., Ovsitser, O.Yu., *Catal. Rev.-Sci. Eng.* **37(3)** (1995) 425
- 6 This thesis, chapter 3
- 7 Grünert, W., Stakheev, A.Y., Mörke, W., Feldkraus, R., Anders, K., Shpiro, E.S., Minachev, K.M. *J. Catal.*, **135** (1992) 269
- 8 van Leerdam, G.C., Ph. D. thesis, Univ. Eindhoven, 1991, chapter 7

- 9 Grasselli, R.K., Burrington, J.D., *Adv. Catal.*, **87** (1987) 363
- 10 Aykan, K., *J. Catal.* **12** (1968) 281
- 11 Rajagopal, S., Marini, H.J., Marzari, J.A., Miranda, R., *J. Catal.* **147** (1994) 417
- 12 van Veen, J.A.R., Hendriks, P.A.J.M., Romers, E.J.G.M., Andréa, R.R., *J. Phys. Chem.* **94** (1990) 5275
- 13 JCPDS-card 23-764
- 14 Giordano, N., Bart, J.C.J., Vaghi, A., Castellan, A., Martinotti, G., *J. Catal.* **36** (1975) 81
- 15 Sonnemans, J., Mars, P., *J. Catal.* **31** (1973) 209
- 16 Asmolov, G.N., Krylov, O.V., *Kinet. Katal.* **11** (1970) 1028
- 17 JCPDS-card 32-671
- 18 Defossé, C., Canesson, P., Rouxhet, P.G., Delmon, B., *J. Catal.* **51** (1978) 269
Shalvoy, R.B., Reucroft, P.J., *J. Electron Spectrosc. Relat. Phenom.* **12** (1977) 351
Angevine, P.J., Vartuli, J.C., Delgass, W.N., *Proc. 6th Int. Congr. Catal.* **2** (1976) 611
Kerkhof, F.P.J.M., Moulijn, J.A., *J. Phys. Chem.*, **83**(12) (1979) 1612
- 19 Kuipers, H.P.C.E., van Leuven, H.C.E., Visser, W.M., *Surf. Interface Anal.* **8** (1986) 235
- 20 Scofield, J.H., *J. Electr. Spectr. Rel. Phen.* **8** (1976) 129
- 21 Seah, M.P., Dench, W.A., *Surf. Interf. Anal.* **1**(1) (1979) 1
- 22 De Jong, A.M., Borg, H.J., Van IJzendoorn, L.J., Soudant, V.G.F.M., De Beer, V.H.J., Van Veen, J.A.R., Niemantsverdriet, J.W., *J. Phys. Chem.*, **97** (1993) 6477
- 23 Haber, J., Marczewski, W., Stoch, J., Ungier, L., *Ber. Bunsen-Ges.* **79** (1975) 970
- 24 Jacobs, J-P, Ph.D. thesis, Univ. Eindhoven, 1995, chapter 2 and references herein
- 25 Davydov, A.A., "Infrared Spectroscopy of Adsorbed Species on the Surface of Transition Metal Oxides." (1990) John Wiley & Sons Ltd, Chichester, England
- 26 Pelmenshikov, A.G., van Santen, R.A., Jänchen, J., Meijer, E., *J. Phys. Chem.* **97**(42) (1993) 11071
- 27 Martin, C., Martin, I., Rives, V., *J. Catal.* **145** (1994) 239
- 28 Yim, S-G, Son, D.H., Kim, K., *J. Chem. Soc., Faraday Trans.* **89**(5) (1993) 837
- 29 Lednor, P.W., de Ruiter, R., Emeis, K.A., "Better Ceramics Through Chemistry", *MRS Symposium Proceedings V* (M.J. Hampden-Smith, W.G. Klemperer, C.J. Brinker, Eds.) **271** (1992) 801
- 30 Vikulo, K.A., Shelimov, B.N., Kazansky, V.B., *J. Mol. Catal.* **65** (1991) 393
- 31 Mol, J.C., Moulijn, J.A., *Catal. Sci. Technol.* **8** (1988) 69
- 32 Lo Jacono, M., Hall, W.K., *J. Colloid and Interface Sci.*, **58**(1) (1977) 76

5

MOLYBDENUM MIXED OXIDES ON $\gamma\text{-Al}_2\text{O}_3$

Abstract.

In order to improve catalytic performance in the formation of acetonitrile from ethylene and ammonia, several secondary compounds were added to $\gamma\text{-Al}_2\text{O}_3$ supported molybdenum catalysts. Transition metals of all series were selected: Mn, Cr, Cu, Ni, Ag, Rh and Pt. Two Mo loadings and different pretreatments were applied and the concentration of some secondary transition metals was varied. Catalytic tests were performed by introducing ethylene to a catalyst pre-adsorbed with ammonia.

Strong promoter effects for the formation of acetonitrile were observed for the oxygen pretreated molybdenum catalyst containing Ni or Cr. Also, the hydrogen pretreated molybdenum catalyst containing Mn in a Mo:Mn ratio of 5:1 and 5:1.75 showed a promoter effect. These three catalysts were submitted to reaction under flow conditions after an oxygen treatment, and showed a higher amount of acetonitrile in both in the semi-steady-state, except for the MoMn catalyst, and the steady-state period, compared to the unpromoted catalyst.

The formation of an $\text{Al}_2(\text{MoO}_4)_3$ phase at higher molybdenum content is suppressed by the presence of Mn, Cr or Ni. It is suggested that the chemical interaction of these transition metals with alumina or molybdenum is more favourable. The formation of NiAlO_4 was confirmed. It was observed that agglomeration of the molybdenum phase was induced by the addition of Mn, Ni or Cr, so a decrease in the interaction of molybdenum with the alumina surface is expected. After reaching the steady-state, Cr was present as Cr_2O_3 and Mn as MnO_2 , whereas Ni was present in different forms, probably Ni^0 and NiO. Manganese appeared to retard the reduction of Mo further than MoO_2 , which resulted in a less active but more selective catalyst. The addition of Cr or Ni resulted in a highly reduced Mo surface, which appeared still MoO_2 -like. The addition of Ni and Cr is not well understood, but a modification of the active site on molybdenum is suggested.

1 Introduction.

Supported metal catalysts are used in a variety of processes in the chemical and petroleum industries. In addition to an active metal and support, industrial catalysts often contain a number of secondary components, known as promoters. Promoters are additives which, although themselves inactive, improve the activity, the selectivity or the stability of the unpromoted catalyst [1]. The term promoter is usually restricted to compounds which are added in small amounts. Unfortunately, the role of promoters in catalysis is only poorly understood. A better insight into the ways in which secondary components influence the behaviour of an active metal may lead to significant improvements in the preparation of supported metal catalysts.

In order to improve catalytic performance in the formation of acetonitrile from ethylene and ammonia, a number of elements of the Group VIII of transition metals were added as promoter to γ - Al_2O_3 supported molybdenum catalysts. The choice of the transition metals concerned members of all three series: of the first series copper, nickel, chromium and manganese; of the second series silver and rhodium and of the third series platinum. Not only possible promoter effects on the formation of acetonitrile were looked at, but also possible changes in the product composition with respect to the nitrogen containing ones. The metals applied will be introduced individually by a short literature survey, in particular focused on molybdenum containing bimetallic catalysts, whenever such information is available.

Catalysts containing platinum and molybdenum species on various supports have been studied for the past two decades by several research groups. In these studies, the catalysts were tested in reactions such as hydrogenolysis [2], hydrogenation [3], dehydrogenation [4], or isomerization of hydrocarbons [5] and in the synthesis of alcohols from CO and H_2 [6]. The synergistic effects of these bimetallic Pt-Mo catalysts has been interpreted in terms of well-dispersed platinum particles on the support, where both Pt and Mo are in contact with each other and where each metal plays an individual role, complementary to the other for the catalytic activity. In its application to ammoxidation reactions, an attempt was made to use this bifunctionality to form amines, where the nitrile formed on the Mo is hydrogenated by the Pt.

In the synthesis of acetonitrile from syngas and ammonia over silica supported molybdenum catalysts, the addition of silver resulted in a strong increase in activity and selectivity to acetonitrile [7]. It was suggested that MoO_2 is the active species for the formation of acetonitrile and that Ag has the effect of making MoO_2 amorphous or more dispersed.

Supported molybdenum catalysts containing rhodium play also an important role in the syngas conversion, enhancing the activity and selectivity to oxygenates [8,9,10]. A textural

promotion role was suggested for molybdenum oxide, wherein it stabilises smaller rhodium aggregates against sintering and agglomeration upon exposure to reaction conditions. Recent success in converting methane to syngas with high selectivity using rhodium monoliths [11] have motivated Bol *et al.* to study the fundamental steps in alkane oxidation on Rh (111) [12], where the rhodium must be precovered with oxygen to obtain aldehydes or ketones.

The Monsanto Company recognised already in 1981 the importance of molybdenum catalysts containing manganese in a process for preparing acetonitrile from syngas mixed with ammonia [13]. It was observed that in some cases manganese retarded the reduction of molybdenum below MoO₂. But also synergy effects by MnMoO₄/MoO₃ have been observed in selective oxidation catalysis by Ozkan *et al.* [14]. In the partial oxidation of C₄ hydrocarbons to maleic anhydride a catalytic job distribution was postulated to explain the synergy. According to this scheme, the active sites for the formation of the selective oxidation products are located on the MoO₃ phase through the use of its lattice oxygen. The MnMoO₄ phase contains the sites that can chemisorb the gas phase oxygen and allow it to migrate to the reduced sites on MoO₃ surfaces in an activated form through a spillover mechanism. Evidence for the existence of such a spillover phenomenon in multi-phase catalysts in selective oxidation reactions have also been reported by Delmon *et al.* [15].

Sulphided molybdenum catalysts supported on γ -Al₂O₃ with Co or Ni as the promoter have long been used in the industrial hydrotreating processes. Extensive studies have been conducted on the subject and have been summarised in several reviews [16]. The Ni-Mo/ γ -Al₂O₃ system is also the most active one when applied in hydrodenitrogenation [17]. The active sites of these catalysts are generated by means of reductive pretreatments. In oxidation reactions, Mazzocchia *et al.* [18] studied the oxidation of butane over NiO-MoO₃ catalysts, and the oxidation of 1-butene over the same catalysts [19]. Unsupported NiMoO₄ is also applied in the oxidation of butane [20].

Supported chromium oxides are well known to possess high catalytic activity in hydrogenation and dehydrogenation reactions of hydrocarbons, dehydrocyclization of paraffins and polymerisation of olefins [21]. Unsupported α -Cr₂O₃ was studied by Yao [22] in the oxidation of hydrocarbons and CO. It was concluded that at the reaction temperature neither the hydrocarbons nor CO would react with the surface lattice oxygen, and that C-H bond breaking was involved in the rate-controlling step of the ethane oxidation, but not in the case of ethylene. However, no literature is available about catalysts containing both Cr and Mo.

In the selective oxidation of propylene, bimetallic Cu-Mo catalysts are known to be active [23]. It was suggested that Cu¹⁺ ions are involved in the formation of active centres responsible for the total oxidation of propylene, probably due to the activation of oxygen,

whereas the presence of Cu^{2+} ions is necessary for the activation of propylene to allylic species, into which oxygen is then inserted to form acrolein.

All these examples show that bimetallic catalysts are at present the subject of considerable interest in catalysis, due to the fact that their properties are superior to those of monometallic catalysts. This chapter describes the study of $\gamma\text{-Al}_2\text{O}_3$ supported molybdenum catalysts containing a secondary compound and their activity towards the formation of acetonitrile, or other nitrogen containing organic compounds, from ethylene and ammonia. The first of the three sections contains the results of catalytic tests of an extensive set of promoted $\gamma\text{-Al}_2\text{O}_3$ supported molybdenum catalysts. The experimental procedure is similar to the sequential pulse method described in Chapter 3. The second section describes the results of a selection of the most promising promoted molybdenum catalysts of the first section submitted to flow conditions. The third section deals with the characterisation, such as HR-TEM, XRD and XPS of the catalysts described in the second section.

2 Catalytic tests by sequentially introducing the reactants.

2.1 Experimental procedure.

The catalysts were prepared according to the method described in Chapter 2, section 2.3, and the apparatus used for catalytic tests is described in section 4. The experimental procedure was identical to the one described in Chapter 3, section 3.2, and two reaction temperatures were compared, viz 425 and 460 °C. The TPD, performed subsequently to the isothermal period of pulsing ethylene consisted of heating in a flow of He with a heating rate 10 °C/min to 600 °C.

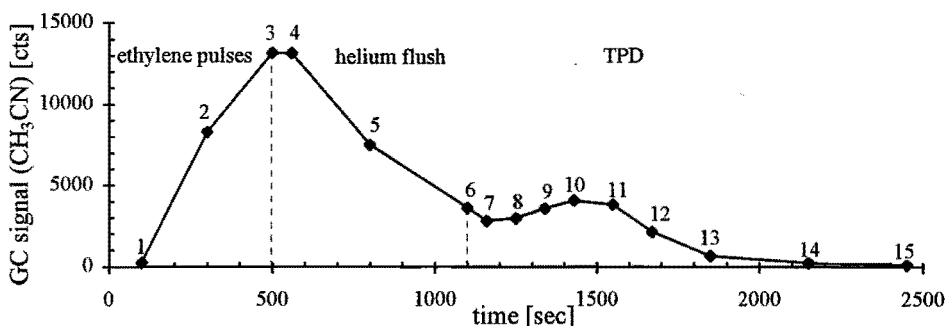
The experiments with the catalysts listed in Table 2.1 of Chapter 2 were done without a 16 loop valve, so only one sample could be analysed by GC. The moment of sampling was kept constant: at the last pulse of ethylene, where acetonitrile formation was at a maximum. Since no calibration data were available at the time, only a qualitative comparison of catalytic performance could be achieved, using the GC peak area. The experiments with the catalysts listed in Table 2.2 of Chapter 2 were done without a mass spectrometer, so saturation of the catalyst with ammonia could not be confirmed. Therefore the number of ammonia pulses was kept constant at 40 (total amount of 128 μmol). Only for the MoCu catalyst, the amount of 90 pulses was compared with 40 pulses of ammonia, since the catalyst coloured dark only in the first region of the catalyst bed, indicating that total saturation was not achieved after 40 pulses of ammonia.

During the introduction of ethylene and the subsequent TPD 15 samples were stored in the 16 loop valve for GC analysis. Since the GC was only equipped with a FID and no TCD was available, only organic components could be detected by the FID. The consecutive actions during an experiment are summarised in Table 5.1.

★ Table 5.1 Consecutive actions of GC-sample collection during a catalytic test.

sample #	$T_{\text{reaction}} = 425\text{ }^{\circ}\text{C}$		$T_{\text{reaction}} = 460\text{ }^{\circ}\text{C}$	
1	number of C ₂ H ₄ pulses	5	number of C ₂ H ₄ pulses	5
2		15		15
3		25		25
4	time after C ₂ H ₄ pulses	1 min	time after C ₂ H ₄ pulses	1 min
5		5 min		5 min
6		10 min		10 min
7	T_{TPD}	435 °C	T_{TPD}	475 °C
8		450 °C		490 °C
9		465 °C		505 °C
10		480 °C		520 °C
11		500 °C		535 °C
12		520 °C		555 °C
13		550 °C		575 °C
14		600 °C		600 °C
15	time at 600 °C	5 min	time at 600 °C	5 min

Since no calibration data of the GC were available, only the total area of acetonitrile could be determined for qualitatively comparing the catalytic performance. All GC data from sample 1 to 15 were used, resulting in an unusual profile of acetonitrile formation. An example of a calcined 10 wt% Mo catalyst is given in Figure 5.1. The numbers correspond with the sample numbers listed in Table 5.1 with corresponding conditions. The total GC area of the curve is calculated and compared for the various catalysts tested under identical conditions.

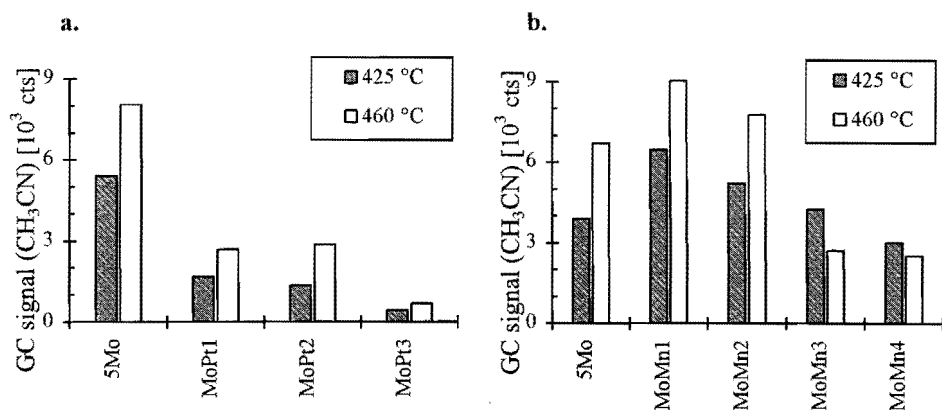


★ Figure 5.1 Example of a profile of the formation acetonitrile during a catalytic test with a calcined 10 wt% Mo catalyst at 425 °C.

2.2 Results and discussion.

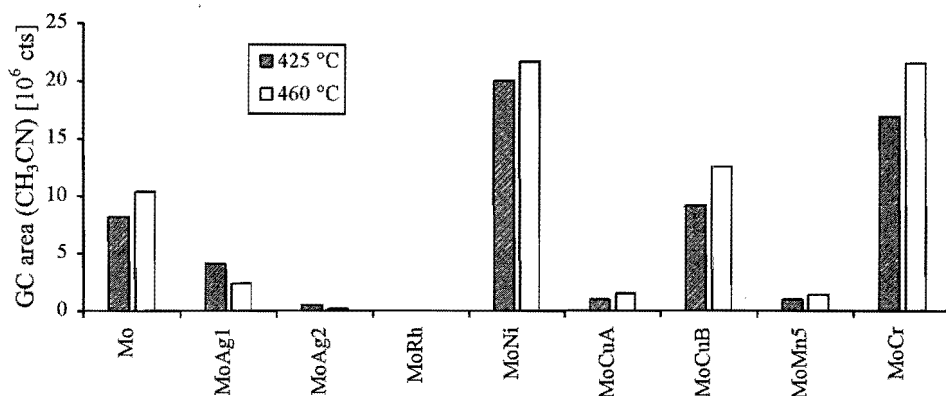
Various transition metals were tested for their promoting effect in γ -Al₂O₃ supported molybdenum catalysts on the formation of acetonitrile from ethylene and ammonia. The catalysts containing different amounts of Pt or Mn were prepared from a hydrogen pretreated 5 wt% Mo catalyst and were also submitted to a reductive treatment prior to reaction. The moment of sampling corresponds with sample number 3 in Table 5.1 and Figure 5.1. As can be seen in Figure 5.2a, the addition of only a little amount of Pt (MoPt1; 0.03 wt%) resulted already in a strong decrease in the formation of acetonitrile. The MoPt2 catalyst, containing 0.3 wt% Pt, showed similar behaviour, whereas MoPt3 (1 wt% Pt) showed a very poor activity towards acetonitrile formation. These catalysts are more active than the unpromoted molybdenum catalyst, producing a large amount of hydrocarbons, such as methane, ethane, propane and butane, and some CO_x. In contrast with the unpromoted molybdenum catalyst, the hydrogen is more strongly adsorbed on the surface than nitrogen, which explains the low activity towards N-insertion.

Figure 5.2b shows the results of the Mn promoted catalysts. When a little amount of manganese was added, a strong promoter effect was observed. The optimum composition was an atomic ratio of approximately 1:0.2 (MoMn1). When an excess of Mn was added, the amount of acetonitrile decreased and the amount at 460 °C was less than at 425 °C, indicating that the optimum temperature for acetonitrile formation had shifted to a lower value. Although the conversion of ethylene for all Mn containing catalysts is lower than for the unpromoted one, the selectivity to acetonitrile is higher. The formation of hydrocarbons was suppressed by the addition of Mn but the amount of CO₂ increased at increasing Mn content.



★ **Figure 5.2** Peak area of the GC signal of acetonitrile for the hydrogen pretreated 5 wt% Mo catalyst containing various amounts of Pt (a) and Mn (b) at 425 °C and 460 °C.

With the set of bimetallic catalysts prepared from a calcined 10 wt% Mo catalyst, the effects on the catalytic performance were observed to be extremely variable, as shown in Figure 5.3. The MoRh catalyst showed a conversion of ethylene of 95-100%, forming mainly CO_x and traces of methane. No acetonitrile was observed but the formation of NO_x or other components not detectable by a FID, could not be excluded. Since the catalyst was not tested after a hydrogen pretreatment, no general conclusion on the promoting effect of Rh can be drawn.



★ **Figure 5.3** The total GC area of acetonitrile for various calcined promoted Mo/ γ -Al₂O₃ catalysts during a catalytic test at 425 °C and 460 °C.

The MoMn5 converted highly selectively some ethylene (a few percent) into acetonitrile. Only traces of CO₂, CH₄, propionitrile and acrylonitrile were observed. This is in contrast with the hydrogen pretreated MoMn1, containing a comparable ratio of Mn and Mo. Apparently, the Mo-Mn catalyst performs better when pretreated in hydrogen (as far as the yield of acetonitrile is concerned).

Also, the addition of Ag did not result in a promoter effect. The conversion was of the same magnitude as the unpromoted catalyst, but the selectivity to acetonitrile was poor, due to high amounts of CO_x, CH₄ and C₆ compounds. Also, the amount of acetonitrile decreased from reaction temperature 425 °C to 460 °C, indicating that the optimum temperature for acetonitrile formation is shifted to a lower value. It cannot be excluded that this catalyst is more selective to acetonitrile when pretreated in hydrogen, because no such experiments were done with this catalyst.

The MoCu catalyst showed a remarkable effect. When the catalyst was not saturated with ammonia (40 pulses; MoCuA in Figure 5.3), it appeared highly active. However, the selectivity to acetonitrile was very poor, producing mainly CO_x, whereas CH₄ was formed in the same amount as acetonitrile. When the MoCu catalyst was saturated with ammonia (90 pulses; MoCuB in Figure 5.3), the conversion of ethylene decreased, due to the decrease in CO₂ and CH₄ formation. This resulted in a strong increase in the selectivity to acetonitrile, thus in a small promoter effect of Cu. This suggests that the Mo-Cu must be reduced to some extent by NH₃ to suppress the combustion of ethylene.

Most striking promoter effects were observed for Ni and Cr. These catalysts appeared not only more active, but were capable of producing highly selectively acetonitrile. The MoNi catalyst formed traces of CH₄ and propionitrile, whereas the main side product for the MoCr combination was CO₂.

2.3 In summary.

The addition of Pt to a reduced Mo catalyst did not result in a higher activity towards acetonitrile formation. Also, no other nitrogen containing organic products were observed. This was also the case when Ag, Rh or Mn were added to a calcined Mo catalyst. When Cu was added, a larger amount of ammonia was needed to obtain a better catalytic performance regarding acetonitrile. This resulted in only a slight promoter effect by Cu. By adding Cr or Ni, strong increases in both activity and selectivity towards acetonitrile were observed. A similar effect was observed for the hydrogen pretreated Mo-Mn catalyst.

3 Catalytic tests under semi-flow conditions.

From the set of promoted Mo/ γ -Al₂O₃ catalysts described in the previous section, the ones with the strongest promoter effect for the formation of acetonitrile were selected for further investigation. This concerned the calcined MoNi and MoCr, and the hydrogen pretreated MoMn catalysts. Although these experiments were not performed, also interesting results are suggested with the MoRh, MoAg and MoCu catalysts after a reductive treatment.

3.1 Experimental procedure.

Catalyst pretreatment and the experimental procedure for catalytic tests is similar to the one described in Chapter 4, section 2, except for the fact that only one reaction temperature was applied, namely 450 °C.

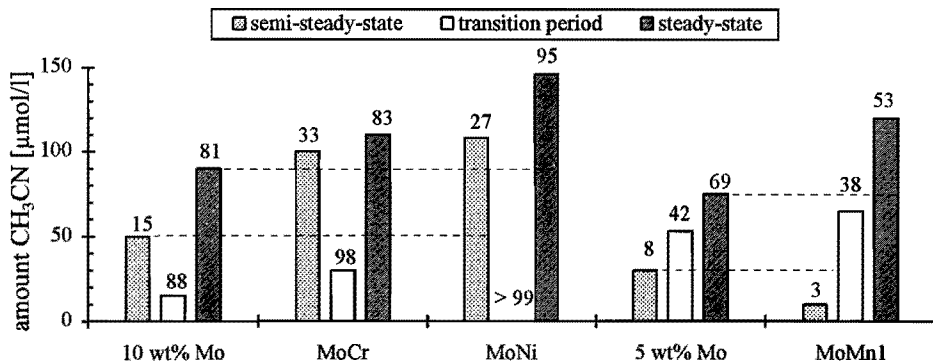
3.2 Results and discussion.

Similar to the unpromoted molybdenum catalyst with higher loading, the calcined 10 wt% Mo catalyst containing a secondary compound showed the three regions of different activity and selectivity, namely the semi-steady-state, the transition period with the non-gradual increase and the steady-state, as discussed in Chapter 4. The differences between the particular regions were even more striking when compared to the unpromoted molybdenum catalyst. The catalyst containing Mn showed a gradual transition period, due to the lower Mo content of 5 wt%.

3.2-1 Catalytic tests.

When the three calcined promoted catalysts were submitted to reaction at 450 °C, the semi-steady-state period showed large differences compared to the molybdenum catalyst under the same conditions (see Figure 5.4). Except for the MoMn catalyst, all these catalysts showed a higher activity, where the main side products in that period were CH₄, C₂H₆ and CO_x. The MoNi catalyst formed more methane, whereas the MoCr and MoMn catalysts formed mainly CO_x as side products.

During the transition period, larger fluctuations were observed for the MoCr and MoNi catalysts. The conversion of ethylene was almost 100%, forming mainly CO, CH₄ and some ethane, while the production of acetonitrile was reduced to almost zero for the MoNi catalyst.



★ **Figure 5.4** The amount of acetonitrile at the various regions of reactivity at 450 °C for various calcined molybdenum and promoted molybdenum catalysts. The number above the bar represents the average conversion of ethylene during the particular period.

The MoCr formed a larger amount of ethane, along with a variety of hydrocarbons, such as propylene, propane, cyclohexadiene and other C_6 compounds.

When reaching the steady-state, the MoNi catalyst showed the highest activity and the largest amount of acetonitrile. Although the MoCr catalyst showed the same activity as the unpromoted molybdenum catalyst, more acetonitrile was observed. The MoMn1 catalyst showed the lowest activity with the highest selectivity to acetonitrile, resulting in also a considerable larger amount of acetonitrile formation than for the base catalyst.

Given the low activity of the molybdenum-only catalyst, it is likely to conclude that the increase in activity and selectivity by adding the promoter is due to an increase in the dispersion of the molybdenum phase. The promoters chromium and nickel are expected to be catalytically active, but no experiments were done to know whether this was towards side reactions or towards acetonitrile. Nickel increased the methane formation, whereas chromium induced more the polymerisation of ethylene. The addition of manganese deactivated the catalyst significantly when pretreated with oxygen. This suggests that Mn is present in a different structure when calcined, and/or masking a larger part of the active sites. Upon hydrogen pretreatment and during reaction, this Mn structure is converted into a different, perhaps reduced one, increasing the selectivity to acetonitrile or suppressing the side reactions.

3.2-2 Catalyst characterisation.

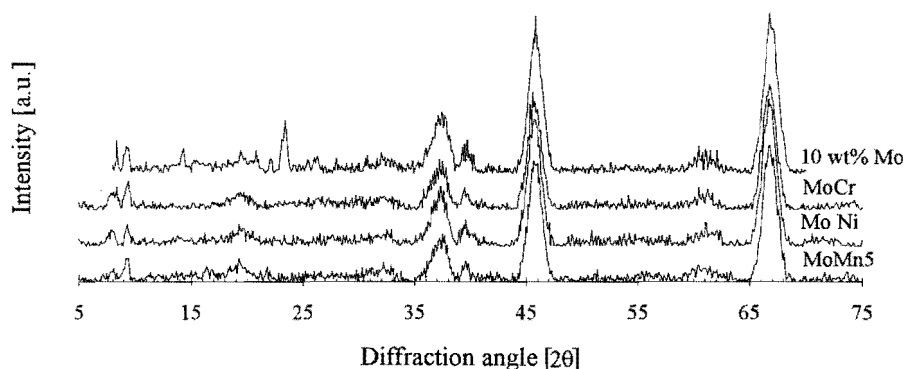
High Resolution Transmission Electron Microscopy.

The MoCr, MoNi and MoMn1 catalysts were investigated by HR-TEM. When freshly calcined, small non-crystalline metal particles were found on the alumina surface. The estimated size was 10 Å or less, so no accurate composition could be determined by EDX. This indicates that the addition of Cr or Ni to a calcined Mo/ γ -Al₂O₃ catalyst with a molybdenum content exceeding the maximum adsorption capacity of alumina, retards the formation of Al₂(MoO₄)₃ and decreases the interaction of the molybdenum with the alumina surface. Even at low molybdenum content (5 wt%) the addition of Mn induced agglomeration of the active phase, which can explain the poor catalytic performance of the calcined MoMn catalyst.

When spent, no significant differences were observed, compared to the fresh catalysts. This implies that no formation of bulk MoO₂ occurred during reaction, suggesting a better dispersion of the molybdenum phase compared to the unpromoted spent one.

X-ray Diffraction.

The XRD spectrum of the freshly calcined 10 wt% Mo catalyst showed small signals of Al₂(MoO₄)₃. When Cr, Ni or Mn has been added, no signals of crystalline phases other than of the alumina support were observed, as is shown in Figure 5.5. This implies that the presence of these secondary components retarded the formation of Al₂(MoO₄)₃. It is known that the formation of NiAl₂O₄ is more favourable, whereas manganese is also capable of forming a spinel structure, MnAl₂O₄. It can not be excluded that also a chemical interaction



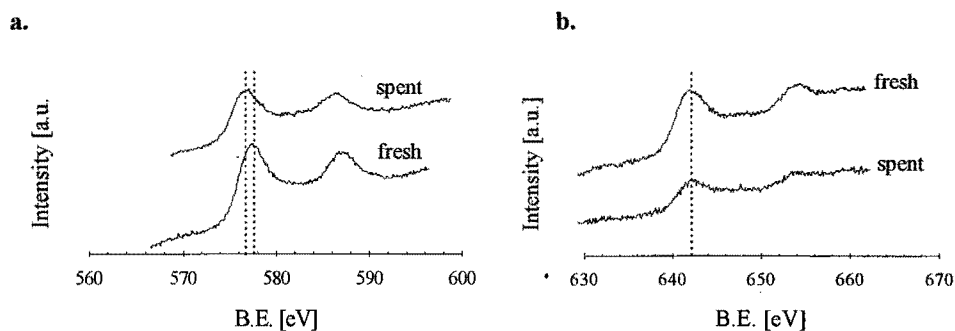
★ Figure 5.5 XRD spectra of calcined 10 wt% Mo, MoNi, MoCr and MoMn5 catalysts.

occurred between chromium and alumina or molybdenum, since the amount of secondary metal added is small and the presence of these spinel structures cannot be detected by XRD.

X-ray Photoelectron Spectroscopy.

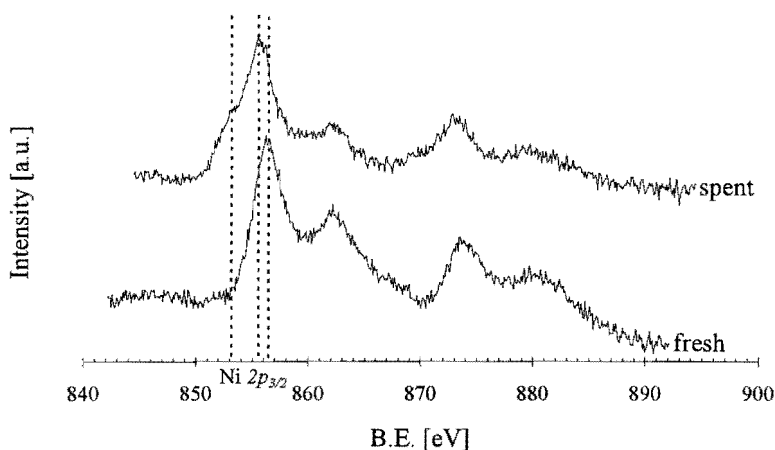
Analysis of the XP signals originating from the promoter added can give information about the structure present in the mixed oxide catalyst. The freshly calcined catalysts showed a different activity compared to the ones that had reached the steady-state, so it is expected that surface species change in structure or dispersion when submitted to reaction conditions. This is shown in Figure 5.6. The spent MoCr showed a Cr $2p_{3/2}$ peak at 576.9 eV, which is typical for Cr^{3+} in bulk Cr_2O_3 (see Figure 5.6a). When calcined, this signal was positioned at 577.6 eV, which cannot be attributed to Cr^{6+} (B.E. at > 578.5 eV in CrO_3). Although it cannot be excluded that a chemical interaction with the alumina or the molybdenum exists when calcined, it is rather likely that a change in dispersion of chromium had occurred upon reaction. The Cr $2p$ signal is known to shift to a higher binding energy when chromium is present as highly dispersed isolated atoms [24], so it is very likely that highly dispersed chromium is present on a calcined catalyst which agglomerates during reaction. This is substantiated by the fact that the intensity of the Cr $2p$ of the spent MoCr had decreased when compared to the freshly calcined one.

The catalyst promoted with manganese showed a different behaviour. No significant shift of the Mn $2p$ signal was observed when a freshly calcined MoMn1 catalyst was compared with a spent one (see Figure 5.6b). The manganese appeared to be present as MnO_2 (B.E. of Mn $2p_{3/2}$ at 642.3 eV).



★ **Figure 5.6** XP spectra of the Cr $2p$ signal of the freshly calcined and spent MoCr catalyst (a) and the Mn $2p$ signal of the freshly calcined and spent MoMn1 catalyst (b).

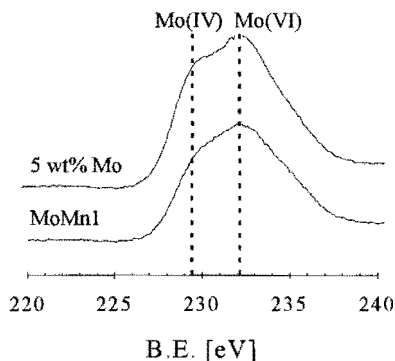
Nickel is known for its complex $2p$ spectrum, which can obstruct the interpretation of these spectra when applied in catalysis, where more than one Ni species can be present. The spectra of the freshly calcined and spent MoNi catalyst are shown in Figure 5.7. When fresh,



★ Figure 5.7 XPS spectra of the Ni $2p$ signal of the freshly calcined and spent MoNi catalyst.

only one Ni component appeared to be present. The Ni $2p_{3/2}$ signal at 856.7 eV is suggested to originate from NiAl₂O₄, which is known to form easily on alumina at higher calcination temperatures and longer calcination times [25]. When submitted to reaction for 24 hours, two different Ni $2p_{3/2}$ signals appeared: at 855.3 eV and a shoulder at 853.5 eV, which are suggested to originate from NiO and Ni⁰, respectively.

Comparing the Mo $3d$ signal of the calcined 5 wt% Mo catalyst with its Mn containing analogue, some difference was observed, as is shown in Figure 5.8. The amount of Mo(IV) was less after reaching the steady-state when manganese was added (55% versus 62% in an unpromoted catalyst). This confirms the idea of Auvil et. al [13] that Mn is responsible for retarding the reduction of molybdenum below MoO₂. It was observed previously a higher amount of Mo(IV) species induced a higher activity towards side reactions [26], so by retarding a further reduction of molybdenum a more selective catalyst to N-insertion is obtained.

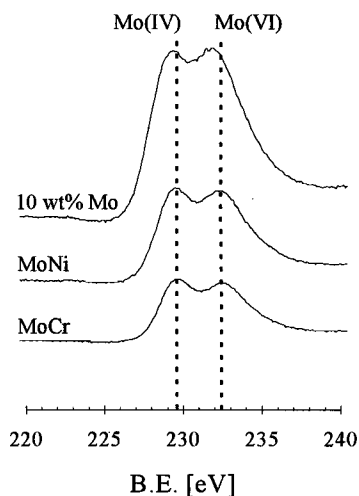


★ Figure 5.8 XPS spectra of the Mo $3d$ signal of a calcined 5 wt% Mo and MoMn1 catalyst after reaching the steady-state at 450 °C.

Differences were found in the $I_{\text{Mo}}/I_{\text{Al}}$ ratio when compared to the unpromoted fresh catalyst. A decrease of the $I_{\text{Mo}}/I_{\text{Al}}$ ratio of 35% was found, due to an increase of the Al signal of 30%, and a decrease of the Mo signal of 15%. This implies that agglomeration of molybdenum occurred by adding manganese. When spent, both the Al and the Mo signal were of the same magnitude, compared to the unpromoted spent molybdenum catalyst. This implies that the increase of activity and selectivity cannot be ascribed to an increase in the dispersion of molybdenum, but to a decrease of the interaction between Mo and $\gamma\text{-Al}_2\text{O}_3$.

The addition of chromium or nickel had a quite different effect on the various oxidation states of molybdenum. Figure 5.9 shows the Mo 3d signals of the calcined 10 wt% Mo catalyst, the MoNi and MoCr catalysts after reaching the steady-state at 450 °C. The addition of chromium or nickel induced a higher amount of Mo(IV) species compared to the unpromoted catalyst. Since it was observed on unpromoted catalysts that a highly reduced molybdenum surface induced a higher activity towards side reactions, the addition of Cr or Ni must modify the properties of the reduced molybdenum, resulting in a higher selectivity to acetonitrile. The MoNi catalyst produced a high amount of methane compared to other products, which demands a higher hydrogen consumption than the formation of higher hydrocarbons. This higher hydrogen consumption might shift the equilibrium between ethylene/ NH_3 and acetonitrile/ H_2 even more to the desired product. To fully understand the role of Ni and Cr in molybdenum supported catalysts, also the catalytic activity of supported nickel and chromium towards ammonia and ethylene should be investigated.

The $I_{\text{Mo}}/I_{\text{Al}}$ ratio of the MoCr was over 50% lower compared to the unpromoted calcined molybdenum catalyst. This was due to an increase in the aluminium signal of 35%, whereas the molybdenum signal decreased 25%. This implies that molybdenum agglomerates when chromium is present. Apparently, by adding Cr the interaction between alumina and molybdenum is decreased, which can explain the higher activity of this catalyst. The spent catalyst showed a $I_{\text{Mo}}/I_{\text{Al}}$ intensity ratio which was of the same magnitude as the spent unpromoted one (only 5% decrease). Although the Mo signal was little lower, the Al signal



★ **Figure 5.9** XP spectra of the Mo 3d signal of a calcined 10 wt% Mo, the MoCr and MoNi catalysts after reaching the steady-state at 450 °C.

was also lower suggesting a better dispersion, where a part of the molybdenum is shielded by Cr₂O₃. Analysis of reference compounds is necessary to elucidate the correct surface morphology.

The $I_{\text{Mo}}/I_{\text{Al}}$ ratio of the freshly calcined MoNi catalyst was 38% lower when compared to the unpromoted molybdenum catalyst, due to an increase of the Al signal of 28% and a decrease of the Mo signal of 21%. When submitted to reaction, this ratio was of the same magnitude of the unpromoted spent catalyst (only 7.5% decrease). Similar to the MoCr catalyst, the molybdenum and the aluminium signals were lower, implying a better dispersed phase where the molybdenum is more shielded by nickel.

4 Conclusions.

Of the set of secondary compounds added to a γ -Al₂O₃ supported molybdenum catalyst, Ni, Mn and Cr showed a strong promoter effect for the formation of acetonitrile. This could not be ascribed to an increase of the dispersion of molybdenum. Instead, agglomeration of the molybdenum phase was induced by the addition of Ni, Cr or Mn, implying a decrease in the interaction between molybdenum and alumina. The formation of Al₂(MoO₄)₃ in freshly calcined catalysts with higher Mo content was suppressed by the presence of the secondary components, and in case of the MoNi catalyst the formation of NiAl₂O₄ was suggested by XPS analysis. The calcined MoNi and MoCr catalysts showed both in the semi-steady-state and in the steady-state a higher activity and selectivity compared to the unpromoted catalyst. At steady-state, a higher amount of Mo(IV) was observed compared to the molybdenum only catalyst. Since a higher amount of Mo(IV) induces a higher activity towards side reactions, it was suggested that Ni and Cr are capable of modifying the active site of Mo.

When adding different amounts of manganese to a Mo/ γ -Al₂O₃ catalyst, an optimum Mo:Mn atomic ratio was found at 10:2. The calcined MoMn appeared to be highly selective to acetonitrile, but with poor activity during the semi-steady-state period. When pretreated with hydrogen, the catalyst activity increased while maintaining its high selectivity, resulting in a strong promoter effect of Mn. At the steady-state, the catalytic performance of the calcined was similar to the hydrogen pretreated one. It was suggested that when calcined, the molybdenum is shielded by not very active MnO₂, and during reaction this MnO₂ is capable of retarding the reduction of molybdenum surface, resulting in a highly selective but less active catalyst for the formation of acetonitrile.

Literature cited

- 1 Trimm, D.L., "Design of Industrial Catalysts", Elsevier, Amsterdam, (1980)
- 2 Yermakov, Yu.I., Kuznetsov, B.V., Ryndin, Yu.A., *React. Kinet. Catal. Lett.* **2** (1975) 151
Yermakov, Yu.I., Kuznetsov, B.V., Ryndin, Yu.A., *J. Catal.* **42** (1976) 73
- 3 Tri, T.M., Candy, J.P., Gallezot, P., Massardier, J., Primet, M., Védérine, J.C., Imelik, B., *J. Catal.* **79** (1983) 196
Tri, T.M., Massardier, J., Gallezot, P., Imelik, B., *J. Catal.* **85** (1984) 151
Tri, T.M., Massardier, J., Gallezot, P., Imelik, B., *J. Catal.* **85** (1984) 244
- 4 Leclercq, G., Romero, T., Pietrzyk, S., Grimblot, L., Leclercq, L., *J. Mol. Catal.* **25** (1984) 67
- 5 Mériaudeau, P., Albano, K., Naccache, C., *J. Chem. Soc., Faraday Trans. I* **83** (1987) 2113
- 6 Petit, C., Katrib, A., Girard, P., Garin, F., Maire, G., *J. Mol. Catal.* **85** (1993) 75
- 7 Hamada, H., Kuwahara, Y., Matsuno, Y., Wakabayashi, K., *Sekiyu Gakkaishi* **30** (1987) 188
- 8 Foley, H.C., Hong, A.J., Brinen, J.S., Allard, L.F., Garratt-Reed, A.J., *Appl. Catal.* **61** (1990) 351
Te, M., Lowenthal, E.E., Foley, H.C., *J. Catal.* **146** (1994) 591
Lowenthal, E.E., Schwarz, S., Foley, H.C., *J. Catal.* **156** (1995) 96
- 9 Kip, B.J., Hermans, E.G.F., van Wolput, J.H.M.C., Hermans, N.M.A., van Grondelle, J., Prins, R., *Appl. Catal.* **35** (1987) 109
- 10 Trunschke, A., Ewald, H., Gutschik, D., Miessner, H., Skupin, M., Walther, B., Böttcher, H.-C., *J. Mol. Catal.* **56** (1989) 95
Trunschke, A., Ewald, H., Gutschik, D., Miessner, H., Fukuoka, A., Ichikawa, M., Böttcher, H.-C., *Mater. Chem. Phys.* **29** (1991) 503
Trunschke, A., Ewald, H., Gutschik, D., Miessner, H., Marengo, S., Martinengo, S., Pinna, F., Zanderighi, L., *J. Mol. Catal.* **74** (1992) 365
- 11 Hickman, D.A., Schmidt, L.D., *Science* **259** (1993) 343
- 12 Bol, C.W., Friend, C.M., *J. Am. Chem. Soc.* **117** (1995) 8053
Bol, C.W., Friend, C.M., *J. Phys. Chem.* **99** (1995) 11930
Bol, C.W., Friend, C.M., *Surf. Sci. Lett.* **337** (1995) L800
- 13 Gambell, J.W., Auvil, S.R., *US Patent* 4 272 451 (1981)
Auvil, S.R., Penquite, C.R., *US Patent* 4 272 452 (1981)
- 14 Ozkan, U.S., Gill, R.C., Smith, M.R., *J. Catal.* **116** (1989) 171
Gill, R.C., Ozkan, U.S., *J. Catal.* **122** (1990) 452
Ozkan, U.S., Moctezuma, E., Driscoll, S.A., *Appl. Catal.* **58** (1990) 305
Ozkan, U.S., Smith, M.R., Driscoll, S.A., "New Developments in Selective Oxidation by Heterogeneous Catalysis, (P. Ruiz and B. Delmon, Eds.), Elsevier, Amsterdam, **72** (1992) 363
- 15 Ruiz, P., Zhou, B., Remy, M., Machef, T., Aoun, F., Doumain, B., Delmon, B., *Catal. Today* **1** (1987) 181
Weng, L.T., Ruiz, P., Delmon, B., *J. Mol. Catal.* **52** (1989) 349
Weng, L.T., Ma, S.Y., Ruiz, P., Delmon, B., *J. Mol. Catal.* **61** (1990) 99
Weng, L.T., Delmon, B., *Appl. Catal.* **81** (1992) 141
- 16 Schuit, G.C.A., Gates, B.C., *AIChEJ* **19** (1973) 417
Grange, P., *Catal. Rev.-Sci. Eng.* **21** (1980) 135
Topsoe, H., Clausen, B.S., *Catal. Rev.-Sci. Eng.* **26** (1984) 395
Prins, R., de Beer, V.H.J. Samorjai, G.A., *Catal. Rev.-Sci. Eng.* **31** (1989) 1
- 17 Ho, T.C., *Catal. Rev.-Sci. Eng.* **30** (1988) 117
Girgis, M.J., Gates, B.C., *Ind. Eng. Chem. Res.* **30** (1991) 2021
Yang, S.H., Scatterfield, C.N., *J. Catal.* **81** (1983) 168
Ledoux, M.J., Djellouli, B., *Appl. Catal.* **67** (1990) 81
Hadjiioizou, G.C., Butt, J.B., Dranoff, J.S., *J. Catal.* **135** (1992) 27
- 18 Mazzocchia, C., Del Rosso, R., Centola, P., *An. Quim.* **79** (1983) 108

- 19 Mazzocchia, C., Del Rosso, R., Centola, P., *Proc. 5th Ibero-American Symp. on Catal.* (M. Farinha Portela, C.M. Pulido, Eds.), Lisbon, **2** (1979) 61
- 20 Ozkan, U.S., Schrader, G.L.C., *J. Catal.* **95** (1985) 120, 137, 147
Martin-Aranda, R.M., Portela, M.F., Madeira, L.M., Freire, F., Oliveira, M., *Appl. Catal.* **127** (1995) 201
- 21 Clark, A., *Catal. Rev.* **3(2)** (1969) 145
Thomas, C.L., *Catalytic Processes and Proven Catalysis*, Academic Press, New York, (1970)
- 22 Yao, Y.-F.Y., *J. Catal.* **28** (1973) 139
- 23 Haber, J., *Proceedings of the 3rd Climax International Conference on the Chemistry and Uses of Molybdenum*, (H.F. Barry, P.C.H. Mitchel, Eds.), Climax Molybdenum, Ann Harbor, MI, (1979) 114
- 24 Merryfield, R., McDaniel, M., Parks, G., *J. Catal.* **77** (1982) 348
- 25 Knözinger, H., *Proceedings of the 9th I.C.C.*, Calgary (M.J. Philips, M. Ternan, Eds.) **5** (1988) 20
- 26 Chapter 4 of this Thesis.

6

CONCLUDING REMARKS AND SUMMARY

Supported molybdenum catalysts are known for the multiplicity of reactions they promote. An important class of such reactions is represented by the catalytic oxidation. Commercially, the most important member of allylic oxidation is the ammoxidation of propylene with ammonia and air to acrylonitrile, which is an example where 30 years of research has elucidated most of the reaction mechanism. In addition, the development and study of selective catalysts for allylic oxidation has led to more understanding concerning selective oxidation and the phenomena of catalysis in general.

In contrast with the allylic (amm)oxidation, only very little research is done on the vinylic ammoxidation of olefins. The aim of this study was to elucidate the reaction mechanism of vinylic ammoxidation over supported molybdenum catalysts, with the conversion of ethylene and ammonia to acetonitrile as a test reaction. No molecular oxygen was added to the reaction stream, so only the lattice oxygen was involved. An attempt was made to find a relationship between catalytic activity and the structural parameters.

Various supported molybdenum catalysts were prepared and submitted to an oxidative or a reductive pretreatment, inducing various concentrations of lattice oxygen and a different catalyst morphology. Comparing various supports, it appeared that $\gamma\text{-Al}_2\text{O}_3$ resulted in a better catalytic performance, regarding the formation of acetonitrile, than SiO_2 . This was due to a stronger interaction between alumina and the active phase, resulting in a better dispersion. On silica, this interaction is much less, resulting in a molybdenum structure that is poorly dispersed MoO_3 -like and not very active towards the formation of acetonitrile. For this reason, the study described in this thesis focuses on $\gamma\text{-Al}_2\text{O}_3$ supported molybdenum oxide catalysts.

Temperature programmed desorption of ammonia showed that dissociative adsorption occurs at an elevated temperature, which shifts for both pretreatments to a lower value with increasing molybdenum content. When pretreated in hydrogen, this temperature was lower than for calcined catalysts. The monomeric Mo surface species present at low molybdenum content, which are resistant to reduction and agglomeration, show a low activity towards ammonia dissociation. At higher molybdenum content, polymeric Mo surface species are present, which are easier to reduce and tend to agglomerate more easily upon a reductive treatment. These larger reduced molybdenum clusters show a higher activity towards complete ammonia dissociation, resulting in the desorption of nitrogen and hydrogen.

From TPD experiments it is also deduced that dissociative adsorption of ammonia can occur via two different mechanisms, dependent on the catalyst pretreatment. When calcined, the dissociation of ammonia proceeds according to a condensation reaction, where water is released from the catalyst using lattice oxygen, forming NH_x species on the surface. When pretreated in hydrogen, the dissociation of ammonia proceeds via the release of hydrogen from the catalyst, so without the use of lattice oxygen. The formation of $=\text{NH}$ species on the catalyst surface is suggested for both pretreatments.

For the catalytic tests a specific experimental procedure was applied, where the reactants were introduced to the catalyst sequentially. It is shown that only the sequence of introducing ammonia first, followed by ethylene results in the formation of acetonitrile. These experiments also showed the presence of two different sites on the molybdenum surface for the formation of acetonitrile. One site, whose concentration is independent of the Mo content, releases the acetonitrile slowly at the reaction temperature. The other site, whose concentration increases with increasing Mo content, strongly adsorbs the acetonitrile, which can only be removed by raising the temperature or by competitive adsorption of ammonia.

Catalytic tests under flow conditions show a remarkable profile of variations in activity and selectivity to acetonitrile. Three regions of interest as a function of time on stream are distinguished: a semi-steady-state, a transition period and the steady-state. The semi-steady-state period is characterised by a constant level of acetonitrile formation, while the selectivity to other products is changing. Typical for the transition period is a strong increase in activity, whereas the amount of acetonitrile formation is changing. Dependent on catalyst pretreatment and molybdenum content this increase is gradual or proceeds via a maximum, while the selectivity to acetonitrile proceeds gradual or via a minimum, respectively. All hydrogen pretreated catalysts and calcined catalysts with Mo content below 10 wt% show a gradual transition to the steady-state. Only calcined catalysts with Mo content of 10 wt% and more show a non-gradual transition period. At steady-state, all catalysts showed a similar reactivity independent of the pretreatment applied.

Two mechanisms for the formation of acetonitrile appear to be operative separately or simultaneously, dependent on catalyst pretreatment and time on stream. One is based on the ammoxidation mechanism with the consumption of lattice oxygen, forming water and acetonitrile. This mechanism is active on freshly calcined catalysts containing only Mo(VI) sites, which are highly selective but not very active. The other is based on synergetic formation of ethane and occurs on catalysts that have reached the steady-state, containing both Mo(VI) and Mo(IV) sites. No lattice oxygen is consumed. Although less selective to acetonitrile, the activity of these catalysts is much higher, resulting in a better yield. The two mechanisms operate simultaneously on hydrogen pretreated catalysts. The existence of these different mechanisms can be related to the different mechanisms of dissociative adsorption of ammonia. Apparently, both mechanisms can generate similar N-inserting species, which are suggested to be Mo=NH.

By combining various characterisation techniques, the catalyst surface was analysed both in the fresh state and after different times on stream. When freshly calcined, it is shown that the molybdenum phase on the alumina surface is not present as MoO₃, but as highly dispersed Al₂(MoO₄)₃ (particle size is less than 5 Å). Furthermore, the maximum adsorption capacity of the γ-Al₂O₃ applied corresponds to approximately 8-9 wt% Mo, whereas the theoretical value is calculated at 15 wt%, assuming the size of one Mo cluster at 20 Å². At a loading exceeding the maximum adsorption capacity of alumina (10 wt% Mo), about 77% of the γ-Al₂O₃ surface is covered, whereas the amount of excess Mo is used to form bulk Al₂(MoO₄)₃. These larger Al₂(MoO₄)₃ crystals are suggested to be responsible for the non-gradual transition period prior to the steady-state. At steady-state a stable molybdenum phase is formed, which is characterised as highly dispersed MoO₂. The large Al₂(MoO₄)₃ crystals present on calcined catalysts with higher loading are converted under reaction conditions to large MoO₂ crystals. Also, upon hydrogen pretreatment these large Al₂(MoO₄)₃ crystals are destroyed, but only at very high Mo contents (15 wt%) traces of a bulk MoO₂ phase are formed. At lower coverage, the molybdenum surface seems further reduced than MoO₂ after a hydrogen pretreatment (contains more Mo(IV) ions), which stabilises to MoO₂ under reaction conditions. Although a reductive pretreatment or long reaction times induces a decrease in Mo dispersion of approximately 50%, the activity increases and the catalysts produce more acetonitrile. This suggests that a decrease in interaction between molybdenum with the support occurs upon reductive treatment, which increases the activity and the desorption rate of products. This high activity shifts the equilibrium between ethylene/ammonia and acetonitrile/hydrogen to the side of the desired product by the high consumption of hydrogen needed for the hydrogenation, forming ethane and some methane.

Since a large number of examples are known of catalytic improvement when secondary compounds are added to molybdenum catalysts, a number of secondary components were tested on their promoter effect in γ - Al_2O_3 supported molybdenum catalysts in the formation of acetonitrile. The addition of chromium, nickel or manganese results in a strong increase in acetonitrile formation. At semi-steady-state, the calcined MoNi and MoCr catalysts shows a higher activity and selectivity to acetonitrile compared to the unpromoted one. The MoMn catalyst shows only a strong promoter effect when pretreated with hydrogen. At steady-state, all three catalysts show a higher selectivity to acetonitrile and, except for the MoMn catalyst, a higher activity, resulting in also a promoter effect. Characterisation techniques show that the formation of $\text{Al}_2(\text{MoO}_4)_3$ in the freshly calcined catalysts is suppressed by the addition of Cr, Ni or Mn, whereas the dispersion of the molybdenum phase decreased (metal particles of approximately 10 Å are present). This suggests a decrease in interaction of molybdenum with the support, which explains the higher activity of the MoNi and MoCr catalysts. The addition of Ni resulted in the formation of NiAl_2O_4 , whereas Cr is present as highly dispersed Cr_2O_3 and Mn as MnO_2 . The presence of MnO_2 in a calcined catalyst obscures the active site. At steady-state, the dispersion of molybdenum is not significantly different from the spent unpromoted catalyst for all three promoted ones. The Cr and Mn are still present as Cr_2O_3 and MnO_2 , respectively. Nickel is present in two different forms, *viz.* NiO and metallic Ni. The presence of Mn retards the reduction of molybdenum further than MoO_2 , which results in a very selective but less active catalyst. The presence of Cr or Ni results in a MoO_2 -like structure, whose surface contains more Mo(IV). Since a higher degree of reduction in an unpromoted catalyst results in a higher activity towards side reactions, it is suggested that the presence of Cr or Ni modifies the active site of molybdenum.

6

CONCLUSIE EN SAMENVATTING

Molybdeenoxide katalysatoren zijn bekend om hun toepasbaarheid in een groot aantal reacties, waarvan de katalytische oxydatie een omvangrijke groep is. Een belangrijk lid van allylische oxydatie is de commercieel meest toegepaste ammoxydatie van propyleen met ammoniak en lucht naar acrylonitril en is een voorbeeld waarbij 30 jaar onderzoek geleid heeft tot de opheldering van een groot deel van het reactiemechanisme. Bovendien heeft de ontwikkeling van selectieve katalysatoren voor allylische oxydatie geleid tot meer inzicht in selectieve oxydatie en katalyse in het algemeen.

In tegenstelling tot (amm)oxydatie waarbij additie aan een eindstandige methylgroep plaatsvindt, is er slechts weinig onderzoek gedaan naar de ammoxydatie waarbij de stikstof aan een eindstandige vinylgroep gekoppeld wordt. Het doel van het onderzoek beschreven in dit proefschrift was het helderen van het reactiemechanisme van het katalytisch koppelen van stikstof aan de =CH₂ groep van olefines. Hierbij is de omzetting van etheen met ammoniak in acetonitril gebruikt als testreactie. Er werd geen gasvormig zuurstof aan het reactiemengsel toegevoegd, zodat alleen het roosterzuurstof betrokken was in de reactie en heroxydatie van het katalysator oppervlak uitgesloten kon worden. Een poging is gedaan om een relatie te vinden tussen katalytische activiteit en structuur van het oppervlak.

Een aantal gedragen molybdeen katalysatoren werd bereid en voorbehandeld met waterstof of zuurstof, daarmee verschillende concentraties van roosterzuurstof en katalysator morfologie creërend. Wanneer dragers met elkaar vergeleken worden, blijkt dat γ -Al₂O₃ een betere katalytische activiteit oplevert wat betreft de vorming van acetonitril, dan SiO₂. Dit wordt veroorzaakt door een sterkere interactie tussen alumina en de actieve fase, waardoor een betere dispersie verkregen wordt. Op silica is deze interactie een stuk zwakker, waardoor een slecht gedispergeerde MoO₃-achtige structuur op het oppervlak ontstaat, die niet erg

actief is voor de vorming van acetonitril. Om deze reden is het onderzoek beschreven in dit proefschrift toegespitst op $\gamma\text{-Al}_2\text{O}_3$ gedragen molybdeenoxide katalysatoren.

Temperatuur geprogrammeerde desorptie van ammoniak op $\text{Mo}/\gamma\text{-Al}_2\text{O}_3$ heeft laten zien dat dissociatieve adsorptie plaatsvindt bij een hogere temperatuur, die voor beide voorbehandelingen naar een lagere waarde verschuift bij een toenemende molybdeen belading. Deze temperatuur is lager voor katalysatoren voorbehandeld met waterstof dan met zuurstof. De monomere Mo oppervlakte species, aanwezig bij een lage molybdeen belading en meer resistent voor reductie en agglomeratie, zijn niet erg actief voor de dissociatie van ammoniak. Bij een hogere belading zijn ook polymere Mo oppervlakte species aanwezig, die makkelijker te reduceren zijn en makkelijker agglomereren onder reducerende condities. Deze grotere gereduceerde molybdeen clusters zijn actiever voor de dissociatie van ammoniak, welke leidt tot de desorptie van stikstof en waterstof.

Uit de TPD experimenten is ook afgeleid dat dissociatieve adsorptie van ammoniak kan plaatsvinden via twee verschillende mechanismen, afhankelijk van de katalysatorvoorbehandeling. Op een gecalcineerde katalysator wordt ammoniak gedissociëerd volgens een condensatiereactie, waarbij water vrijkomt via de consumptie van roosterzuurstof, en oppervlakte $=\text{NH}$ species worden gevormd. Voorbehandeld in waterstof wordt ammoniak gesplitst waarbij waterstof vrijkomt, dus zonder het gebruik van roosterzuurstof. De vorming van $=\text{NH}$ species op het katalysatoroppervlak is verondersteld voor beide voorbehandelingen.

Voor de katalytische tests werd een bepaalde experimentele procedure gebruikt waarbij de reactanten opeenvolgend in de reactor worden gebracht. Er is aangetoond dat alleen de volgorde van het aanbieden van eerst ammoniak, gevolgd door etheen resulteert in de vorming van acetonitril. Deze experimenten laten ook zien dat er twee verschillende actieve sites aanwezig zijn op het molybdeen oppervlak die verantwoordelijk zijn voor de vorming van acetonitril. Eén site, waarvan de concentratie onafhankelijk is van de molybdeen belading, laat het gevormde acetonitril langzaam desorberen bij de reactie temperatuur. Een tweede site, waarvan de concentratie toeneemt bij toenemende molybdeen belading, adsorbeert het gevormde acetonitril zo sterk dat het alleen van het katalysatoroppervlak verwijderd kan worden door verwarmen of door competitieve adsorptie met ammoniak.

Katalytische tests onder flow condities laten een opmerkelijk profiel zien van veranderingen in activiteit en selectiviteit naar acetonitril als functie van de reactietijd. Drie gebieden als functie van reactietijd kunnen worden onderscheiden: een semi-steady-state, een overgangperiode en de steady-state. De semi-steady-state periode wordt gekenmerkt door een constante productie van acetonitril, terwijl de selectiviteit naar andere producten verandert. Karakteristiek voor de overgangperiode is een sterke toename in activiteit, terwijl de acetonitril productie ook sterk varieert. Afhankelijk van de katalysator voorbehandeling en molybdeen belading, is deze toename geleidelijk of via een maximum, terwijl de selectiviteit

naar acetonitril respectievelijk geleidelijk of via een minimum verloopt. Alle waterstof voorbehandelde en gecalcineerde katalysatoren met een molybdeen belading van 5 gew% of minder vertonen een geleidelijke overgang naar de steady-state. Alleen gecalcineerde katalysatoren met een molybdeen belading van 10 gew% en hoger laten een niet geleidelijke overgangperiode zien. In de steady-state periode hebben alle katalysatoren een overeenkomstige reactiviteit die onafhankelijk is van de voorbehandeling.

Twee mechanismen blijken mogelijk voor de vorming van acetonitril en kunnen zowel gelijktijdig als apart actief zijn, afhankelijk van katalysator voorbehandeling en reactietijd. De één is gebaseerd op het ammoxydatiemechanisme met de consumptie van roosterzuurstof, waarbij water en acetonitril worden gevormd. Dit mechanisme is actief op vers gecalcineerde katalysatoren die alleen Mo(VI) sites bevatten, die zeer selectief maar niet erg actief zijn. Het andere mechanisme is gebaseerd op het synergetisch vormen van ethaan en vindt plaats op katalysatoren die de steady-state bereikt hebben en zowel Mo(IV) als Mo(VI) sites bevatten. Er wordt dan geen roosterzuurstof meer verbruikt. Hoewel minder selectief voor acetonitril, is de activiteit van deze katalysatoren veel hoger, wat resulteert in een hogere opbrengst aan gewenst product. De mechanismes zijn gelijktijdig actief op waterstof voorbehandelde katalysatoren in de semi-steady-state periode. De oorsprong van deze twee mechanismes voor de vorming van acetonitril kan gezocht worden in de twee mechanismes die gevonden zijn bij de dissociatieve adsorptie van ammoniak. Blijkbaar kunnen beide mechanismes overeenkomstige species voor N-insertie genereren, welke verondersteld worden als Mo=NH.

Door het combineren van verschillende karakteriseringstechnieken werd het katalysatoroppervlak geanalyseerd zowel in de verse toestand als gebruikt na variabele reactietijden. Op vers gecalcineerde katalysatoren blijkt het molybdeen niet aanwezig te zijn als MoO₃, maar als zeer hoog gedispergeerd Al₂(MoO₄)₃ (deeltjesgrootte kleiner dan 5 Å). Bovendien blijkt de maximale adsorptiecapaciteit van het hier gebruikte γ-Al₂O₃ overeen te komen met ongeveer 8-9 gew% Mo, terwijl de theoretische berekende waarde 15 gew% is, waarbij de afmeting van één Mo cluster van 20 Å² is aangenomen. Bij een belading die de maximum adsorptiecapaciteit van alumina overschrijdt (10 gew% Mo) is ongeveer 77% van het γ-Al₂O₃ bedekt, terwijl het overshot Mo gebruikt wordt voor de vorming van bulk Al₂(MoO₄)₃. Deze grotere Al₂(MoO₄)₃ kristallen worden verantwoordelijk geacht voor de niet geleidelijke overgangperiode voorafgaand aan de steady-state. In de steady-state is een stabiele molybdeen fase gevormd welke gekarakteriseerd is als hoog gedispergeerd MoO₂. De grote Al₂(MoO₄)₃ kristallen aanwezig in gecalcineerde katalysatoren met een hogere molybdeen belading, worden onder reactiecondities omgezet naar grote MoO₂ kristallen. Ook met behulp van een waterstof voorbehandeling zijn deze Al₂(MoO₄)₃ kristallen te vernietigen, hoewel pas bij zeer hoge Mo belading (15 gew%) sporen van bulk MoO₂ worden gevormd. Bij een

lagere belading lijkt het molybdeenoppervlak verder gereduceerd dan MoO_2 (bevat meer Mo(IV) ionen) na een waterstof voorbehandeling, en stabiliseert naar MoO_2 onder reactiecondities. Hoewel een reducerende voorbehandeling en lange reactietijden een afname in de Mo dispersie induceren van ongeveer 50%, neemt the activiteit enorm toe, terwijl ook de hoeveelheid acetonitril toeneemt. Dit suggereert dat er een afname in de interactie plaats heeft gevonden tussen molybdeen en de drager, waardoor er grotere molybdeen deeltjes ontstaan die actiever zijn en een hogere desorptiesnelheid van produkten mogelijk maken. De hoge activiteit verschuift het evenwicht tussen etheen/ammoniak en acetonitril/waterstof naar de kant van het gewenste product door de hoge consumptie van waterstof die nodig is voor de hydrogenering, waarbij ethaan en methaan worden gevormd.

Er zijn een groot aantal voorbeelden bekend van katalysator verbetering wanneer er secundaire componenten aan molybdeen katalysatoren worden toegevoegd. Daarom zijn er een aantal secundaire componenten getest op hun promotor effect in $\gamma\text{-Al}_2\text{O}_3$ gedragen molybdeen katalysatoren wat betreft de vorming van acetonitril. De toevoeging van chroom, nikkel of mangaan resulteert in een sterke toename van de acetonitril produktie. In de semi-steady-state hebben de gecalcineerde MoNi en MoCr katalysatoren een hogere activiteit en selectiviteit naar acetonitril vergeleken met een niet-gepromoteerde. The MoMn katalysator laat alleen een sterk promotor effect zien wanneer voorbehandeld met waterstof. In de steady-state laten alle drie de katalysatoren een hogere selectiviteit naar acetonitril zien en, behalve de MoMn katalysator, een hogere activiteit. Karakteriseringstechnieken toonden aan dat de vorming van $\text{Al}_2(\text{MoO}_4)_3$ in vers gecalcineerde katalysatoren met hoge belading wordt onderdrukt door de toevoeging van Cr, Ni of Mn, terwijl de molybdeen dispersie afneemt (metaaldeeltjes van ongeveer 10 Å zijn aanwezig). Dit suggereert dat er een afname in de interactie tussen molybdeen en de drager is opgetreden, wat de hogere activiteit verklaard van de MoNi en MoCr katalysatoren. De toevoeging van Ni resulteert in de vorming van NiAl_2O_4 , terwijl Cr als hoog gedispergeerd Cr_2O_3 en Mn als MnO_2 aanwezig zijn. De aanwezigheid van MnO_2 in een gecalcineerde katalysator schermt de actieve Mo site af. In de steady-state verschilt de dispersie van molybdeen voor alle drie de gepromoteerde katalysatoren niet substantieel van de niet-gepromoteerde gebruikte katalysator. Chroom en mangaan zijn nog steeds aanwezig als Cr_2O_3 en MnO_2 , terwijl nikkel in twee valentietoestanden aanwezig is, te weten NiO en metallisch Ni. De aanwezigheid van Mn onderdrukt de reductie van molybdeen verder dan MoO_2 , wat resulteert in een zeer selectieve maar minder actieve katalysator. De aanwezigheid van Cr of Ni leidt tot de vorming van een MoO_2 -achtige structuur, waarvan het oppervlak meer Mo(IV) bevat. Omdat een hogere graad van reductie bij een niet-gepromoteerde katalysator resulteert in een hogere activiteit voor nevenreacties, is geopperd dat de aanwezigheid van Cr of Ni de actieve site van molybdeen modificeert.

I

APPENDIX

The conversion of ethylene and the selectivities in the semi-steady-state period for different pretreated Mo/ γ -Al₂O₃ catalysts with various molybdenum content.

★ Table I.1 The oxygen pretreated 3 wt% Mo/ γ -Al₂O₃ catalyst.

T [°C]	X C ₂ H ₄ [%]	S CH ₃ CN [%]	S C ₂ H ₆ [%]	S CH ₄ [%]	S CO ₂ [%]	S CO [%]
450	2.86	94.85	0	0	5.15	0
475	3.18	92.40	0	0	7.60	0
500	2.92	82.07	0	0	17.35	0.57
525	7.04	64.22	0	0	25.71	10.07
550	18.35	27.60	19.13	11.25	21.21	20.80

★ Table I.2 The hydrogen pretreated 3 wt% Mo/ γ -Al₂O₃ catalyst.

T [°C]	X C ₂ H ₄ [%]	S CH ₃ CN [%]	S C ₂ H ₆ [%]	S CH ₄ [%]	S c-C ₆ [%]	S CO ₂ [%]	S CO [%]
425	2.01	100	0	0	0	0	0
450	2.88	100	0	0	0	0	0
475	2.97	95.33	0	0	0	4.67	0
500	13.00	59.89	26.24	0	0	9.60	4.27
525	25.83	39.29	30.09	12.15	0	6.75	11.73
550	70.23	3.03	17.14	22.35	26.53	2.77	28.18

★ Table I.3 The oxygen pretreated 5 wt% Mo/ γ -Al₂O₃ catalyst.

T [°C]	X C ₂ H ₄ [%]	S CH ₃ CN [%]	S C ₂ H ₆ [%]	S CH ₄ [%]	S CO ₂ [%]	S CO [%]
425	3.52	90.58	0	0	9.42	0
450	4.60	86.62	0	0	13.38	0
475	6.78	85.75	0	0	14.25	0
500	11.15	79.95	0	0	17.34	2.71
525	48.49	28.04	33.12	12.07	16.65	10.12

★ Table I.4 The hydrogen pretreated 5 wt% Mo/ γ -Al₂O₃ catalyst.

T [°C]	X C ₂ H ₄ [%]	S CH ₃ CN [%]	S C ₂ H ₆ [%]	S CH ₄ [%]	S CO ₂ [%]	S CO [%]
400	2.31	96.21	0	0	3.79	0
425	4.37	95.25	0	0	4.75	0
450	15.27	61.99	30.66	0	7.35	0
475	36.15	42.31	36.89	0	8.99	11.81
500	70.99	4.60	36.98	36.52	1.47	20.43

★ Table I.5 The oxygen pretreated 10 wt% Mo/ γ -Al₂O₃ catalyst.

T [°C]	X C ₂ H ₄ [%]	S CH ₃ CN [%]	S C ₂ H ₆ [%]	S CH ₄ [%]	S c-C ₆ [%]	S CO ₂ [%]	S CO [%]
350	4.52	73.17	0	0	0	25.07	1.76
400	7.17	81.94	0	0	0	18.06	0
425	9.18	85.66	0	0	0	14.34	0
450	12.31	88.31	0	0	0	11.69	0
475	21.03	76.94	10.26	0	0	11.27	1.53
500	29.79	72.19	11.78	5.27	0	8.16	2.60
550	89.69	1.30	4.76	35.25	17.74	8.14	32.82

★ **Table I.6** The hydrogen pretreated 10 wt% Mo/ γ -Al₂O₃ catalyst.

T [°C]	X C ₂ H ₄ [%]	S CH ₃ CN [%]	S C ₂ H ₆ [%]	S CH ₄ [%]	S CO ₂ [%]	S CO [%]
350	1.95	100	0	0	0	0
400	5.16	94.07	0	0	5.93	0
425	15.95	57.65	35.20	0	7.15	0
450	27.65	53.62	31.96	5.00	9.42	0
475	59.64	29.86	34.04	4.57	12.12	19.41
500	98.71	1.00	10.85	40.43	1.05	46.67

★ **Table I.7** The oxygen pretreated 15 wt% Mo/ γ -Al₂O₃ catalyst.

T [°C]	X C ₂ H ₄ [%]	S CH ₃ CN [%]	S C ₂ H ₆ [%]	S CH ₄ [%]	S CO ₂ [%]	S CO [%]
400	9.75	82.98	0	0	17.02	0
425	9.90	88.02	0	0	11.98	0
450	18.99	79.08	11.79	0	9.13	0
475	30.29	70.92	17.07	0	12.01	0
500	50.69	56.26	17.07	4.68	18.86	3.13
550	84.81	1.41	3.86	38.85	17.50	38.38

★ **Table I.8** The hydrogen pretreated 15 wt% Mo/ γ -Al₂O₃ catalyst.

T [°C]	X C ₂ H ₄ [%]	S CH ₃ CN [%]	S C ₂ H ₆ [%]	S CH ₄ [%]	S CO ₂ [%]	S CO [%]
350	4.22	44.28	55.72	0	0	0
400	9.23	55.14	40.73	0	4.13	0
425	15.15	58.50	36.86	0	4.65	0
450	36.59	48.19	39.88	0	11.92	0
475	84.30	2.15	41.59	28.74	1.43	26.09
500	86.88	1.57	12.96	49.25	1.82	34.39

Dankwoord.

Ik heb mijn onderzoek ervaren als een zoektocht in het donker naar de lichtknop. Toen de lichtknop gevonden werd is de oogst van resultaten en conclusies begonnen en samengevat in dit boekje. Zowel het zoeken als het oogsten zou ik nooit zonder de hulp van anderen hebben kunnen voltooien.

Allereerst wil ik mijn ouders bedanken. Jullie hebben mij altijd de vrijheid hebben gegeven om datgene te doen wat ik wilde, en ook als dat weleens verkeerd uitpakte, stonden jullie altijd klaar om mij te steunen.

Rutger, bedankt, omdat je zelfs in de meest donkere dagen het kleinste spootje van optimisme nog aanwezig bij mij wist aan te sporen. Met de meest curieuze vragen kon ik altijd bij Rob van Veen terecht en de daarop volgende verfrissende discussies met jou heb ik ook altijd erg op prijs gesteld. Joop is niet alleen technisch en wetenschappelijk van onschatbare waarde gebleken. Je wist ook met je eerlijke en duidelijke kijk op zaken mij te leren hoofd en bijzaken te onderscheiden. San de Beer bedankt dat ik ook gebruik heb mogen maken van jou als wandelende molybdeen encyclopedie.

De "oppervlaktegroep" wil ik bedanken omdat ik redelijk onbeperkt heb mogen hobbyen op jullie XPS. Met name Cees Verhagen bedankt voor je heldere uitleg, Tiny dat ik je altijd wel lastig mocht/kon vallen met technische problemen en Arthur, Pieter en Peter Thüne voor de ruggespraak met jullie die ik wel eens nodig had.

Adelheid Elemans bedankt voor het uitvoeren van de vaak lastige molybdeen analyses m.b.v. AAS en voor de lange XRD metingen. Eugène van Oers bedankt voor de BET metingen en Jos van Wolput voor de vaak zeer "exotische" IR metingen, die achteraf toch zeer waardevol bleken te zijn. Martien Haanen bedank ik voor zijn hulp bij de SEM/EDX metingen. Het feit dat geen enkele SEM foto in dit boekje verschenen is heeft niet aan jou gelegen, maar jouw metingen hebben wel aanleiding gegeven tot het contact zoeken met de TU Delft.

De groep van Hidde Brongersma bedank ik omdat ik bij jullie terecht kon voor de LEIS metingen. Met name de vasthoudendheid van Amoud heeft ervoor gezorgd dat er in korte tijd toch zeer waardevolle LEIS metingen zijn gegenereerd.

Patricia Kooyman van het Nationale Centrum voor HREM aan de TU Delft; jouw medewerking en doorzettingsvermogen (zelfs toen de apparatuur niet echt meewerkte) heeft een groot aantal puzzelstukjes op zijn plaats doen vallen bij de interpretatie.

De hoeveelheid data had ik nooit kunnen genereren zonder het bloed, zweet en tranen van mijn afstudeerders Marjan Rijckaert, Marco van Son, Simon Liebrechts en René Houben en stagiaire Sjoerd Alkema. Bovendien maakte jullie aanwezigheid het meestal een stuk gezelliger.

Mijn (ex-)kamerogenoten en "medemetalers" Marius, Robert, Annemieke, Noud, Marnix, Piet, Bruce, Frank en Pieter wil ik bedanken dat jullie altijd beschikbaar waren voor het bespreken van mijn dagelijkse problemen en het (meestal) accepteerden dat ik mijn overvloedige agressie op jullie botvierde....

Verder zouden deze afgelopen jaren zeer saai verlopen zijn zonder de zwarte humor tijdens lunchpauzes, voornamelijk afkomstig van "de elementen van vloer 10", zonder de verfrissende gesprekken tijdens de koffie, zonder de soms (vaak?) uit de hand gelopen borrels en vreetpartijen erna, zonder het feit dat ik een groot deel van TAK op het paard gezien heb (de paarden zijn overigens na een zeer intensieve therapie weer redelijk hersteld) en zelfs tegen de muur heb laten klimmen.

Tenslotte Wim bedankt dat je mijn buien maar op de koop toe hebt genomen en als ik de realiteit een beetje dreigde te verliezen mij weer tot mijn enkels in de grond wist te verankeren.

Curriculum Vitae.

Imre Peeters werd geboren op 4 mei 1966 in Den Haag. Na in Voorschoten de lagere school te hebben doorlopen, begon zij in 1978 met de HAVO opleiding aan het Lucas College in dezelfde gemeente. In 1979 is zij verhuisd naar Noord-Limburg waar de HAVO werd voortgezet aan het Bouwens van der Boye College in Panningen en voltooid in 1983. Vervolgens heeft zij daar in 1985 het VWO eindexamen behaald.

In september van dat jaar werd gestart met de studie Scheikundige Technologie aan de Technische Universiteit Eindhoven. Haar afstudeeronderzoek betrof de chemische hydrolyse van modelverbindingen voor cyclisch adenosine monofosfaat en werd verricht onder leiding van dr.ir. N.L.H.L. Broeders en prof.dr. R.A. Sheldon in de vakgroep Organische Chemie. In augustus 1991 werd de ingenieurs titel behaald.

Van 15 december 1991 tot 16 maart 1996 was zij als assistent in opleiding in dienst van SON/NWO en verrichtte het in dit proefschrift beschreven onderzoek onder leiding van prof.dr. van Santen in de vakgroep Anorganische Chemie en Katalyse.

Stellingen behorende bij het proefschrift:

The Oxidative Ammonolysis of Ethylene to
Acetonitrile over Supported Molybdenum
Catalysts

door: Imre Peeters

1. De conclusie van Grünert *et al.*, verkregen met behulp XPS, dat bij de reductie van alumina gedragen molybdeen katalysatoren er oppervlakken ontstaan waarop Mo(VI), Mo(V), Mo(IV), Mo(II) en Mo(0) kunnen coëxisteren kan gezien worden als een knap staaltje fitwerk, echter de wetenschappelijke juistheid ervan is onwaarschijnlijk.

Grünert, W., Stakheev, A.Yu., Mörke, W., Feldhaus, R., Anders, K., Shpiro, E.S., Minachev, K.M., *J. Catal.* 35 (1992) 269

2. Ook al is Eindhoven één van de eerste gemeenten waar de groene golf is ingevoerd, toch geeft deze gemeente veruit de meeste voorkeur om de rode golf in de praktijk toe te passen.

- 3 The remote control mechanism in catalysis is just as impossible to imagine as for a woman in Europe to conceive a baby from a man in America.

R.K. Grasselli in discussie met P. Ruiz tijdens het ACS symposium "Heterogeneous Hydrocarbon Oxidation." in New Orleans, LA, USA, maart 1996.

4. Het is heel goed mogelijk om in vier jaar te promoveren, mits dit niet de eerste vier zijn.
5. Het is discutabel om een conclusie te trekken over de aanwezigheid van een reactie intermediair door deze als reactant aan te bieden, aangezien de concentratie en het adsorptie gedrag niet vergelijkbaar zijn met de reactiecondities.

Sokolovskii, V.D., Davydov, A.A., Ovsitser, O.Yu., *Catal. Rev.-Sci. Eng.* 37 (1995) 425

6. Het is makkelijker anderen hun fouten te vergeven dan hen die getuigen waren van jouw fouten.
7. Wetenschappelijke artikelen worden pas echt waardevol als ze ook de mislukte experimenten vermelden en verklaren.

8. Voetbal zou een stuk aantrekkelijker schouwspel worden indien er twee ballen in het spel zouden zijn.

9. Het feit dat een molybdeen katalysator gebruik kan maken van verschillende reactiemechanismen om hetzelfde, gewenste produkt te vormen, is weer een voorbeeld van de veelzijdigheid van dit metaal.

10. Diploma's zijn de sleutels waarmee je deuren opent. Maar om binnen te blijven moet je wel iets presteren.

11. Bureaucratie wordt pas vervelend als ze te omzeilen valt.

12. Het bereiden van een monolaag molybdeenoxide op alumina is onmogelijk.

13. De enige plek waar liefde altijd vóór seks komt, is in het woordenboek.

14. Sommige misdaden vragen om de herinvoering van lijfstraffen.

15. The search for the perfect pint should take a life time.

Imre Peeters
Eindhoven, 1 september 1996